Synthesis, Characterisation and Evaluation of Ferrocene-containing Novobiocin Analogues for Anticancer and Antiplasmodial Activity through Inhibition of Hsp90

THESIS

Submitted in fulfilment of the requirements for the degree of

Master of Science

of

Rhodes University

Mziyanda Mbaba

B.Sc.Hons (Rhodes)

January, 2017

DEDICATION

To my late mother,

Nonzondelelo Miriam Mbaba.

ACKNOWLEDGEMENTS

Kuqala, ndingathanda ukubulela uMdali wam uThixo ngesipho sobom, amandla kunye nolondolozo. Ndibulela abazali bam, uTata noMama uMbaba, oodade nabantakwethu bobasixhenxe uyokuqhina kubatshana neentombi zam ngenxaso nothando enindibonise lona ngalo lonke ixesha ndingumfundi. Niyinto yonke kum! Ndibulela kakhulu nakuMaSabatha, abantu beNkonzo yasekhaya, ngeminqweno emihle, ubunye kunye nenkathalo enindinike yona.

To my supervisor, Dr. S.D. Khanye, thank you for all your support, patience and guidance throughout the duration of this project and my academic hustles. Working under your supervision was a privilege and has moulded me into the aspiring researcher I am today. I could not wish for a better supervisor! I would equally like to thank my co-supervisor, Assoc. Prof. A.L. Ekdins, for her most invaluable input and advice in this project. To her research lab, Lab 301, your assistance with the biological assays is most appreciated. I would also like to acknowledge Mrs. M. Isaacs for conducting the antiplasmodial and cytotoxicity assays.

I am thankful to the Rhodes Chemistry Department, especially the technical and support staff, for their undying spirits of ensuring every bit of research goes smoothly and as planned. Without you, this project would have suffered greatly. To my friends and colleagues from Lab F22, past and present, I am grateful for having worked with people like you. Thank you for your support and constructive criticism throughout this project.

My heartfelt thanks to my close friends: Ewald Kruger, Sivuyile "S'vig" Mnqovu, Khethobole Sekgotha, Mpho Ngoepe, Christian Nkanga, Arthur Manda, Asanda Saba, Gwiba Makalima, Ogunyemi "Yemist" Oderinlo and Justin "Juzzy" Rodriguez (Dootch Fund bursary scheme). Thank you for your undying love, support and encouragement.

Finally, to my best friend, Athandwe "Pineapples" Paca, thank you for the gift of your presence, the laughter and for always keeping me on track.

This work was supported by the National Research Foundation (NRF) of South Africa. Opinions expressed and conclusions arrived at are those of the author and are not necessarily to be attributed to the NRF.

ABSTRACT

Novobiocin (Nb) is a coumarin type antibiotic isolated from the bacterium species of *Streptomyces* and possesses modest anticancer and antimalarial activities. Nb and analogues have been extensively explored as potential anticancer agents through inhibition of the *C*-terminal domain of heat shock protein 90 (Hsp90), which plays a pivotal role in the protein-folding machinery of cells. There has been little effort in the exploration of Nb and derivatives for antimalarial activity.

Incorporation of organometallic units, such as ferrocene (Fc), into bioactive chemical scaffolds remains an attractive approach for developing new therapeutic agents for treatment of several ailments. The current study sought to investigate the anticancer and antiplasmodial effects of incorporating ferrocene (Fc) into Nb scaffold presumably through inhibition of Hsp90. The ferrocenyl Nb analogues containing simplified structural motifs such as phenyl, benzyl, and piperidine were synthesized in six to nine steps employing conventional synthetic organic protocols adapted from literature, and the compounds were accessed in reasonable yields. For comparison purposes, a selection of organic Nb analogues were also included in the study. The target compounds were characterized by spectroscopic techniques including 1-dimensional nuclear magnetic resonance (1D NMR) and high-resolution mass spectroscopy.

The synthesized compounds were evaluated *in vitro* for potential anticancer and antiplasmodial activities using the breast cancer cell line (HCC38) and chloroquine-sensitive strain (3D7) of the malaria parasite, *Plasmodium falciparum*. The presence of the Fc unit was found to enhance both anticancer and antiplasmodial activities of the resultant ferrocenyl Nb compounds with IC_{50} values in the low to mid micromolar range. Hsp90 inhibitory studies of the ferrocenyl Nb analogues possessing superior activities (**2.13a** and **2.20c**) were also conducted using different yeast strains expressing both human and malarial Hsp90 isoforms: hHsp90α/β and *Pf*Hsp90, respectively. The results of Hsp90 inhibitory studies suggested no direct correlation between the observed activities of the analogues and Hsp90 inhibition. However, since the conditions of the assay were not optimised due to time constrains of the project, these observed data remained to be confirmed.

TABLE OF CONTESTS

Dedication (i)

Acknowledgements (ii)

Abstract (iii)

Table of contents (iv)

List of abbreviations and symbols (vii)

Publication and conference participation (ix)

1. INTRODUCTION 1

1.1. BACKGROUND: HEAT SHOCK PROTEIN 90 1

1.1.1. Hsp90 Structure 1

1.1.2. Hsp90 as a drug target 4

1.1.2.1. Hsp90 inhibition for anticancer activity 4

1.1.2.2. Hsp90 inhibition for antiplasmodial activity 7

1.2. MEDICINAL CHEMISTRY OF NOVIBIOCIN: CANCER AND MALARIA 10

1.2.1. Biological activities of novobiocin 11

1.2.1.1. Antibacterial activity of novobiocin 11

1.2.1.2. Antiplasmodial activity of novobiocin 12

1.2.1.3. Antitumour activity of novobiocin 14

1.3. NOVOBIOCIN ANALOGUES WITH ANTITUMOUR ACTIVITY 15

1.4. MEDICINAL CHEMISTRY OF FERROCENE AND ITS DERIVATIVES 19

1.4.1. Incorporation of ferrocene into bioactive chemical scaffolds 20

1.4.2. Ferrocenyl compounds with biological activity 23

1.5. AIMS AND OBJECTIVITIES OF THE PROJECT 26

REFERENCES 28

2. SYNTHESIS OF TARGET NOVOBIOCIN ANALOGUES 35

2.1. OVERVIEW OF SYNTHESIS OF COUMARIN COMPOUNDS 35

2.1.1. Pechmann reaction 36

2.1.2. Knoevenagel reaction 36

2.1.3. Witting reaction for coumarin synthesis 37
2.1.4. Perkin reaction 38
2.2. SYNTHESIS OF NOVOBIOCIN ANALOGUES 40
2.2.1. Preparation of coumarin nucleus of Nb analogues 41
2.2.2. Synthesis of 7-*O*-phenyl Nb analogues 47
2.2.2.1. Synthesis of *N*-Boc 7-phenyloxy-3-aminocoumarins (**2.6a-f**) 48
2.2.2.2. *N*Boc deprotection of phenylated 3-aminocooumarins 51
2.2.2.3. Preparation of biphenyl **A** 52
2.2.2.4. Synthesis of target phenylated Nb analogues (**2.13a-f** and **2.14a-f**) 55
2.2.2.5. Attempted amidation procedures 61
2.2.3. Synthesis of target piperidinyl Nb analogues 62
2.2.3.1. Preparation of benzyl-protected 3-aminocoumarins (**2.16a-b**) 64
2.2.3.2. Amidation with *n*-propylphosphonic acid (T3P®) 66
2.2.3.3. Synthesis of 7-hydroxy Nb analogues (**2.19a-d**) 68
2.2.3.4. Synthesis of target piperidinyl Nb analogues (**2.20a-k**) 69
2.3. CONCLUSIONS AND FUTURE WORK 78

REFERENCES 79

3. BIOLOGICAL EVALUATION STUDIES 82

3.1. ANTICANCER ACTIVITY OF TARGET NOVOBIOCIN ANALOGUES 82
3.1.1. Anticancer activity of phenylated Nb analogues (**2.13a-f** and **2.14a-f**) 82
3.1.2. Anticancer activity of OBn/OH and piperidinyl Nb analogues 84
3.1.3. Summary of anticancer activity studies 87
3.2. CYTOTOXICICY ASSAY STUDIES 89
3.3. ANTIPLASMODIAL ACTIVITY OF TARGET NOVOBIOCIN ANALOGUES 89
3.3.1. Antiplasmodial activity of phenylated Nb analogues (**2.13a-f** and **2.14a-f**) 89
3.3.2. Antiplasmodial activity of OBn/OH and piperidinyl Nb analogues 91
3.3.3. Summary of antiplasmodial activity studies 92
3.4. HSP90 INHIBITION STUDIES 93
3.5. CONCLUSIONS AND FUTURE WORK 95

REFERENCES 96

4. EXPERIMENTAL 97

4.1. GENERAL DETAILS 97

4.2. SYNTHESIS OF TARGERT NOVOBIOCIN ANALOGUES 97

4.2.1. General procedure for synthesis of salicylaldehydes (**2.2a-b**) 98

4.2.2. General procedure for synthesis of acetamidocoumarins (**2.3a-b**) 99

4.2.3. General procedure for synthesis of *N*-Boc 7-hydroxy-3-aminocoumarins (**2.4a-b**) 99

4.2.4. General procedure for synthesis of *N*-Boc 7-phenyloxy-3-aminocoumarins (**2.6a-f**) 101

4.2.5. General procedure for synthesis of free 7-phenyloxy-3-aminocoumarins (**2.7a-f**) 103

4.2.6. Synthesis of methyl 3-iodo-4-methoxybenzoate (**2.9**) 106

4.2.7. Synthesis of methyl 4-methoxy-3-(3-methoxy)phenylbenzoate (**2.10**) 106

4.2.8. Synthesis of 4-methoxy-3-(3-methoxy)-phenyl benzoic acid (**2.11**) 106

4.2.9. General procedure for synthesis of phenylated Nb analogues (**2.13a-f** and **2.14a-f**) 107

4.2.10. General procedure for synthesis pf *N*Boc-protected piperidinols (**2.15e-f**) 114

4.2.11. General procedure for synthesis of *N*-Boc-protected 7-benzyloxy-3-aminocoumarins (**2.16a-b**) 115

4.2.12. General procedure for Synthesis of free 7-benzyloxy-3-aminocoumarins (**2.17a-b**) 116

4.2.13. General procedure for synthesis of 7-OBn Nb analogues (**2.18a-d**) 117

4.2.14. General procedure for synthesis of 7-OH Nb analogues (**2.19a-d**) 119

4.2.15. Mitsunobi etheration for synthesis of piperidinyl Fc-Nb analogues (**2.20a-f**) 121

4.2.16. General procedure for synthesis of 3'- and 4'-NH piperidinyl Fc-Nb analogues (**2.20g-h**) 124

4.2.17. Synthesis organic piperidinyl Nb analogues (**2.20i-k**) 125

4.3. HCC38 BREST CANCER CELL LINE INHIBITION ASSAY 128

4.4. HeLa CELL CYTOTOXICITY ASSAY 128

4.5. 3D7 ANTIPLASMODIAL ASSAY 128

4.6. HSP90 INHIBITION ASSAY 129

REFERENCES 130

LIST OF ABBREVIATIONS AND SYMBOLS

EDCI	1-Ethyl-3-(3-imethylaminopropyl)carbodiimide
ATP	Adenosine triphosphate
atm.	Atmosphere
CQR	Chloroquine-resistant
CQS	Chloroquine-sensitive
$CuSO_4$	Copper(II) sulphate
^oC	Degrees Celsius
DNA	Deoxyribonucleic acid
DCM	Dichloromethane
CQ^{2+}	Diprotonated chloroquine
ESI	Electrospray Ionisation
eq.	Equivalents
E. coli	*Escherichia coli*
FDA	Food and Drug Administrattion
ν	Frequency
GryA	Gyrase subunit A
GryB	Gyrase subunit B
IC_{50}	Half-maximal inhibitory concentration
Δ	Heat
Hex	Hexane
hHsp90	Human heat shock protein 90
HCl	Hydrochloric acid
H-bond	Hydrogen bond
H-bonding	Hydrogen bonding
HOBt	Hydroxybenzotriazole
LHS	Left-hand side
$MgSO_4$	Magnesium sulphate
m/z	Mass-to-ratio charge
M.p.	Melting point
MeOH	Methanol
μM	Micromolar concentration

mL	Milliliter
mmol	Millimole
nM	Nanomolar
mmol	Millimole
M	Molar concerntration
M^+	Molecular ion
RNA	Ribonucleic Acid
RHS	Right-hand side
%T	Percentage transmittance
rpm	Revolutions per minute
TFA	Trifluoroacetic acid
$NaHCO_3$	Sodium bicarbonate
Na_2SO_3	Sodium sulphite
UV	Ultra-violet
w/v	Weight by volume

PUBLICATION AND CONFERENCE PARTICIPATION

Publication

"Ferrocenyl and organic novobiocin derivatives: Synthesis and their *in vitro* biological activity."

Authors: Mbaba, M., Mabhula, A., Boel, N., Edkins, A.L., Isaacs, I., Hoppe, H. and Khanye, S.D.

Paper submitted for publication to the *Journal of Inorganic Biochemistry* (16 December 2016).

Conference participation

"Novel ferrocenyl novobiocin analogues: anticancer and antiplasmodial activity."

Oral presentation given at the Frank Warren conference, Rhodes University (04 December 2016).

1. INTRODUCTION

This chapter provides a brief background on heat shock protein 90 as a drug target particularly in cancer and malaria (**Section 1.1**), and investigation of novobiocin (**Section 1.2**) and novobiocin-based compounds on the two diseases (**Section 1.3**). At the end of the chapter, attention is given to the medicinal chemistry of ferrocenyl derivatives (**Section 1.4**) and aims and objectives of the current work (**Section 1.5**).

1.1. BACKGROUND: HEAT SHOCK PROTEIN 90

Heat shock protein 90 (Hsp90) is a protein that belongs to a class of chaperones known as heat shock proteins (HSPs). The HSPs are molecular chaperones whose primary role is to carry out protein folding in cells. Under normal circumstances, heat shock proteins work in partnerships whereby unfolded proteins in metastable state are partially folded by one group of chaperones and passed down to another until full functional conformation is achieved.[1] HSPs are constitutively expressed in all organisms under normal conditions, but can also be inductively expressed, especially in pathogenic cells, upon induction of stress stimuli, like temperature elevation, nutrient deprivation, hypoxia, and presence of metabolic inhibitors, heavy metals and amino acids.[1] Like other HSPs, Hsp90 plays a crucial role in maturing nascent proteins and re-folding denatured proteins into their respective bioactive conformations.[2] Over 200 proteins involved in various important cellular processes, particularly in signal transduction pathways, are substrates of Hsp90 (i.e. Hsp90 client proteins).[3] As such, Hsp90 has been widely investigated as a therapeutic target for various afflictions, including cancer and infections caused by protozoan parasites.

1.1.1. Hsp90 Structure

There are four isoforms of Hsp90 in humans: Hsp90α, Hsp90β, GRP94 and TRAP1.[4] Hsp90α and Hsp90β are the most studied of the four isoforms. They are localized in the cytoplasm and constitute 1 – 2% of the cytosolic protein content, whereas GRP94 and TRAP1, respectively, are found in the endoplasmic reticula and mitochondria. Hsp90 functions as a homodimer.[5, 6] The monomeric form of Hsp90 consists of three functional domains, namely: the *N*-terminal domain (25 kDa), the middle domain (35 kDa) and the *C*-terminal domain (12 kDa) (**Figure 1.1**).[5, 6] A linker characterized by charged amino acid residues connects the middle and *N*-terminal domains.

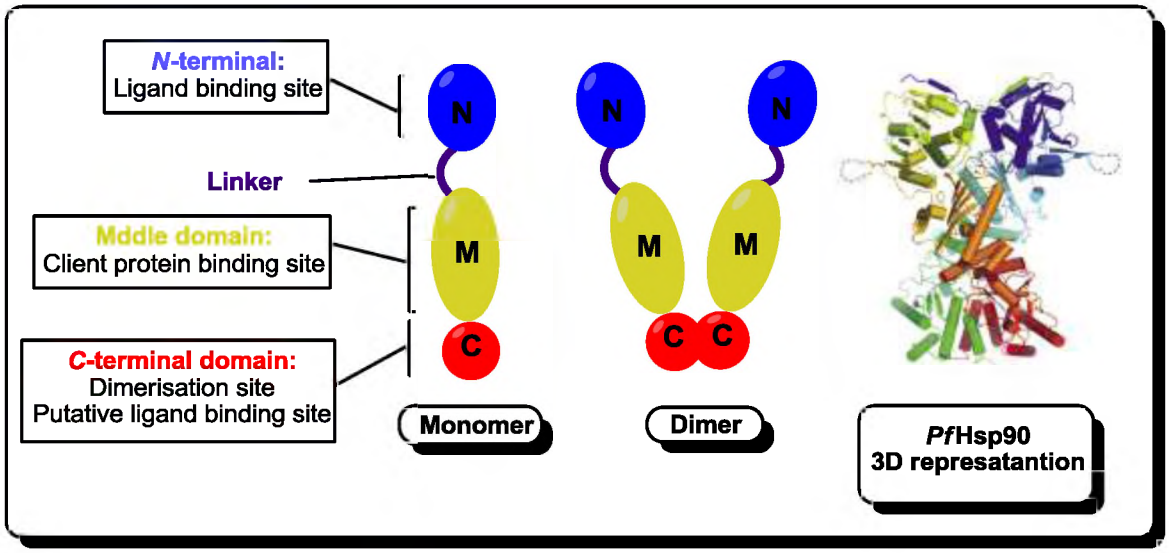

Figure 1.1: A three-dimensional representation of *Pf*Hsp90 showing all three domains: *N*-terminal, Middle and *C*-terminal domains with their functional roles.[7] The rods in *Pf*Hsp90 represent α-helices of the protein while the arrows represent the β-sheets.

Of the three functional domains, the *N*-terminus is the most studied and well-understood, both functionally and structurally.[8] There is high abundance of isolated and fully characterised co-crystal structures of the *N*-terminus complexed with different ligand molecules that have been deposited into the protein data bank website (PDB search: hsp90 n-terminal domain). The *N*-terminus is defined by an ATP-binding site that is connected by a 'linker' to the middle domain, forming a well-recognised 'split' ATPase site to which other molecules such as geldanamycin (**1.1**), radicicol (**1.2**) and harmine (**1.3**) can competitively bind (**Figure 1.2**).

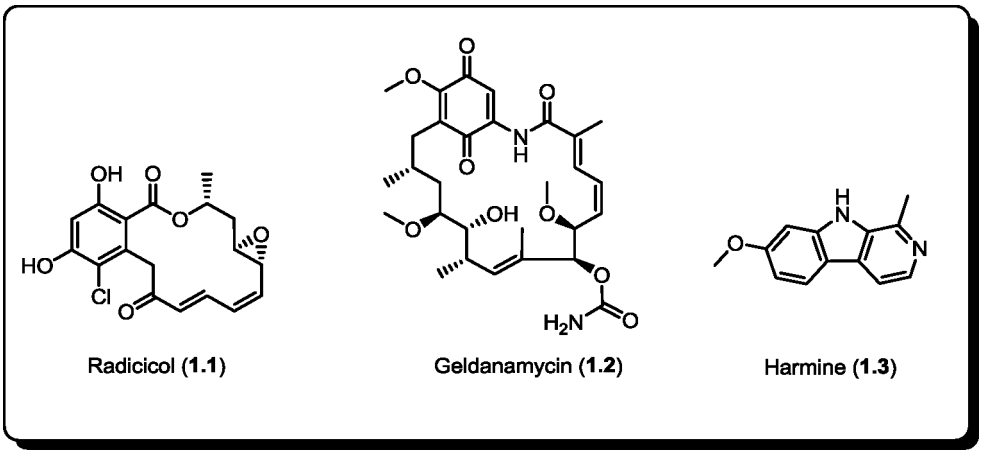

Figure 1.2: Examples of traditional Hsp90 *N*-terminal inhibitors.

Binding of such molecules inhibits the function of the protein. *N*-terminal inhibition of Hsp90 depletes the protein-folding machinery and Hsp90 client proteins and induces their proteasomal degradation.[6] These have undesirable effects for the cell, which include induction of cell arrest and apoptosis. Surprisingly, the same inhibition at the *N*-terminus is also associated with induction of heat shock response as a survival mechanism for stressed cells.[9] The middle domain is characterised by highly charged amino acid residues and has high affinity for co-chaperones and client proteins.[5] In *Plasmodium falciparum* heat shock protein 90 (*Pf*Hsp90), this charged region is unusually larger compared to Hsp90s from other species, signifying one of the unique features of *Pf*Hsp90.[7]

Unlike the *N*-terminal domain, much still remains unknown about the *C*-terminus. The primary function of this domain is to act as the chaperone's site of dimerization.[5, 6] It is characterised by an MEEVD motif that is recognised by Hsp90 co-chaperones that synergistically function with Hsp90 during protein folding.[10] Additionally, the *C*-terminus contains a second putative ATP-binding site that lacks ATPase activity.[11] The function of ATP binding to this site is to allosterically facilitate nucleotide exchange at the *N*-terminus. Molecules such as novobiocin (Nb, **1.4**), epigallocatechin-3-gallate (**1.5**) and cisplatin (**1.6**) are known to also competitively bind to the same site (**Figure 1.3**). As with *N*-terminal inhibition, occupation of this site by these molecules disrupts the function of Hsp90 and has similar consequences for client proteins as well as the cell. However, *C*-terminal inhibition lacks the pro-survival heat shock response associated with *N*-terminal inhibition.

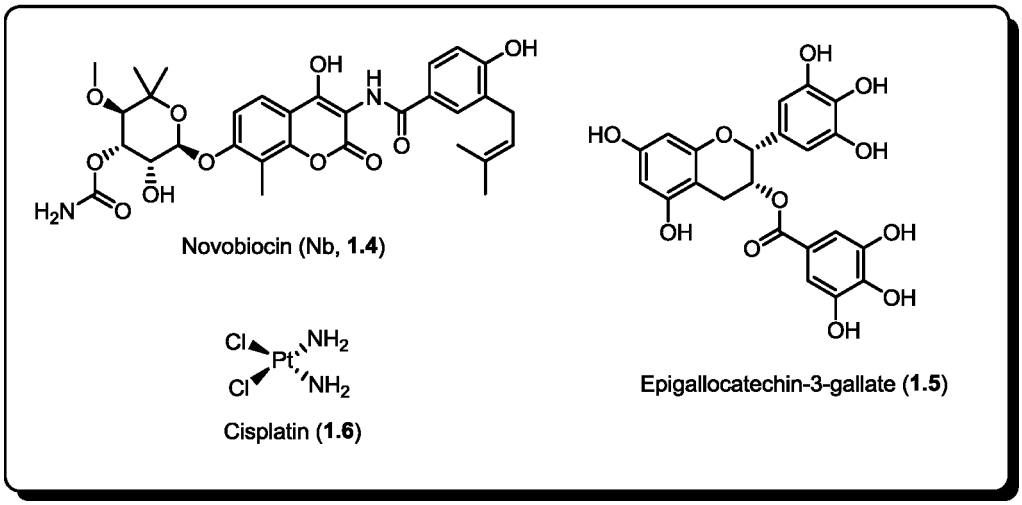

Figure 1.3: Examples of some traditional Hsp90 *C*-terminal inhibitors.

1.1.2. Hsp90 as a drug target

As a molecular chaperone, Hsp90 is principally involved in the folding and maturation of newly synthesised polypeptides into fully functional proteins.[2] These proteins are structurally and functionally diverse; a vast majority are signal transduction and transcription factors and regulatory kinases all of which are essential for normal cell growth.[12] Thus, Hsp90 forms a global hub of cellular processes. A wide variety of Hsp90 client proteins are involved in crucial cellular processes such as signal transduction, cellular trafficking, chromatin re-modelling, cell growth, differentiation, and reproduction, cell growth and, more importantly, maintaining normal cellular function.[6, 12] Disrupting the function of Hsp90 subsequently leads to proteasomal degradation of its client proteins suggesting that the processes in which they are involved will in turn be affected. The effects of Hsp90 blockade are far-reaching and detrimental for the cell, and include induction of cell apoptosis and cell arrest.[12] Hence, Hsp90 has been immensely explored as an attractive therapeutic target for many diseases, from neurodegenerative disorders[13] and cancer to parasitic diseases such as malaria. The following sections discuss the roles of Hsp90 in cancer and malaria, and its exploration as a drug target for the two diseases.

1.1.2.1. Hsp90 inhibition for anticancer activity

Cancer is a global problem and one of the leading causes of mortality worldwide. In 2012 alone, there were 14 million reported cancer cases and 18.2 million cancer-related deaths.[14] By definition, cancer is a disease or a collection of diseases caused by uncontrolled division of cells which clump together to form malignant tumours. These cells are invasive and can spread to other parts of the body, leading to more formation of tumour cells that are capable of growing in any part of the body that can produce tissues. One of the most significant factors that make cancer such a dreadful disease is the development of tenacious malignant tumours against therapeutic agents in clinical use for treatment of the disease.[15] Thus, there is a medical need for expansion of the anticancer drug arsenal targeting innovative therapeutic targets.

In 2004, Hanahan and Weinberg in their critical review described the six hallmarks of cancerous cells.[16] These hallmarks include: i) self-sufficiency in growth signals, ii) insensitivity to growth inhibition, iii) evasion of cell apoptosis, iv) limitless replicative potential, v) sustained angiogenesis, and (vi) tissue invasion and metastasis. Thus, an effective anticancer agent should ideally affect all the six hallmarks of cancer. Classical anticancer chemotherapeutics act by targeting proteins associated with at least one, but not all, of these hallmarks.[15]

As an integral component of protein folding complexes, Hsp90 is known to play a pivotal role in the manifestation of all six cancer hallmarks. Indeed, a number of Hsp90 client proteins are associated with each of the six hallmarks as illustrated in **Table 1.1** below.[17, 18] Since inhibition of Hsp90 induces degradation of client proteins, Hsp90 is logically the most promising target for design and development of anticancer therapeutics that are capable of simultaneously disrupting all six cancer traits with minimal incidences of development of drug resistance.

Table 1.1: Hsp90 client proteins associated with the hallmarks of cancer.

Cancer hallmark	Client Protein
i. Self-sufficiency in growth signals	Raf-1, AKT, Her2, MEK, Bcr-Alb, ErbB-2, Src, AKT, MEK
ii. Insensitivity to growth inhibition	CDK4, CDK6, Plk-1, Myt-1, cyclin D
iii. Evasion of cell apoptosis	RIP, AKT, mutant p53, AKT, c-MET, Apa-1, Survivin, Bcl2, IGF-IR
iv. Limitless replicative potential	Telomerases: h-TERT and α-TERT
v. Sustained angiogenesis	FAK, AKT, Hif-1α, VEGFR, Flt-3, Src
vi. Tissue invasion and metastasis	c-MET, MMP-2

Numerous Hsp90 inhibitors have been investigated as potential anticancer agents.[19, 20] In 2014, there were 13 structurally diverse Hsp90 inhibitors undergoing clinical evaluation as anticancer chemotherapeutics.[17] A vast majority of these inhibitors is dominated by *N*-terminal inhibitors. The *N*-terminal inhibitor of Hsp90, 17-allylamino-17-desmethoxygeldanamycin (17-AAG), a derivative of **1.2**, is amongst the first generation of Hsp90 inhibitors to be demonstrated to possess high antitumour efficacy that reached phase I clinical trials under the name Tanespimycin®.[21]

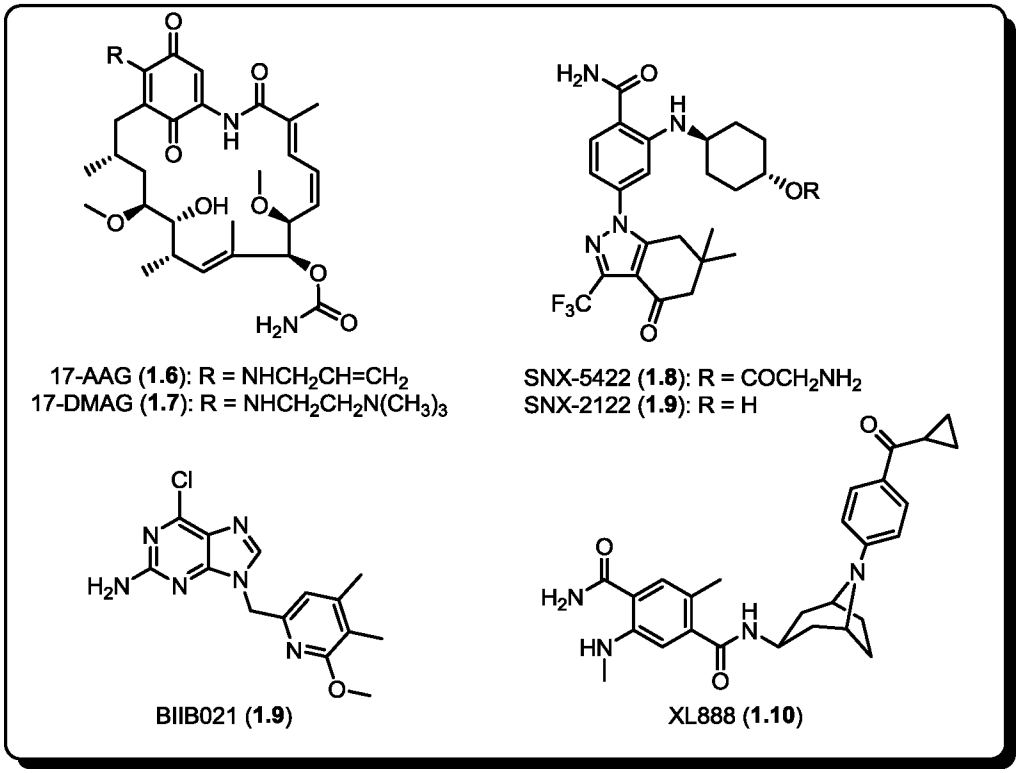

Figure 1.5: Some of Hsp90 *N*-terminal inhibitors that have reached clinical trials for treatment of cancer.

However, progression of this drug to phase I/II clinical development was halted by its sponsor, Bristol-Myers Squibb, possibly due to financial constraints.[17] Other *N*-terminal inhibitors undergoing clinical evaluation are shown in **Figure 1.5**. On the other hand, the *C*-terminal inhibitors of Hsp90 are increasingly attracting interest as potential anticancer agents. Among *C*-terminal inhibitors explored for anticancer activity, analogues of Nb are the most studied (**Figure 1.6**).[17, 22-24] Although none of these have entered clinical trials, they have been demonstrated *in vitro* to effectively supress tumour cells with impressive potency.

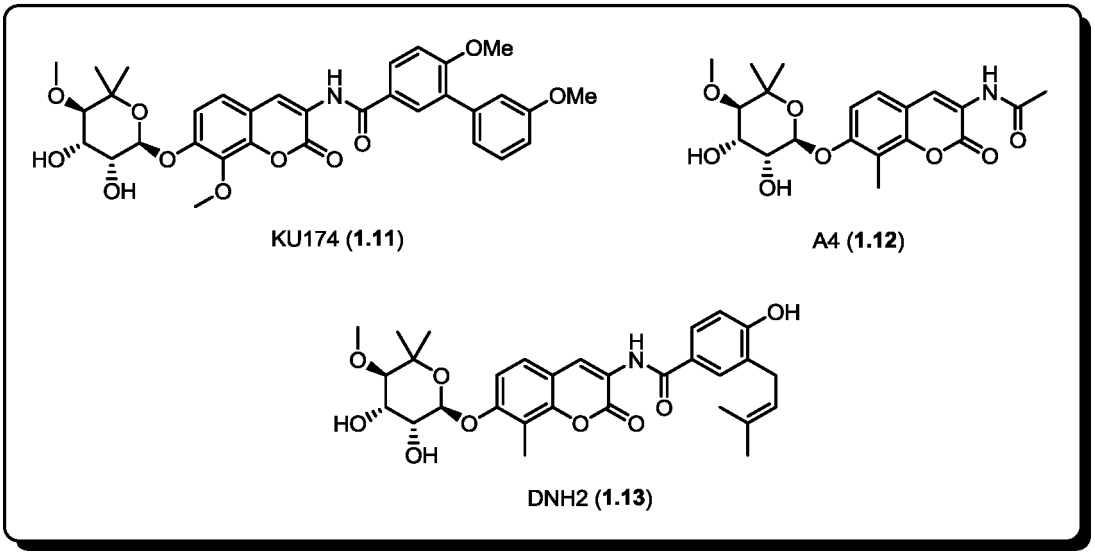

Figure 1.6: Novobiocin analogues explored as Hsp90 *C*-terminal inhibitors.

1.1.2.2. Hsp90 inhibition for antimalarial activity

Malaria is caused by a *Plasmodium* parasite transmitted through a bite by the *Anopheles* female mosquito. Of the five *Plasmodium* species that infect humans, *Plasmodium falciparum* (*P. falciparum*) is the most burdensome due to its high tenacity as a result of resistance to clinical drugs used for treatment of malaria. Despite the recent successes and average global decline of malaria infections over the last 15 years, malaria still remains a life-threatening disease globally, which claimed about half a million deaths in 2015.[25] Resistance to traditional antimalarial therapeutics (**Figure 1.7**), including the highly active artesunate, poses a great socio-economic burden especially to developing countries in tropical and subtropical regions.[26, 27]

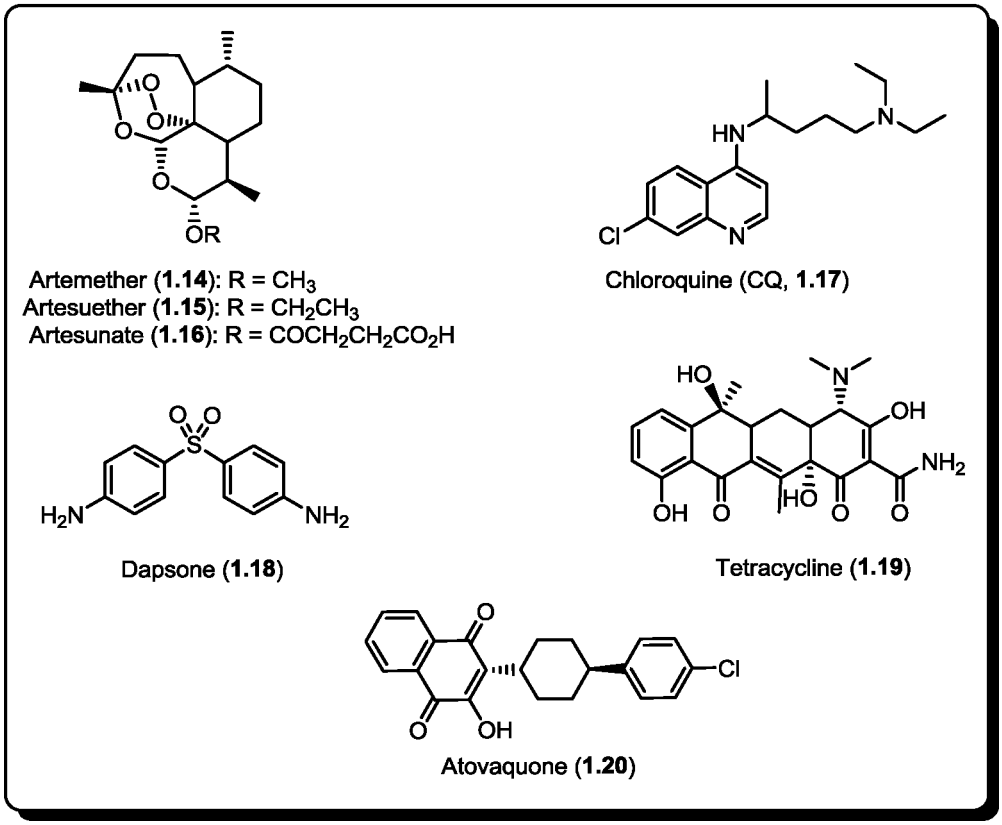

Figure 1.7: Representative examples of traditional antimalarial chemotherapeutics.

To address resistance, the World Health Organisation (WHO) implemented the use of artemisinin-combination therapies (ACTs) in 2001 to treat uncomplicated malaria in endemic regions where antimalarial resistance is prevalent.[28] ACTs employ a combination of two antimalarials with different modes of action: a long-lived non-artemisinin drug and a short-lived artemisinin-based drug, which work synergistically to eliminate the parasite.[28] Undoubtedly, ACTs proved effective as they significantly reduced malaria incidences and mortalities in endemic regions since their introduction.[25] However, development of artemisinin resistance by *P. falciparum* in 2009 has put ACTs under a great threat as an effective antimalarial regimen.[26, 27] Development of resistance in antimalarial drugs is associated with genetic mutations in the drug targets and pathways on which the drug acts, which alter the phenotype of the parasitic cell as to circumvent the lethal effects of a drug used for treatment of the disease.[29] Typical examples of targets and/or pathways on which traditional antimalarials act include: the purine salvage pathway, pyrimidine biosynthesis pathway, apicoplast processes and hemozoin formation.[29] With ACTs currently at the verge of facing full-blown antimalarial resistance, the quest for antimalarial drugs which act against novel targets could counter the issue of resistance, and thus their investigation is of imminent importance.

As a highly conserved protein across species, Hsp90 is ubiquitously expressed in *P. falciparum* and plays a vital role in the development of the parasite, especially during the asexual growth stages of the parasite's erythrocytic life cycle during its tenure in the human host.[30-33] Studies by Banumathy *et al.* confirmed the significance of *Pf*Hsp90 in the parasite's development by demonstrating that the *N*-terminal Hsp90 inhibitor GA (**1.2**) could repress *P. falciparum* growth *in vitro* by arresting transitions from the trophozoite stage to ring stage of the parasite's life cycle (**Figure 1.8**, (**5**)).[30] Additionally, *Pf*Hsp90 is more expressed in the parasite than in the human host cells during the erythrocytic stages (**Figure 1.8**, (**B**)), suggesting the importance of the chaperone in growth and development of the parasite.[30] It has also been postulated that since *Pf*Hsp90 plays a pivotal role in survival of the parasite, it mediates the mechanisms that allow the parasite to survive in stressful environments like drug-induced stress, thereby potentiating drug resistance.[31] Indeed, Hsp90 is implicated in CQ (**1.7**) resistance by interacting with the CQ-resistance-associated protein, Cg4.[34]

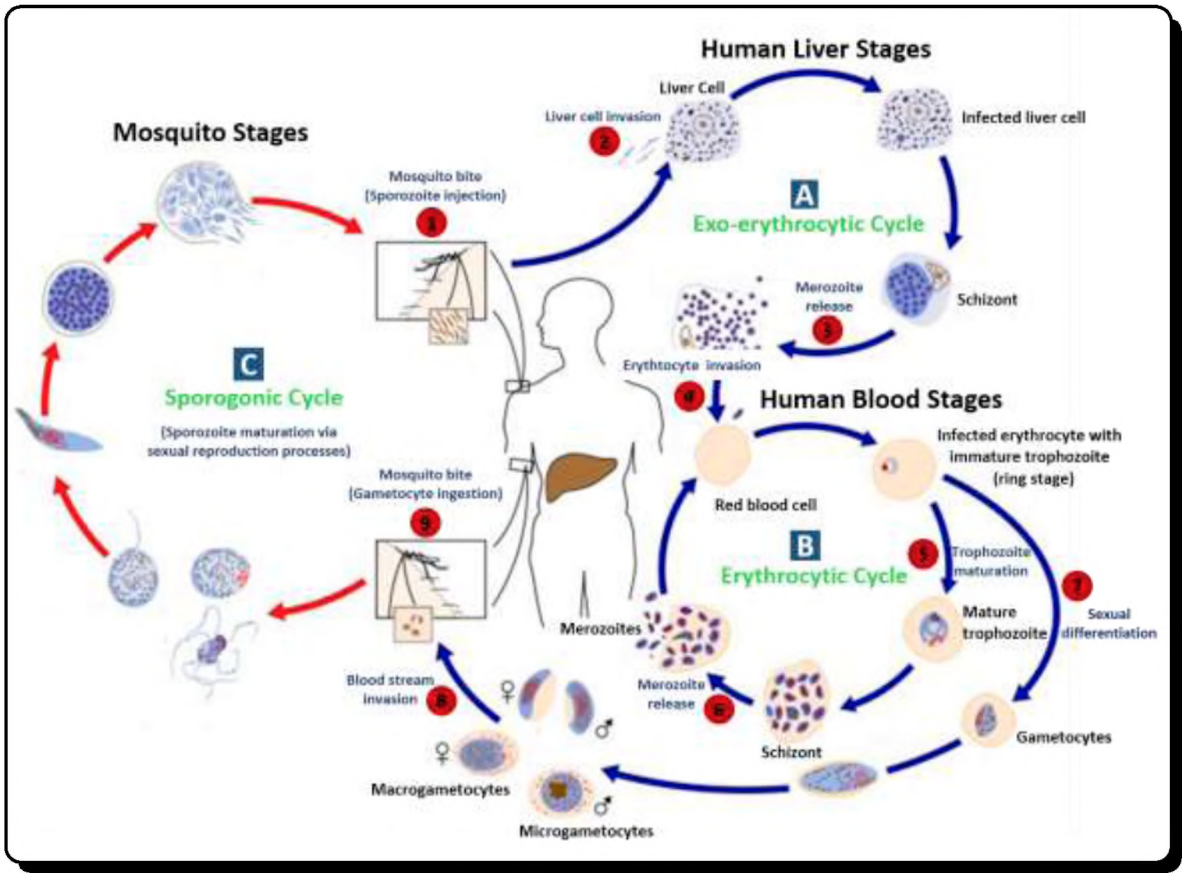

Figure 1.8: Life cycle of Plasmodium falciparum parasite.[35]

Various Hsp90 inhibitors have been studied for antimalarial activity, including *C*-terminal inhibitors Nb and **1.6**.[31, 32, 36-39] Some inhibitors have been shown to restore the efficacy of

previously ineffective traditional antimalarials.[31, 32, 36-39] Evidently, Hsp90 is a promising target for exploration of its inhibitors as antimalarial agents. Nevertheless, there is still little knowledge regarding structure-activity relationship (SAR) profiles of *Pf*Hsp90 inhibitors for antimalarial activity.

Despite the limitations associated with *N*-terminal inhibitors that have reached clinical evaluation for treatment of cancer, a majority of Hsp90 inhibitors investigated for antimalarial activity target the same *N*-terminal ATP-binding site of the chaperone. On the other hand, there is little evidence in literature about exploration of *C*-terminal Hsp90 inhibitors as potential antimalarial agents, which could circumvent issues related with *N*-terminal inhibition. Insights into Hsp90 *C*-terminal inhibition could lead to viable solutions to antimalarial resistance, and could possibly restore the efficacy of traditional antimalarial drugs if used in combination with *C*-terminal inhibitors.

1.2. MEDICINAL CHEMISTRY OF NOVOBIOCIN: CANCER AND MALARIA

Novobiocin (Nb, **1.4**) is a naturally occurring antibiotic of the coumarin family of antibiotics that was first isolated from *Streptomyces* strains and described in mid-1950s as the first antibiotic in its class.[40] Other coumarin type antibiotics, which are also isolable from the same strains, are coumermycin A_1 (**1.21**) and clorobiocin (**1.22**) (**Figure 1.9**). Besides its antibiotic activity, Nb has also been screened for anticancer and antimalarial activity. This section reviews the biological properties of Nb, its application as an antiseptic and its exploratory studies in malaria and cancer.

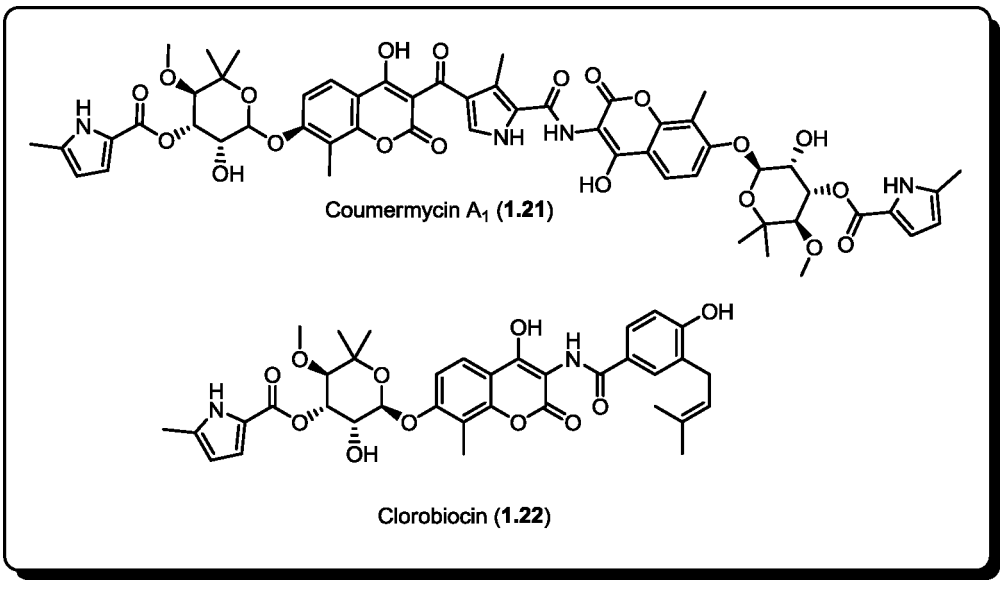

Figure 1.9: Chemical structures of coumermycin A_1 (**1.21**) and clorobiocin (**1.22**).

1.2.1. Biological activities of novobiocin

Since its discovery, the medicinal chemistry of Nb has been primarily focused on treatment of bacterial infections. Similarly, research on Nb has been on improving its antibacterial efficacy through structural modifications.[41-46] It was not until 1988 that Nb was exclusively tested for activity other than antibacterial by Bia and co-workers who screened fluoroquinolone antibiotics in parallel with Nb for potential antimalarial activity *in vitro*.[47] Prior to this, Nb had only been investigated in combination with known antimalarial drugs that had become ineffective in an attempt to restore their efficacy. Despite its modest repressive effects on *Plasmodium* parasite growth, there has been limited literature on structural modifications of Nb to improve its antiplasmodial activity. Apart from malaria, Nb has also been shown to suppress tumour cell growth through inhibition of Hsp90 by the research group of Neckers.[48] This discovery prompted research into further structural modifications of Nb to identify novel analogues with improved Hsp90 inhibitory effects for better antitumour efficacy. The following sections describe the activity and investigation of Nb as an antibacterial, antiplasmodial and antitumour agent.

1.2.1.1. Antibacterial activity of novobiocin

Nb has been applied to treat infections caused by *Staphylococci* bacterial strains since its approval in 1964 as an oral antibiotic under the trade name Albamycin®, which is a monosodium salt of Nb. Despite its period in the market as a reliable antibiotic, its clinical usage was discontinued in 2008 for efficacy or safety concerns.[49] The mode of action of Nb is associated with inhibition of the ATPase activity of the DNA gyrase enzyme. Indeed, Nb does inhibit the function of DNA gyrase.[50, 51] DNA gyrase is a bacterial type IIA topoisomerase that is integrally involved in DNA processes, namely: replication, transcription, catalysis of reactions pertaining DNA supercoiling and repair processes.[52] It consists of two subunits: GyrA and GyrB. Whilst GryA is involved in breaking and relinking DNA strands and DNA-protein interactions, GyrB facilitates the binding of gyrase to DNA. This enzyme is vital for normal bacterial cell growth.

Other coumarin type antibiotics, including **1.21** and **1.22**, have also been reported to target this enzyme.[51] As with Hsp90 blockade, interruption at either subunit of DNA gyrase induces cytostatic effects to the cell. Nb and other coumarin-based inhibitors of gyrase (**Figure 1.11**) bind to the GyrB subunit of the enzyme and inhibit its ATPase activity.[51] This is the proposed mode by which Nb and related antibiotics work for treatment of *Staphylococci* infections.

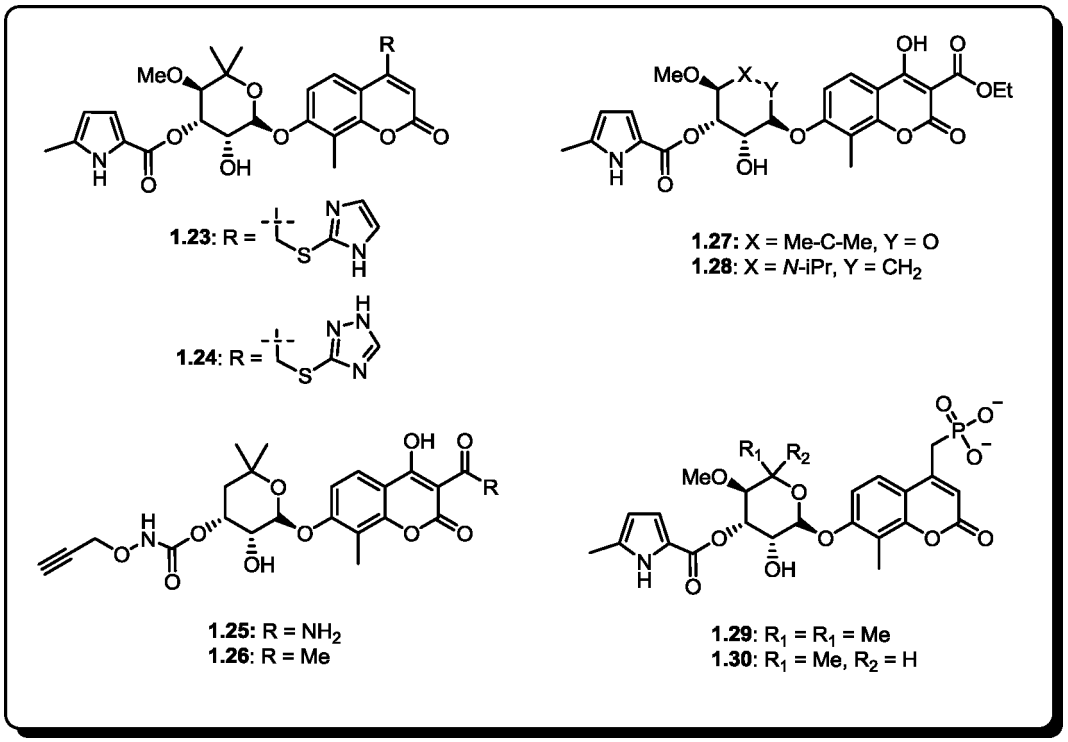

Figure 1.11: Other DNA gyrase B inhibitors containing coumarin scaffold.[42-46]

1.2.1.2. Antiplasmodial activity of novobiocin

Antimalarial activity of Nb first came into light in 1988 when Bia *et al.* investigated the antiplasmodial effects of fluoroquinolone antibiotics in parallel with Nb (**1.4**) and coumermycin A_1 (**1.21**) against two strains of *P. falciparum*, FCC_1 (CQS) and VNS (CQR) strains.[47] Both **1.4** and **1.21** were found to possess modest antimalarial activity against both strains. The IC_{50} values after 48 hours of exposure were 28 and 21 μM for Nb and 28 and 6 μM for coumermycin A_1 against FCC_1 and VNS strains, respectively (**Table 1.2**).

Table 1.2: IC_{50} values of Nb and coumermycin A_1 against FCC_1 and VNS strains of *P. falciparum* strains.[47]

Coumarin Antibiotic	IC50 (μM)	
	FCC_1	VNS
Nb	28	21
Coumermycin A1	28	6

The plausible mechanism of in vitro antimalarial effects of the tested antibiotics was not investigated. However, both types of antibiotics, i.e. fluoroquinolone and coumarin types, are known to possess inhibitory activity against DNA gyrase.[53] The plausible mode of action of Nb for antiplasmodial activity remained unclear until recently when it was discovered by the group of Habib that Nb targets the DNA gyrase B subunit of the *P. falciparum* parasite (*Pf*GyrB) expressed in *E. coli*.[54] In their study, Nb strongly inhibited the ATPase activity of *Pf*GyrB with the inhibition constant (K_i) of 1.24 μM. Furthermore, the downstream effects of Nb were investigated. The study revealed that Nb repressed DNA replication in the apicoplast of the parasite, whilst mitochondrial DNA replication was not significantly affected. The apicoplast is a validated target for development of antimalarial agents.[55] These findings unequivocally demonstrated Nb to be an interesting lead for design and development of novel antimalarial agents by disrupting the apicoplast DNA replication machinery through inhibition of *Pf*GyrB.

Despite the lack of derivatives of Nb that have been investigated against the *P. falciparum* parasite, there are other coumarin derivatives, though not based on Nb scaffold, that have been investigated for antimalarial activity (**Figure 1.18**).[56-63] These have been demonstrated to suppress *in vitro* the growth of both CQ-sensitive and -resistant strains of the *P. falciparum* parasite. Some have also been investigated *in vivo* and shown to have unfavourable effects against malaria.[61-63] It is important to note that, unlike Nb and its analogues, none of these coumarin compounds have been shown to exhibit antimalarial activity that is associated with inhibition of Hsp90 function. In all instances of the synthetic antimalarial coumarins (**1.52-1.57**) in **Figure 1.18**, the coumarin moiety principally serves as a backbone scaffold to which other pharmacophoric units (e.g trioxane, pyrozoline, chalcone) are appended.

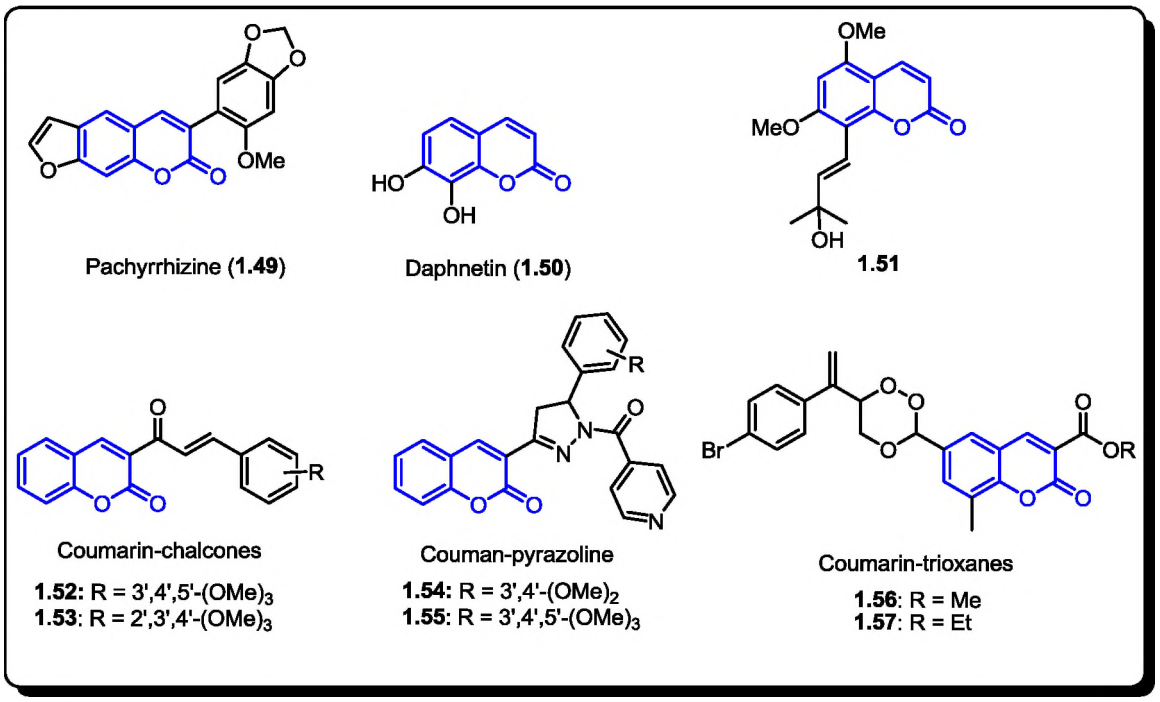

Figure 1.18: Some naturally occurring (**1.49-1.51**) and synthetic (**1.52-1.57**) coumarin-containing compounds possessing antimalarial activity.

1.2.1.3. Antitumour activity of novobiocin

For decades the anticancer activity of Nb remained unknown until the beginning of the twenty-first century. In 2000, Neckers and co-workers sought to investigate the anticancer and Hsp90 inhibitory activities of known DNA gyrase B inhibitors: Nb, clorobiocin and coumermycin A_1, with specific focus on Nb.[48] This study was inspired by the intriguing similarities in homology between the *N*-terminal ATP-binding pockets of Hsp90 and bacterial DNA gyrase. As highlighted in **Section 1.1.1** the structurally diverse antibiotics, **1.1** and **1.2**, are known to competitively bind to the *N*-terminal ATP binding pocket of Hsp90 and deplete the chaperone, and thus induce antitumour activity in cancerous cells.

Neckers *et al.* proposed Nb and other coumarin antibiotics (**1.21** and **1.22**) that inhibit DNA gyrase could inhibit Hsp90 in a similar manner as **1.1** and **1.2**, and thus induce anticancer activity. As expected, Nb and related antibiotics (**1.21** and **1.22**) inhibited the ATPase activity of Hsp90 and induced the depletion of Hsp90 client proteins: Raf-1, $p185^{erbB2}$, mutant p53, and $p60^{v\text{-}src}$. Interestingly, when Nb and non-coumarin inhibitors (**1.1** and **1.2**) were investigated to ascertain whether both types of inhibitors bound Hsp90 in a similar manner, Nb was found to bind to a different fragment (designated 2Δ, with 380 – 728 amino acid residues) of Hsp90 located at the *C*-terminus of the protein. The non-coumarin inhibitors, **1.1** and **1.2**, on the other

hand did not bind to this fragment, but instead to an *N*-terminal fragment corresponding to the *N*-terminal ATP-binding pocket of Hsp90. These findings suggested that Nb binds to a putative *C*-terminal ATP-binding pocket to induce its anticancer activity.

Since the recognition of this putative ATP-binding pocket, there have been numerous studies that have focused on probing the *C*-terminal ATP-binding pocket of Hsp90.[64-68] Similar studies, spearheaded by the research group of Blagg have focused on the design, synthesis and development of Nb analogues as potential anticancer therapeutic agents through inhibition of Hsp90. In the following section, investigation of Nb analogues as potential anticancer agents through *C*-terminal Hsp90 inhibition is discussed.

1.3. NOVOBIOCIN ANALOGUES WITH ANTITUMOUR ACTIVITY

The discovery of Hsp90 inhibitory activity of Nb by Marcu and co-workers attracted immense interest to investigate compounds based on the scaffold of Nb, i.e. novobiocin analogues, as potential therapeutic agents to treat cancer. With the limitations of associated with inhibiting the Hsp90 *N*-terminus, Nb analogues as Hsp90 *C*-terminal inhibitors are increasingly gaining more interest as alternative means of disrupting Hsp90 function for potential anticancer activity.

Neckers and co-workers demonstrated that Nb possessed modest anticancer activity against the SkBr3 cancer cell line with IC_{50} of ~700 μM.[48] Different research groups have since explored structural modifications of Nb in the search of novel Nb analogues with better Hsp90 inhibitory activity and anticancer efficacy. The first library of Nb analogues with better efficacy was first reported by the research group of Blagg.[22] **Figure 1.13** summarises the key structural modifications in this library of compounds.

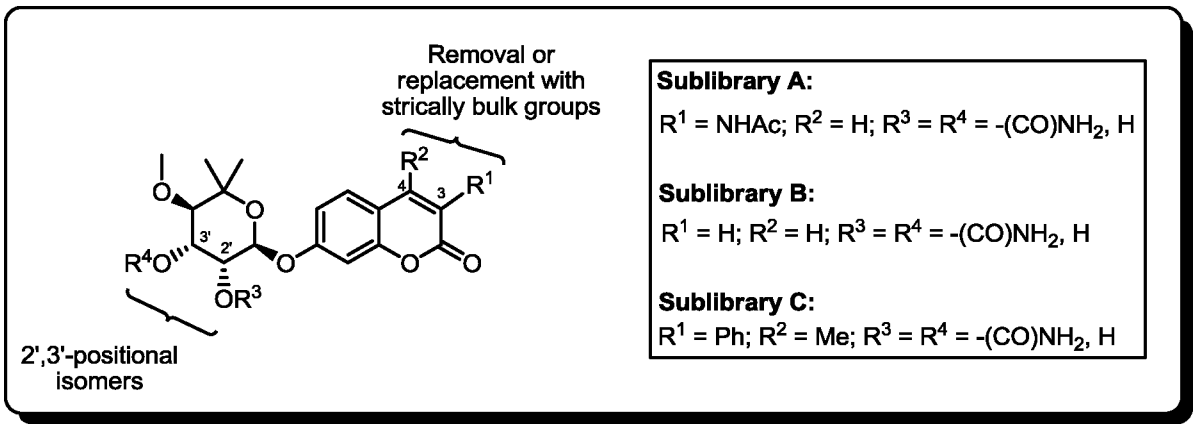

Figure 1.13: First library of Nb analogues designed for improved efficacy.

The most active analogue in the whole library was identified from **Sublibrary A** (**Figure 1.13**) and consisted of the *N*-acetyl motif in place of the benzamide side chain, and was devoid of both 4-hyroxyl and 2',3'-carbamoyl groups. This analogue, designated A4 (**1.12**) (**Figure 1.6**), severely degraded phospho-AKT (an Hsp90 client protein) in SKBr3 cells upon incubation with the concentration of 100 μM. This, in addition to the reduction of Hsp90-dependent androgen receptors, AKT and Hif-1α, at ~1 μM concentration of A4 (**1.12**) indicated effective inhibition of Hsp90 by the compounds A4 **Figure 1.14**).

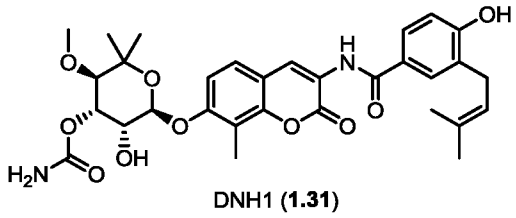

DNH1 (**1.31**)

Entry	MIC for client protein depletion (μM)
A4	~ 1
DNH1	5
DNH2	0.1

Figure 1.14: First generation of Nb analogues with antitumour activity through Hsp90 inhibition.

These findings provided the first meaningful preliminary SAR data of Nb analogues: the 4-hydroxyl and carbamoyl groups reduced efficacy of Nb analogues. To verify these findings a second library of Nb analogues was prepared.[23] This library was similar to the first library in all aspects except the 8-methyl and benzamide side chain groups were retained as in the parental compound, Nb. Two analogues, one with 3'-carbamoyl (DHN1, **1.31**) and one without (DHN2, **1.13**) were evaluated for Hsp90 inhibition and anticancer activity (**Figure 1.14**). Indeed, the results confirmed the initial findings: the presence of carbamoyl appeared to retard anti-Hsp90 activity of the prepared analogues.

Another class of Nb analogues that had been investigated for improved activity contained bulky structural moieties as replacements of the benzamide appendage. Both research groups of Blagg and Alami were independently at the forefront of these investigations.[24, 69-72] In this class of Nb analogues, replacement of the benzamide with bulky substituents appeared to be favourable for anticancer and Hsp90 inhibitory efficacies of the analogues. The main focus of Blagg and co-workers was on the replacement of the benzamide with aryl, biaryl and fused heterocycle ring groups to probe the bonding capabilities of the putative hydrophobic pocket

into which the benzamide of Nb presumably projects when bound to the *C*-terminal ATP-binding pocket of Hsp90 (**Figure 1.15**).[24, 69] As with the first library of Nb analogues, the new library was devoid of 4-hydroxy and 3'-carbomoyl groups.

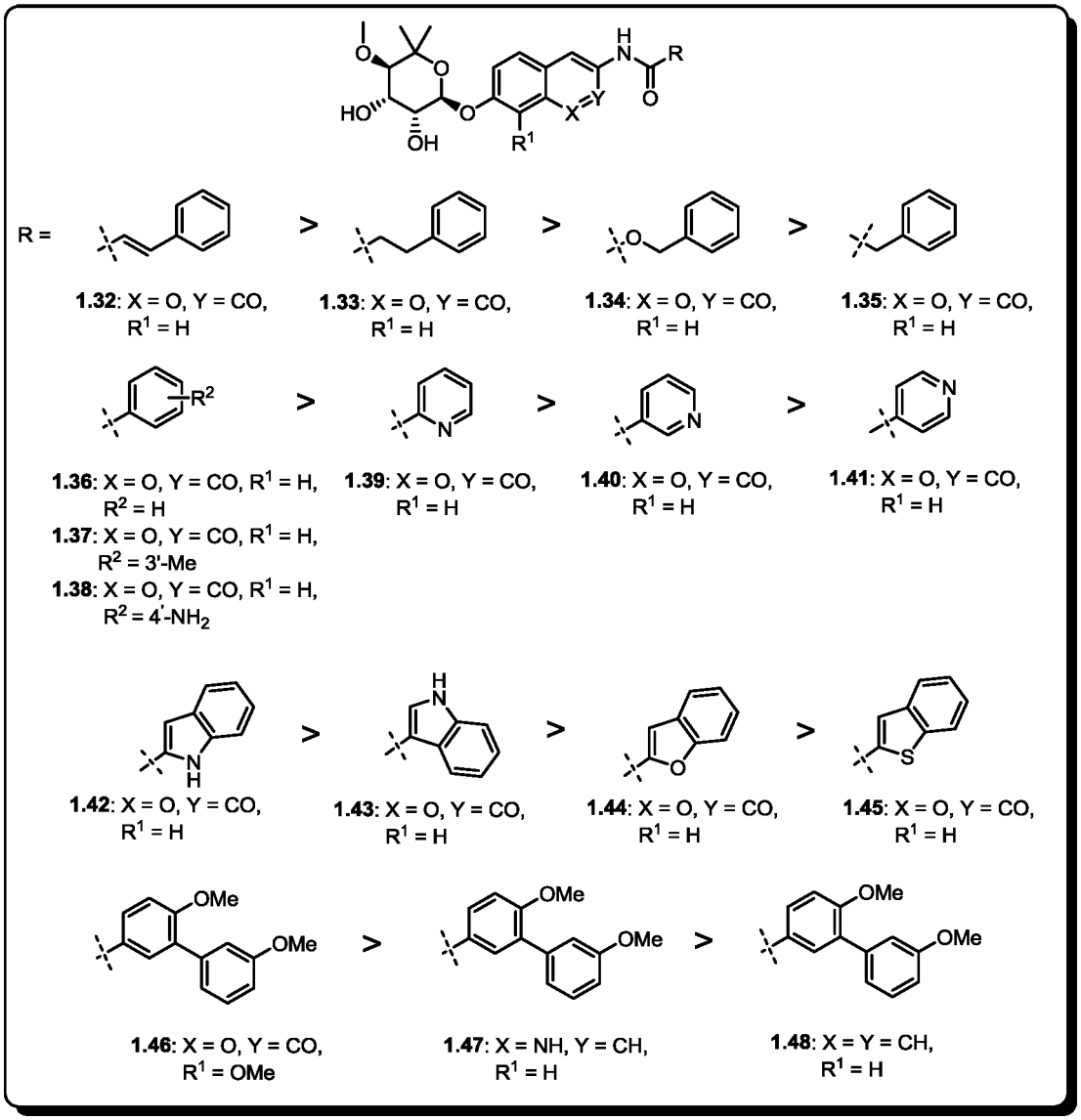

Figure 1.15: Second generation of Nb analogues.

The presence of bulky groups was found to augment the efficacy of Nb analogues for anticancer and Hsp90 inhibitory activity. In the biaryl series, compound KU174 (**1.11**) possessed the most efficacy, whilst **1.42** had greatest activity in the indole series (**Figure 1.15**). These findings suggested that the hydrophobic pocket of the ATPase site of the HSp90 *C*-terminal is tolerant of bulky moieties for better binding affinity and increased anticancer activity. On the other hand, the lactone moiety was found to be important for participation in H-bonding interactions with amino acid residues from the *C*-terminal Hsp90 ATPase pocket. Interestingly, the

quinoline (**1.47**) and naphthalene **(1.48)** variants exhibited similar, but lower, activities as the coumarin derivatives. These results suggested that the lactone functionality was favourable but not necessary for activity, and thus dispensable.

Investigations by Alami and co-workers corroborated the findings by Blagg *et al*: bulky functional groups in place of benzamide chain favour the efficacy of Nb analogues.[70-72] Similarly, these investigations focused on: 1) replacement the benzamide chain with bulkier groups and 2) removal or replacement of the noviose appendage with simpler structural motifs (**Figure 1.16**). More importantly, these findings revealed that the noviose sugar moiety could be replaced with simpler motifs whilst retaining activity since some of the analogues devoid of noviose structure showed impressive anticancer and Hsp90 inhibitory activities. It is important to note, however, that the hydroxyl groups of the noviose sugar were found to be favourable for interactions with Hsp90.

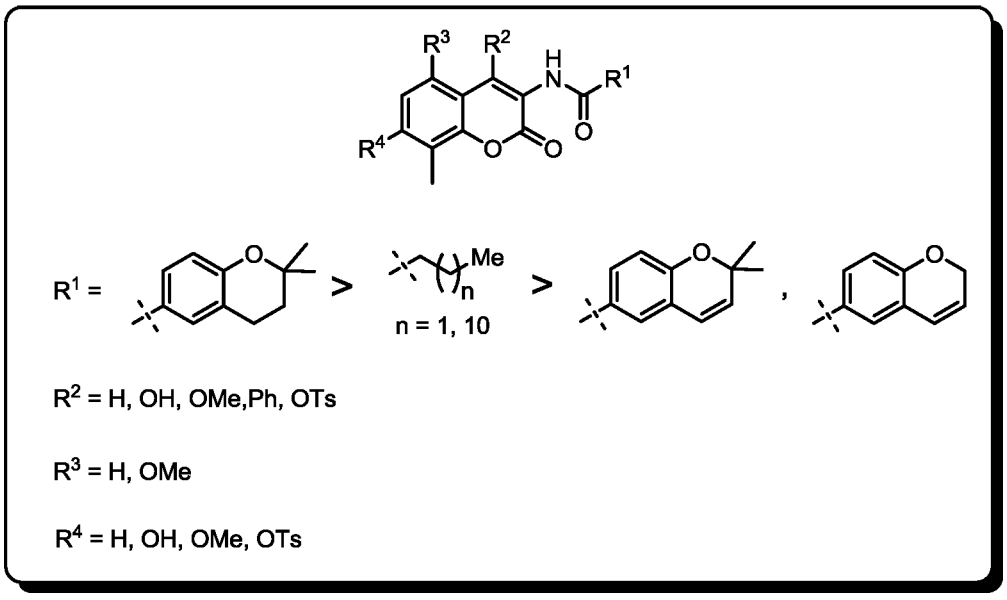

Figure 1.16: Non-noviose Nb analogues with bulky benzamide replacements.

Findings by Alami *et al*., revealed that the noviose sugar was not requisite for antiproliferative and Hsp90 inhibitory activity of Nb analogues.[70-72] Consequently, Blagg and co-workers prepared a library of Nb analogues with simpler structural motifs as replacements of the synthetically complex noviose sugar.[73-78] The simplified replacements consisted of amine-containing groups (*viz*. acyclic amines and piperidines), sugar based derivatives (*viz*. dehydroxylated, mono- and di-hyroxylated furanose and paranose sugars), phenyl derivatives and other miscellaneous groups favourable for solubility (**Figure 1.17**).[73-78] The results

emanating from this study confirmed that the activity was retained for Nb analogues lacking the noviose moiety: *des*-noviose analogues had similar activities to noviosylated analogues.

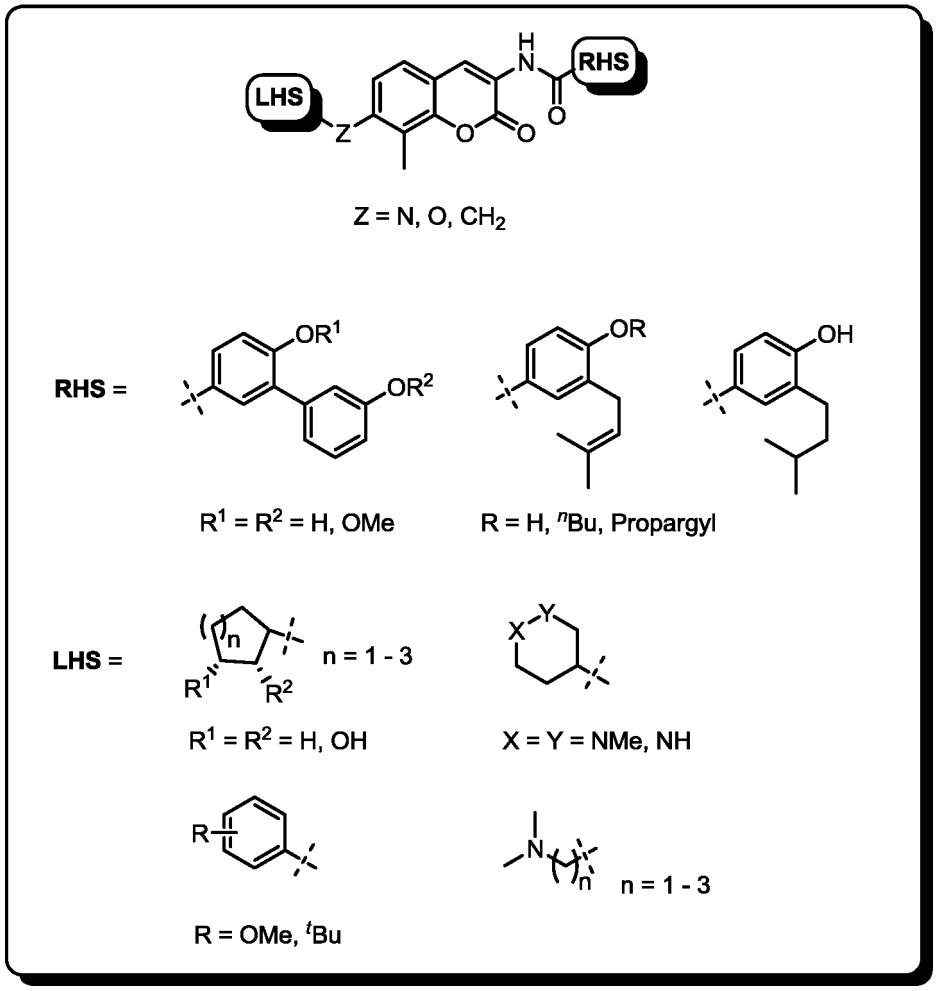

Figure 1.17: Simplified des-noviose Nb analogues with retained efficacy.[73-78]

1.4. MEDICINAL CHEMISTRY OF FERROCENE AND ITS DERIVATIVES

Ferrocene (Fc) is a synthetic organometallic complex which was first discovered in 1951[79] and its structure confirmed and disclosed in 1952.[80, 81] It was discovered by serendipity when Kealy and Pauson attempted to prepare fulvalene (i.e. bicyclopentadienylidene) from cyclopentadiene magnesium bromide in the presence of iron(III) chloride as a catalyst, but instead formed dicyclopentadienyl iron (i.e. ferrocene) as the major product.[79] Although Fc was not the first organometallic complex ever made at the time of its discovery, it was the first metallocene to be synthesized. Metallocenes are a class of organometallic compounds characterized by a "sandwich" structure comprising a central metal atom that is connected via covalent metal-carbon bonds to two cyclopentadienyl (Cp) anion rings on opposite sides of the metal (**Figure 1.19**). More interestingly, the discovery of Fc accented the field of bioorganometallic

chemistry, and many other metallocenes and their derivatives have since been synthesized and shown to possess antitumour activities.[82, 83]

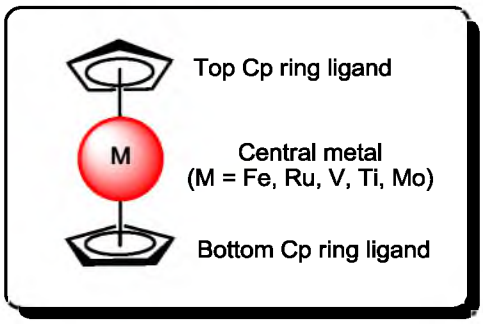

Figure 1.19: Representative structure of a metallocene.

Amongst metallocenes, Fc is notably of most important medicinal interest in the fields of medicinal and biorganometallic chemistry due to its broad spectrum of remarkable properties. These include high aromaticity, high chemical stability, favourable redox behaviour, ability to form reactive oxygen species (ROS) and absence of cytotoxicity in human cells.[84, 85] These properties have rendered Fc and its derivatives appealing in medicinal inorganic chemistry and drug discovery fields. There have been numerous endeavours to tailor various bioactive organic compounds to Fc-bearing derivatives possessing different biological activities against a number of diseases from cancer to parasitic infections. Most notable example of such endeavours is the development of ferroquine (FQ, SSR97193), which is currently in phase II clinical evaluation (in combination with artesunate (**1.16**)) as the first antimalarial drug containing the Fc moiety.[86]

Fc has a redox potential of –0.54 V and can undergo anaerobic oxidation in the presence of strong acids, halogens or salts such as ferric chloride, silver and ceric sulphate.[80] Its oxidation is reversible without major structural alterations. This is effected anodically at the central Fe(II) atom, which gets oxidized to Fe(III), essentially rendering the whole molecule cationic to form a water soluble ferrocenium ion. Fc in its neutral form is insoluble in water, but readily soluble in most organic solvents. The moderate ease of oxidation of Fc together with its low aqueous solubility and high aromaticity have significant implications on the physicochemical and medicinal properties of the compound.

1.4.1. Incorporation of ferrocene into bioactive chemical scaffolds

Ferrocene is regarded as a privileged structure in the medicinal chemistry context. First, the non-toxicity of Fc, high lipophilicity and favourable pharmacokinetic properties immediately

make Fc appealing for incorporation into bioactive chemical scaffolds in the design and development of small molecules with drug-like properties. Second, the presence of Cp rings on opposite sides of the tightly bound central iron metal imparts aromaticity, thickness and rigidity into the molecule. Thus, the Fc moiety can bind to a variety of biomolecules such as nucleic acids (DNA and RNA), lipids and proteins, and it can fit into and block many enzyme active sites.[87, 88] Third, the low redox potential of Fc allows ease of oxidation of Fe(II) metal to Fe(III) by O_2, forming cytotoxic ferrocenium ions with concomitant generation of highly reactive oxygen species (ROS), such as hydroxyl ($^{\bullet}OH$) and superoxide anion radicals.[82, 83] These radicals are disruptive to the targeted biological cells.[82, 83] The role of the Fc moiety in biologically active Fc-containing compounds is best presented in the mechanism of action of FQ (antimalarial agent), which exhibits a dual mode of action for antimalarial activity in which Fc moiety plays a crucial role.

FQ is a highly active antimalarial compound developed by Sanofi-Aventis and is currently in phase II clinical trials.[86] It is more potent than chloroquine (CQ) and is active against a panel of chloroquine-resistant *P. falciparum* strains.[89] It has been proposed that its mechanism of action resembles that of CQ by causing the accumulation of toxic heme in the *Plasmodium* cell and forming a highly toxic heme-CQ complex.[90] Both processes are supposed to disrupt the cell membrane function of the parasite, leading to its death.[90] Heme is a soluble, toxic by-product that forms during digestion of host cell haemoglobin by the parasite for nourishment. To prevent cell disruption by this toxic molecule, the parasite biocrystallizes heme into non-toxic and insoluble haemozoin crystals. These crystals collect in the putative digestive vacuole of the parasitic cell. Following diffusion of CQ into the acidic food vacuole (pH 5.2), the molecule gets diprotonated to CQ^{2+}, which binds hemozoin to prevent further bio-crystallization of heme. This causes a massive accumulation of the toxic heme in the parasitic cells, which leads to cell death by disruption of the cell membrane function of the cell.

FQ is proposed to act in a similar manner. Indeed, FQ has been shown to bind β-hematin (synthetic hemozoin) even more effectively than CQ.[90] Inside the digestive vacuole, the diprotonated form of FQ (i.e. FQ^{2+}) has a smaller pK_a value than CQ^{2+}.[90] This would suggests low accumulation of FQ in the vacuole. However, FQ^{2+} adopts a closed conformation via "H-bond flip/flop" mechanism which exposes the Fc moiety, making the molecule more hydrophobic (**Figure 1.20**).[91] This offsets the implied effects of low pK_a and enhances interactions of the compound with hydrophobic membranes, hence its accumulation inside the vacuole.[91]

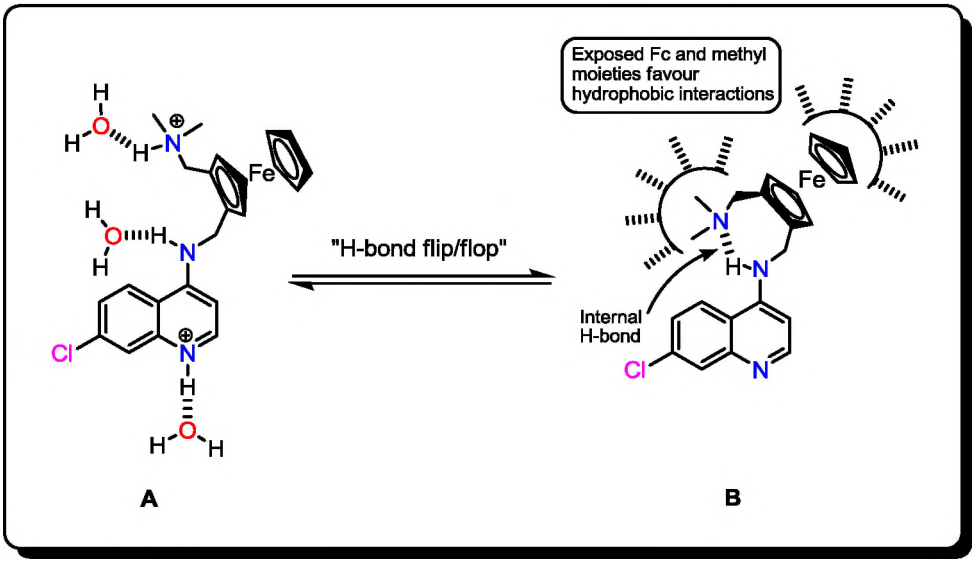

Figure 1.20: H-bond "flip/flop" mechanism illustrating open (**A**) and closed (**B**) conformers of FQ.[91]

High hydrophobicity of FQ^{2+} means low concentration of the drug in water. This circumvents transportation of the molecule by efflux transporters (associated with CQ resistance) to the exterior of the vacuole, retaining it in the targeted site.[91] High hydrophobicity of FQ^{2+} (owing to Fc) also allows it to bind to lipid structures at the catalytic sites of hemozoin formation. This could be an explanation for higher affinity of the drug for hematin, hence its impressive antimalarial potency.[92] In addition to hemozoin inhibition, FQ produces ROS, specifically $^{\bullet}OH$ radicals, which are degradative to the cell membrane of the parasite.[93] This is proposed to take place inside the digestive vacuole and requires hydrogen peroxide (H_2O_2). During oxidation by H_2O_2, the Fe(II) central atom gets converted to Fe(III), forming a ferrocenium ionic form of FQ and $^{\bullet}OH$ radicals (**Figure 1.21**).

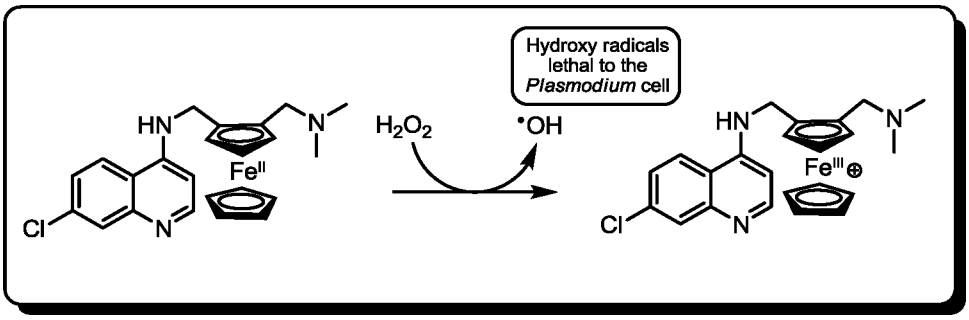

Figure 1.21: Proposed mechanism of FQ for production of hydroxyl radicals ($^{\bullet}OH$) by peroxidative oxidation inside the digestive vacuole of the *Plasmodium* parasite.

Great amounts of H_2O_2 are known to be expended in the peroxidative degradation of heme,[94] and would imply limited formation of $^{\bullet}OH$ radicals.[93] However, these radicals (in combination with hemozoin formation mechanism) are said to be enough to effect cell damage to the parasite regardless of the level of production. Roles of the Fc moiety in FQ and other biologically active Fc-containing compounds, i.e. ferrocifens, are summarised in **Table 1.3** below.

Table 1.3: Role of Fc moiety in known biologically active compounds.

Compound	Disease	Role of Fc	Ref.
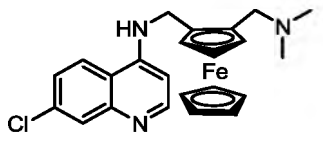 FQ	Malaria	i. Enhances activity. ii. Allows ease of compound to cross membrane to target site (digestive vacuole) iii. Targets catalytic site for hemozoin formation. iv. Retains compound in target site. v. Facilitates strong hematin binding. vi. Produces ROS.	90, 91
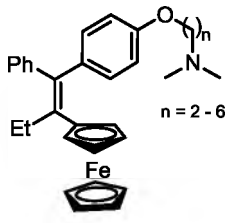 Ferrocifens	Cancer	i. Enhances activity ii. Allows ease of compound to cross membranes into tumour cells. iii. Allows binding to DNA. iv. Retains compound in target site. v. Produces ROS	84, 95

In summary, it is apparent from the discussion above that the pharmacoric and medicinal roles of the Fc moiety in biologically active compounds seem to be vested in its physicochemical and redox properties.

1.4.2. Ferrocenyl compounds with biological activity

In addition to favourable physicochemical properties of the Fc moiety, another important trait of Fc is its amenability to several chemical transformations. This is principally due to the presence of two highly aromatic Cp rings on opposite sides of central iron metal. The high aromaticity of these rings is retained in Fc, thus making the molecule elicit chemistry of typical aromatic compounds. Chemical transformations of Fc take place on the Cp rings. It is noteworthy that although Fc exhibits facile electrophilic aromatic substitution, its sensitive redox character makes it impossible to undergo some oxidative substitution reactions such

direct halogenation and nitration. Equally important is the mentioning of the lack of established synthetic routes for specific synthesis of monosubstituted Fcs due to the difficulty of isolating the desired isomer from a mixture of disubstituted isomers that form when employing typical chemical transformation.

Synthesis of monosubtituted Fcs can only be effected via non-oxidative electrophilic aromatic substitution reactions and metalation (with lithium, mercury or tin) (**Figure 1.22**).[96-99] Metalation yields monosubstituted metalloferrocenes as vital intermediates for insertion of various functional groups such as hydroxy, amine, halogens and boric acids by conventional substitution methods. Various strategies for difunctionalisation of ferrocenes are reviewed in reference 96.[96] Through these functional groups, Fc can be easily grafted into a variety of known bioactive chemical scaffolds for the design and development of novel potential therapeutic agents with improved biological activities.

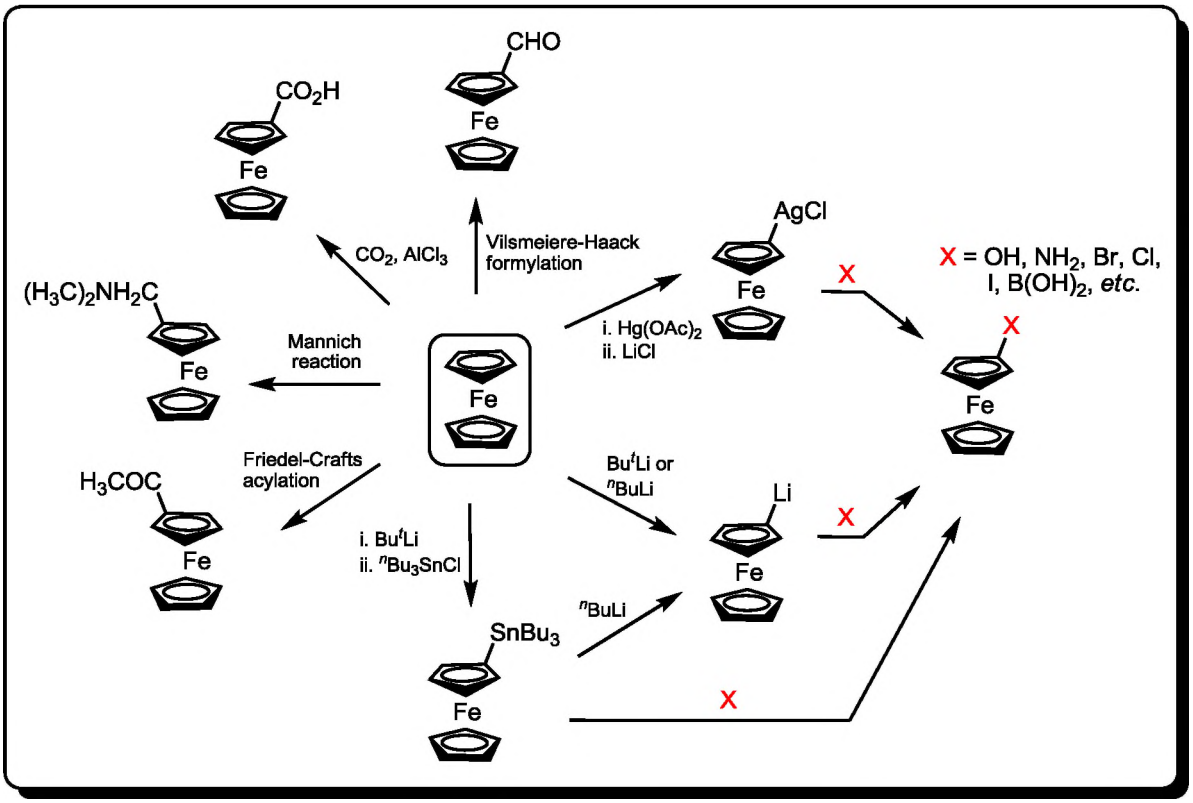

Figure 1.22: Different approaches to mono-functionalization of Fcs. Different functional groups can be inserted by simple substitution reactions directly or via intermediate reactions.

The ease of structural modification of Fc (via such transformations on the Cp rings), and thus its convenient insertion to known bioactive scaffolds has led to the synthesis of several Fc derivatives possessing a wide range of biological activities. In almost all the reported cases of

Fc-containing bioactive compounds, most Fc derivatives have higher activities than their organic counterparts. Some of these are exemplified in **Table 1.4** below.

Table 1.4: Examples of ferrocenyl derivatives of known bioactive scaffolds and their biological activities.

Compound	Activity	Remark	Ref
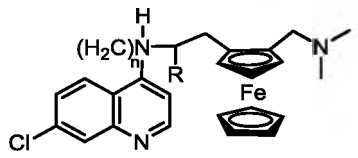 Ferrocenyl quinolines	Antimalarial	R = -CONHBn, n = 2, IC_{50} (D10) : 16.20 ± 0.54 nM R = -CONHBn, n = 6, IC50 (D10): 19.01 ± 6.24 nM	100
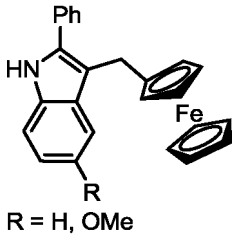 Ferrocenyl indoles	Anticancer	R = H, IC_{50} (A549): 5 ± 1 μM R = OMe, IC_{50} (A549): 7 ± 1 μM	101
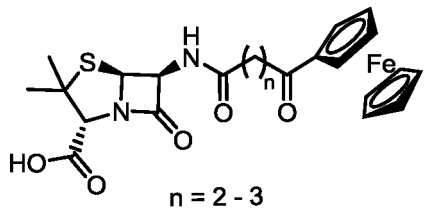 Ferrocenyl penicilins	Antibacterial	n = 2, IC_{50} (MSSA): 10 μg/mL n = 3, IC_{50} (MSSA): 40 μg/mL	102
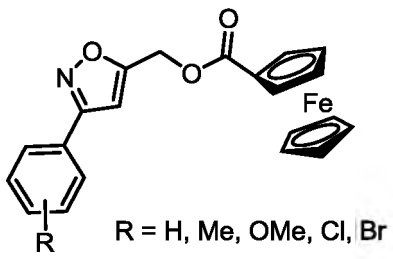 Ferrocenyl isoxazoles	Anticancer	R = 2'-Cl, IC_{50} (A549): 3.65 nM R = 4'-Me, IC_{50} (A549): 34.18 μM	103

1.5. AIMS AND OBJECTIVES OF THE PROJECT

Nb (**1.4**) possesses modest anticancer and antimalarial activities.[47, 48] Efforts to improve the anticancer activity of Nb through structural modifications, yielding Nb analogues, by targeting the *C*-terminus of Hsp90 have been extensive and fruitful.[22-24, 69-78] Among other findings, these efforts have suggested the presence of a putative hydrophobic binding pocket within the *C*-terminal domain, which allows desirable interactions between the benzamide side chain of Nb and the *C*-terminus of Hsp90 for enhanced anticancer activity.[24, 69-72] Furthermore, Blagg and co-workers have identified biphenyl **A** (**Figure 1.24**) as one of the most favoured motifs for activity if appended in place of the benzamide side chain of Nb.[69] In the present work, we reasoned that incorporating Fc in the same position as this moiety would result to new compounds with enhanced anticancer and antiplasmodial activities. A selection of the organic counterparts of the Fc-Nb analogues bearing biaryl **A** in lieu of Fc were also included in the study for comparison purposes.

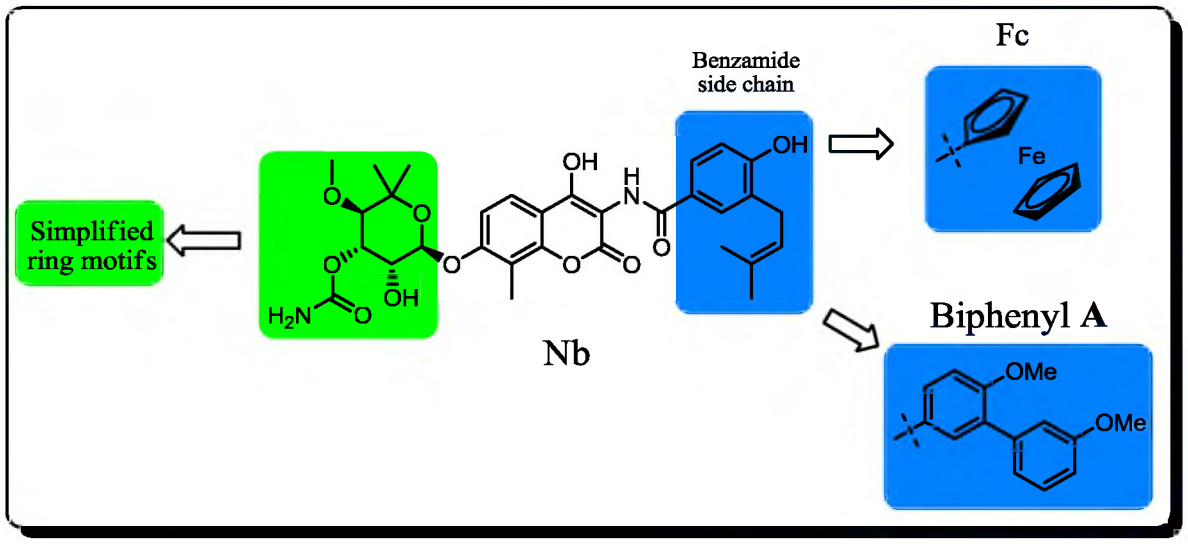

Figure 1.24: Nb analogues pursued in this work.

Contrary to anticancer investigation of Nb analogues, there have been no reports in literature with regards to improving the antimalarial activity of Nb although there is evidence of its potency against strains of *P. falciparum* and the plausible target(s). Similarly, there is no evidence in literature of the incorporation of Fc into the Nb scaffold for investigation of anticancer and/or antiplasmodial activities despite it being known to impart favourable effects on the biological activities of known bioactive organic compounds. In light of the above assertions, the overall objective of the current work was as follows.

Objective: To investigate the effects of incorporating Fc into Nb scaffold to form novel compounds with anticancer and antimalarial activities.

The specific aims entailed the following:

1. Incorporation of Fc into Nb scaffold to create a novel class of bioactive ferrocenyl compounds.
2. Synthesis of ferrocenyl Nb analogues and a selection of their corresponding organic variants bearing biphenyl **A**.
3. Pharmacological evaluation of ferrocenyl Nb analogues and their corresponding organic derivatives *in vitro* against cancer cell lines and *P. falciparum* strains for potential anticancer and antiplasmodial activities.
4. To gain insights into the plausible mechanism of action of the most promising compounds with respect to inhibition of the proposed targets: human and *P. falciparum* Hsp90 (hHsp90 and *Pf*Hsp90) for anticancer and antiplasmodial activity, respectively.

REREFENCES

1. J. C. Young, V. R. Agashe, K. Siegers and F. U. Hartl, *Nat. Rev. Mol. Cell Biol.*, **2004**, *5*, 781-791.
2. J. C. Young, I. Moarefi and F. U. Hartl, *J. Cell Biol.*, **2001**, *154*, 267-274.
3. HSP90 INTERACTARS, http://www.picard.ch/downloads/Hsp90interactors.pdf., (accessed 05 November 2016)
4. A. Subbarao Sreedhar, É. Kalmár, P. Csermely and Y.-F. Shen, *FEBS Lett.*, **2004**, *562*, 11-15.
5. P. Csermely, T. Schnaider, C. So, Z. Prohászka and G. Nardai, *Pharmacol. Ther.*, **1998**, *79*, 129-168.
6. W. B. Pratt and D. O. Toft, *Exp. Biol. Med.*, **2003**, *228*, 111-133.
7. R. Kumar, S. R. Pavithra and U. Tatu, *J. Biosci.*, **2007**, *32*, 531-536.
8. M. M. Ali, S. M. Roe, C. K. Vaughan, P. Meyer, B. Panaretou, P. W. Piper, C. Prodromou and L. H. Pearl, *Nature*, **2006**, *440*, 1013-1017.
9. L. Whitesell and S. L. Lindquist, *Nat. Rev. Cancer.*, **2005**, *5*, 761-772.
10. L. H. Pearl and C. Prodromou, *Annu. Rev. Biochem.*, **2006**, *75*, 271-294.
11. C. Söti, A. Rácz and P. Csermely, *J. Biol. Chem.*, **2002**, *277*, 7066-7075.
12. A. Zuehlke and J. L. Johnson, *Biopolymers*, **2010**, *93*, 211-217.
13. M. Waza, H. Adachi, M. Katsuno, M. Minamiyama, F. Tanaka, M. Doyu and G. Sobue, *J. Mol. Med.*, **2006**, *84*, 635-646.
14. Cancer, http://who.int/mediacentre/factsheets/fs297/en/, (accessed 07 November 2016)
15. C. Holohan, S. Van Schaeybroeck, D. B. Longley and P. G. Johnston, *Nat. Rev. Cancer.*, **2013**, *13*, 714-726.
16. D. Hanahan and R. A. Weinberg, *Cell.*, **2000**, *100*, 57-70.
17. K. Sidera and E. Patsavoudi, *Recent Pat. Anticancer Drug. Discov.*, **2014**, *9*, 1-20.
18. L. B. Peterson and B. S. Blagg, *Future Med. Chem.*, **2009**, *1*, 267-283.
19. L. Neckers, *Trends Mol. Med.*, **2002**, *8*, S55-S61.
20. T. Taldone, A. Gozman, R. Maharaj and G. Chiosis, *Curr. Opin. Pharmacol.*, **2008**, *8*, 370-374.

21. Tanespimycin in Treating Young Patients With Recurrent or Refractory Leukemia or Solid Tumors, https://clinicaltrials.gov/ct2/show/study/NCT00093821, (accessed 04 November 2016)

22. X. M. Yu, G. Shen, L. Neckers, H. Blake, J. Holzbeierlein, B. Cronk and B. S. Blagg, *J. Am. Chem. Soc.*, **2005**, *127*, 12778-12779.

23. J. A. Burlison, L. Neckers, A. B. Smith, A. Maxwell and B. S. Blagg, *J. Am. Chem. Soc.*, **2006**, *128*, 15529-15536.

24. J. A. Burlison, C. Avila, G. Vielhauer, D. J. Lubbers, J. Holzbeierlein and B. S. Blagg, *J. Org. Chem.*, **2008**, *73*, 2130-2137.

25. World Health Organization, World Malaria Report, 2015. Geneva, Switzerland, http://apps.who.int/iris/bitstream/10665/200018/1/9789241565158_eng.pdf?ua=1, (accessed 23 March 2016)

26. World Health Organization, Status report on artemisinin resistance, 2014. Geneva, Switzerland, http://www.who.int/malaria/publications/atoz/status_rep_artemisinin_resistance_sep2014.pdf, (accessed 23 March 2016)

27. World Health Organization, Global report on antimalarial efficacy and drug resistance: 2000-2010, 2010. Geneva, Switzerland, http://apps.who.int/iris/bitstream/10665/44449/1/9789241500470_eng.pdf, (accessed 24 March 2016)

28. D. Sinclair, B. Zani, S. Donegan, P. Olliaro and P. Garner, *Cochrane Database Syst. Rev.*, **2009**.

29. C. Bustamante, C. N. Batista and M. Zalis, *Curr. Drug Targets*, **2009**, *10*, 279-290.

30. G. Banumathy, V. Singh, S. R. Pavithra and U. Tatu, *J. Biol. Chem.*, **2003**, *278*, 18336-18345.

31. D. Shahinas, A. Folefoc and D. R. Pillai, *Pathogens*, **2013**, *2*, 33-54.

32. R. Kumar, A. Musiyenko and S. Barik, *Malar. J.*, **2003**, *2*, 1.

33. R. Pallavi, N. Roy, R. K. Nageshan, P. Talukdar, S. R. Pavithra, R. Reddy, S. Venketesh, R. Kumar, A. K. Gupta and R. K. Singh, *J. Biol. Chem.*, **2010**, *285*, 37964-37975.

34. P. S. Raghavan, R. Kumar and U. Tatu, *PLoS Comput. Biol.*, **2007**, *3*, e168.

35. Malaria, http://www.cdc.gov/malaria/about/biology/, (accessed 08 November 2016)

36. Y. Tanaka, K. Shiomi, K. Kamei, M. Sugoh-Hagino, Y. Enomoto, F. Fang, Y. Yamaguchi, R. Masuma, C. G. Zhang and X. W. Zhang, *J. Antibiot.*, **1998**, *51*, 153-160.

37. L. Nair and V. K. Bhasin, *Jpn. J. Med. Sci. Biol.*, **1994**, *47*, 241-252.

38. R. Kumar, A. Musiyenko and S. Barik, *Mol. Biochem. Parasitol.*, **2005**, *141*, 29-37.

39. D. Shahinas, G. MacMullin, C. Benedict, I. Crandall and D. R. Pillai, *Antimicrob. Agents Chemother.*, **2012**, *56*, 4207-4213.

40. A. K. Bryskier, M, Coumarin Antibiotics: Novobiocin, Coumermycin, and Clorobiocin. In *Antimicrobial Agents: Antibacterials and Antifungals*, ed. A. Bryskier, American Society for Microbiology: Washington, **2005**, Ch. 29, p 816-824.

41. P. Laurin, D. Ferroud, M. Klich, C. Dupuis-Hamelin, P. Mauvais, P. Lassaigne, A. Bonnefoy and B. Musicki, *Biorg. Med. Chem. Lett.*, **1999**, *9*, 2079-2084.

42. P. Laurin, D. Ferroud, L. Schio, M. Klich, C. Dupuis-Hamelin, P. Mauvais, P. Lassaigne, A. Bonnefoy and B. Musicki, *Bioorg. Med. Chem. Lett.*, **1999**, *9*, 2875-2880.

43. A.-M. Periers, P. Laurin, D. Ferroud, J.-L. Haesslein, M. Klich, C. Dupuis-Hamelin, P. Mauvais, P. Lassaigne, A. Bonnefoy and B. Musicki, *Bioorg. Med. Chem. Lett.*, **2000**, *10*, 161-165.

44. B. Musicki, A.-M. Periers, P. Laurin, D. Ferroud, Y. Benedetti, S. Lachaud, F. Chatreaux, J.-L. Haesslein, A. Iltis and C. Pierre, *Bioorg. Med. Chem. Lett.*, **2000**, *10*, 1695-1699.

45. D. Lafitte, V. Lamour, P. O. Tsvetkov, A. A. Makarov, M. Klich, P. Deprez, D. Moras, C. Briand and R. Gilli, *Biochemistry.*, **2002**, *41*, 7217-7223.

46. B. Musicki, A.-M. Periers, L. Piombo, P. Laurin, M. Klich, C. Dupuis-Hamelin, P. Lassaigne and A. Bonnefoy, *Tetrahedron Lett.*, **2003**, *44*, 9259-9262.

47. A. Divo, A. Sartorelli, C. Patton and F. Bia, *Antimicrob. Agents Chemother.*, **1988**, *32*, 1182-1186.

48. M. G. Marcu, T. W. Schulte and L. Neckers, *J. Natl. Cancer Inst.*, **2000**, *92*, 242-248.

49. Determination That ALBAMYCIN (Novobiocin Sodium) Capsule, 250 Milligrams, Was Withdrawn From Sale for Reasons of Safety or Effectiveness https://www.gpo.gov/fdsys/pkg/FR-2011-01-19/pdf/2011-1000.pdf, (accessed 21 October 2016)

50. M. Gellert, M. H. O'Dea, T. Itoh and J.-I. Tomizawa, *Proc. Natl. Acad. Sci. USA.*, **1976**, *73*, 4474–4478.
51. N. A. Gormley, G. Orphanides, A. Meyer, P. M. Cullis and A. Maxwell, *Biochemistry*, **1996**, *35*, 5083-5092.
52. C. Mayer and Y. L. Janin, *Chem. Rev.*, **2013**, *114*, 2313-2342.
53. M. A. Kohanski, D. J. Dwyer and J. J. Collins, *Nat. Rev. Microbiol.*, **2010**, *8*, 423-435.
54. E. R. Ram, A. Kumar, S. Biswas, A. Kumar, S. Chaubey, M. I. Siddiqi and S. Habib, *Mol. Biochem. Parasitol.*, **2007**, *154*, 30-39.
55. S. A. Ralph, M. C. D'Ombrain and G. I. McFadden, *Drug Resist. Update*, **2001**, *4*, 145-151.
56. R. Pingaew, A. Saekee, P. Mandi, C. Nantasenamat, S. Prachayasittikul, S. Ruchirawat and V. Prachayasittikul, *Eur. J. Med. Chem.*, **2014**, *85*, 65-76.
57. G. Wanare, R. Aher, N. Kawathekar, R. Ranjan, N. K. Kaushik and D. Sahal, *Bioorg. Med. Chem. Lett.*, **2010**, *20*, 4675-4678.
58. K. V. Sashidhara, A. Kumar, R. P. Dodda, N. N. Krishna, P. Agarwal, K. Srivastava and S. Puri, *Bioorg. Med. Chem. Lett.*, **2012**, *22*, 3926-3930.
59. H. A. Oketch-Rabah, J. W. Mwangi, J. Lisgarten and E. K. Mberu, *Fitoterapia*, **2000**, *71*, 636-640.
60. W. Akhter, A. Marella, M. Shaquiquzzaman, M. Akhter and M. M. Alam, *J. Pharm, Res.*, **2015**, 318-322.
61. Y.-Z. Yang, A. Ranz, H.-Z. Pan, Z.-N. Zhang, X.-B. Lin and S. R. Meshnick, *Am. J. Trop. Med. Hyg.*, **1992**, *46*, 15-20.
62. I. Kostova, *Curr. Med. Chem. Anticancer Agents*, **2005**, *5*, 29-46.
63. F. Borges, F. Roleira, N. Milhazes, L. Santana and E. Uriarte, *Curr. Med. Chem.*, **2005**, *12*, 887-916.
64. M. Sgobba, G. Degliesposti, A. M. Ferrari and G. Rastelli, *Chem. Biol. Drug. Des.*, **2008**, *71*, 420-433.
65. M. Sgobba, R. Forestiero, G. Degliesposti and G. Rastelli, *J. Chem. Inf. Model.*, **2010**, *50*, 1522-1528.
66. R. L. Matts, A. Dixit, L. B. Peterson, L. Sun, S. Voruganti, P. Kalyanaraman, S. D. Hartson, G. M. Verkhivker and B. S. Blagg, *ACS Chem. Biol.*, **2011**, *6*, 800-807.
67. S. Khalid and S. Paul, *Med. Hypotheses*, **2014**, *83*, 39-46.

68. S. S. Roy and M. Kapoor, *J. Mol. Graph. Model.* **2016**, *70*, 253-274.

69. A. C. Donnelly, J. R. Mays, J. A. Burlison, J. T. Nelson, G. Vielhauer, J. Holzbeierlein and B. S. Blagg, *J. Org. Chem.*, **2008**, *73*, 8901-8920.

70. G. Le Bras, C. Radanyi, J.-F. Peyrat, J.-D. Brion, M. Alami, V. Marsaud, B. Stella and J.-M. Renoir, *J. Med. Chem.*, **2007**, *50*, 6189-6200.

71. C. Radanyi, G. Le Bras, V. Marsaud, J.-F. Peyrat, S. Messaoudi, M.-G. Catelli, J.-D. Brion, M. Alami and J.-M. Renoir, *Cancer Lett.*, **2009**, *274*, 88-94.

72. C. Radanyi, G. Le Bras, S. Messaoudi, C. Bouclier, J.-F. Peyrat, J.-D. Brion, V. Marsaud, J.-M. Renoir and M. Alami, *Bioorg. Med. Chem. Lett.*, **2008**, *18*, 2495-2498.

73. H. Zhao, A. C. Donnelly, B. R. Kusuma, G. E. Brandt, D. Brown, R. A. Rajewski, G. Vielhauer, J. Holzbeierlein, M. S. Cohen and B. S. Blagg, *J. Med. Chem.*, **2011**, *54*, 3839-3853.

74. H. Zhao, B. Reddy Kusuma and B. S. Blagg, *ACS Med. Chem. Lett.*, **2010**, *1*, 311-315.

75. B. R. Kusuma, A. S. Duerfeldt and B. S. J. Blagg, *Bioorg. Med. Chem. Lett.*, **2011**, *21*, 7170-7171.

76. A. C. Donnelly, H. Zhao, B. R. Kusuma and B. S. Blagg, *Med. Chem. Commun.*, **2010**, *1*, 165-170.

77. S. N. Shelton, M. E. Shawgo, S. B. Matthews, Y. Lu, A. C. Donnelly, K. Szabla, M. Tanol, G. A. Vielhauer, R. A. Rajewski and R. L. Matts, *Mol. Pharmacol.*, **2009**, *76*, 1314-1322.

78. H. Zhao, E. Moroni, B. Yan, G. Colombo and B. S. Blagg, *ACS Med. Chem. Lett.*, **2012**, *4*, 57-62.

79. T. Kealy and P. Pauson, *Nature*, **1951**, *168*, 1039-1040.

80. G. Wilkinson, M. Rosenblum, M. Whiting and R. Woodward, *J. Am. Chem. Soc.*, **1952**, *74*, 2125-2126.

81. E. Fischer and W. Pfab, *Z. Naturforsch. B.*, **1952**, *7*, 377-379.

82. H. Tamura and M. Miwa, *Chem. Lett.*, **1997**, *1997*, 1177-1178.

83. G. Tabbì, C. Cassino, G. Cavigiolio, D. Colangelo, A. Ghiglia, I. Viano and D. Osella, *J. Med. Chem.*, **2002**, *45*, 5786-5796.

84. M. F. R. Fouda, M. M. Abd-Elzaher, R. A. Abdelsamaia and A. A. Labib, *Appl. Organomet. Chem.*, **2007**, *21*, 613-625.

85. N. Chavain and C. Biot, *Curr. Med. Chem.*, **2010**, *17*, 2729-2745.

86. To Evaluate the Efficacy of a Single Dose Regimen of Ferroquine and Artefenomel in Adults and Children With Uncomplicated Plasmodium Falciparum Malaria (FALCI), https://clinicaltrials.gov/ct2/show/NCT02497612, (accessed 24 March 2016)

87. K. E. Dombrowski, W. Baldwin and J. E. Sheats, *J. Organomet. Chem.*, **1986**, *302*, 281-306.

88. D. R. Van Staveren and N. Metzler-Nolte, *Chem. Rev.*, **2004**, *104*, 5931-5986.

89. W. A. Wani, E. Jameel, U. Baig, S. Mumtazuddin and L. T. Hun, *Eur. J. Med. Chem.*, **2015**, *101*, 534-551.

90. C. Biot, D. Taramelli, I. Forfar-Bares, L. A. Maciejewski, M. Boyce, G. Nowogrocki, J. S. Brocard, N. Basilico, P. Olliaro and T. J. Egan, *Mol. Pharm.*, **2005**, *2*, 185-193.

91. C. Biot and D. Dive, Bioorganometallic Chemistry and Malaria. In *Med. Org. Chem.*, eds. G. Jauen and N. Metzler-Nolte, Springer: Heidelberg, **2010**, Ch. 32, p 155-193.

92. F. Dubar, J. Khalife, J. Brocard, D. Dive and C. Biot, *Molecules*, **2008**, *13*, 2900-2907.

93. N. Chavain, H. Vezin, D. Dive, N. Touati, J.-F. Paul, E. Buisine and C. Biot, *Mol. Pharm.*, **2008**, *5*, 710-716.

94. W. H. Schaefer, T. M. Harris and F. P. Guengerich, *Biochemistry*, **1985**, *24*, 3254-3263.

95. G. Jaouen, A. Vessières and S. Top, *Chem. Soc. Rev.*, **2015**, *44*, 8802-8817.

96. R. C. J. Atkinson and N. J. Long, Monodentate Ferrocene Donor Ligands. In *Ferrocenes: Ligands, Materials and Biomolecules*, ed. P. Stepnicka, John Wiley & Sons, Ltd: Chichester, **2008**, Ch. 1, p 1-32.

97. D. Astruc, *Eur. J. Inorg. Chem.*, **2017**, *1*, 6-29.

98. D. Guillaneux and H. B. Kagan, *J. Org. Chem.*, **1995**, *60*, 2502-2505.

99. M. Herberhold, Ferrocene compounds containing heteroelements. In *Ferrocenes: Homogeneous Catalysis, Organic Synthesis, Materials Science*, eds. A. Togni and T. Hayashi, VCH Publishers: Weinheim, **1995**, Ch. 5, p 219-278.

100. K. Chibale, J. R. Moss, M. Blackie, D. van Schalkwyk and P. J. Smith, *Tetrahedron Lett.*, **2000**, *41*, 6231-6235.

101. J. Quirante, F. Dubar, A. González, C. Lopez, M. Cascante, R. Cortés, I. Forfar, B. Pradines and C. Biot, *J. Organomet. Chem.*, **2011**, *696*, 1011-1017.

102. J. Skiba, A. Rajnisz, K. N. de Oliveira, I. Ott, J. Solecka and K. Kowalski, *Eur. J. Med. Chem.*, **2012**, *57*, 234-239.

103. J. Yong, C. Lu and X. Wu, *Med. Chem. Commun.*, **2014**, *5*, 968-972.

2. SYNTHESIS OF TARGET NOVOBIOCIN ANALOGUES

This chapter focuses mainly on the synthesis and characterisation of target Nb analogues. The synthetic methods for preparation of coumarin compounds are briefly reviewed at the beginning of the chapter (**Section 2.1**) before delving into the synthesis and characterisation of the target analogues (**Section 2.2**). Conclusions of this part of the study are drawn at the end of the chapter (**Section 2.3**).

2.1. OVERVIEW OF SYNTHESIS OF COUMARIN COMPOUNDS

The structure of Nb comprises three units: **A** – noviose sugar, **B** – coumarin ring and **C** – benzoic acid side chain (**Figure 2.1**). Of the three units, the coumarin ring is arguably the most important as it serves as a backbone for appending the noviose and benzamide units. Additionally, Nb and compounds **1.21-1.22** are known as aminocoumarin antibiotics, a name attributable to the coumarin nucleus common in all three antibiotics. In literature, synthesis of Nb analogues is typically initiated by preparation of the coumarin nucleus to which other substituents can be appended.[1-3] Some researchers start with the parental structure of Nb and modify it to synthesize the desired analogues.[4, 5]

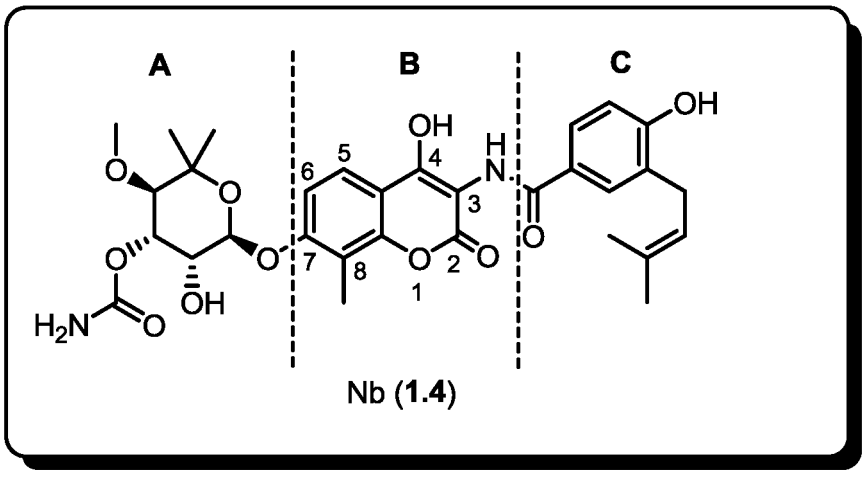

Figure 2.1: Structure of Nb showing different subunits: **A** – noviose ring, **B** – coumarin ring and **C** – benzoic acid side chain.

Coumarins belong to the α-benzopyrone sub-family of the benzopyrone family of coumpounds.[6] The other group within the benzopyrone family is the γ-benzopyrone whose prime members are flavonoids. Coumarins have a wide spectrum of properties including applications in pharmaceutical, agrochemical and photochemical industries.[6] Due to their wide

applicability, various synthetic methods have been developed for synthesis of coumarin compounds. The most common methods for coumarin synthesis include the Pechmann reaction, Knoevenagel condensation, Perkin condensation and Wittig reactions tailored for coumarin synthesis.

2.1.1. Pechmann reaction

The Pechmann reaction involves condensing a phenol with a *β*-keto ester or carboxylic acid in the presence of a strong acid like sulphuric acid (H_2SO_4) as illustrated in **Scheme 2**.[6] It is by far the most high-yielding method compared to other classical methods mentioned above.[6] The method is widely used for synthesis of coumarins with various substituents. However, it is somewhat limited in substrate variability due to the direct use of H_2SO_4, which presents corrosion problems and leads to formation of many by-products. The reaction has since been modified to circumvent the use of H_2SO_4 for milder reaction conditions.

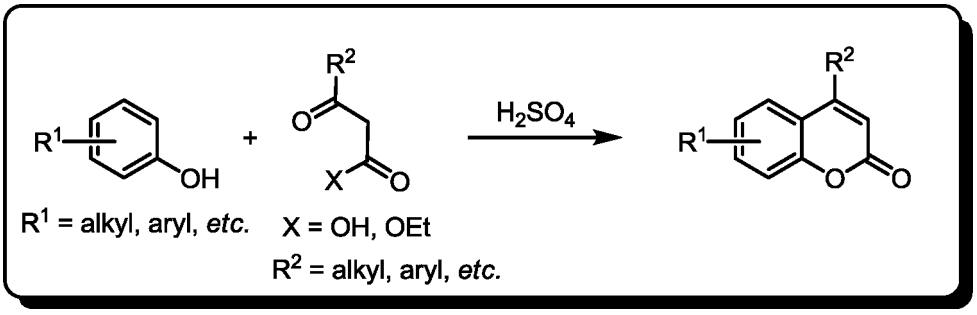

Scheme 2.1: Representative reaction of the Pechmann reaction.

Among other variations of the Pechmann reaction are the use of Lewis acids ($AlCl_3$, $TiCl_4$, $ZnCl_2$, $InCl_3$),[7-9] ionic liquids[10, 11] and microwave irradiation.[12, 13] Other variations employing Brønsted bases (NaOMe, NaOEt, NaOAc) have also been explored, but there is inadequate data regarding their efficacy compared to H_2SO_4.[6] Another efficient and mild variation of the Pechmann reaction makes use of grinding the reactants in solid phase with catalytic amounts of an acid.[14]

2.1.2. Knoevenagel reaction

A typical Knoevenagel reaction utilizes an amine as a base to couple an active methylene compound to a carbonyl group, yielding an α,β-unsaturated adduct.[15] This method has proven invaluable for synthesis of cinnamic acid derivatives. In coumarin synthesis, an activated methylene is added to a benzaldehyde substrate carrying a hydroxyl group in the *ortho*-position, i.e. a salicylaldehyde, to effect an "open ring", cinammic acid-like intermediate which

subsequently cyclizes (lactonization) to give the desired coumarin product (**Scheme 2.2**).[15] This is usually achieved in a one-pot synthesis. Most methylene substrates are usually malonic esters and derivatives (e.g. carboxylic acids and amides), but cyanide (-CN) has also been reported as an activating group.[16, 17]

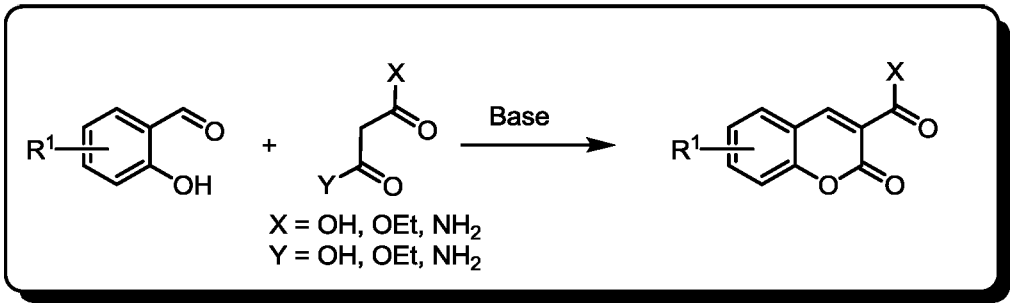

Scheme 2.2: Representative reaction of the Knoevenagel reaction.

Like other methods for coumarin synthesis, the Knoevanegel condensation yields coumarins with various substituents on the benzene ring and is compatible with quite a number of sensitive functional groups.[15]

2.1.3. Wittig reaction for coumarin synthesis

The Wittig reaction is a C=C bond forming reaction that has been widely applied in the synthesis of unsaturated acyclic systems since its inception. Due to limited generality of the classical coumarin synthetic methods, efforts to develop better procedures for coumarin preparation have led to the modification of the Wittig reaction for coumarin synthesis.[18, 19] Harayama *et al.* reported a modified Wittig method in which they reacted (Carbethoxymethylene)triphenylphosphorane (i.e. a Wittig reagent) with various salicylaldehydes under reflux.[18] The method afforded milder reaction conditions and reasonable yields of the desired coumarin products.

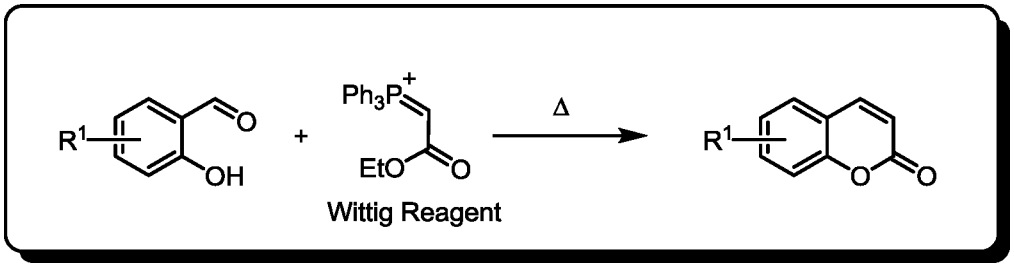

Scheme 2.3: Synthesis of coumarin via modified Wittig reaction.

Mechanistically, the reaction is thought to proceed via a typical Wittig pathway, forming a cinnamic ester derivative as an intermediate, which self-cyclizes to give the desired coumarin

product. Another modification by Yavari *et al.* employed a Wittig reagent formed *in situ* by treating dimethyl acetylenedicarboxylate (DMAD) with tripenyl phosphine (PPh_3) and reacting it with substituted phenols, similarly to the Pechmann reaction.[19]

2.1.4. Perkin reaction

The Perkin reaction was first reported by Sir William Perkin in 1868.[20] The reaction involved refluxing salicylaldehyde in acetic anhydride (Ac_2O) in the presence of a base, sodium acetate (NaOAc), as a catalyst which gave coumarin as a product (**Scheme 2.4**). To this day, the Perkin reaction is one of the most direct and simplest methods for synthesis of substituted coumarins. However, it bears a major drawback of low yields which is attributable to harsh reaction conditions such as the use of excess amounts of Ac_2O and NaOAc, and refluxing at elevated temperatures (>110 °C). These conditions lead to a tedious reaction workup, giving unsatisfactory product yields.

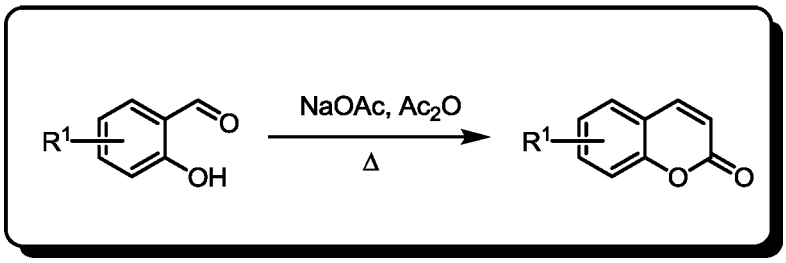

Scheme 2.4: Perkin condensation.

The mechanism of the Perkin reaction is not yet fully understood. There are, however, two propositions regarding the mechanistic details of this reaction. One take suggests the product forms by internal lactonisation of an intermediary *trans*-cinnamic acid derivative formed by normal aldol condensation of salicylaldehyde and Ac_2O (**Scheme 2.5**).[21-23] This is known as the intermolecular Perkin reaction mechanism.

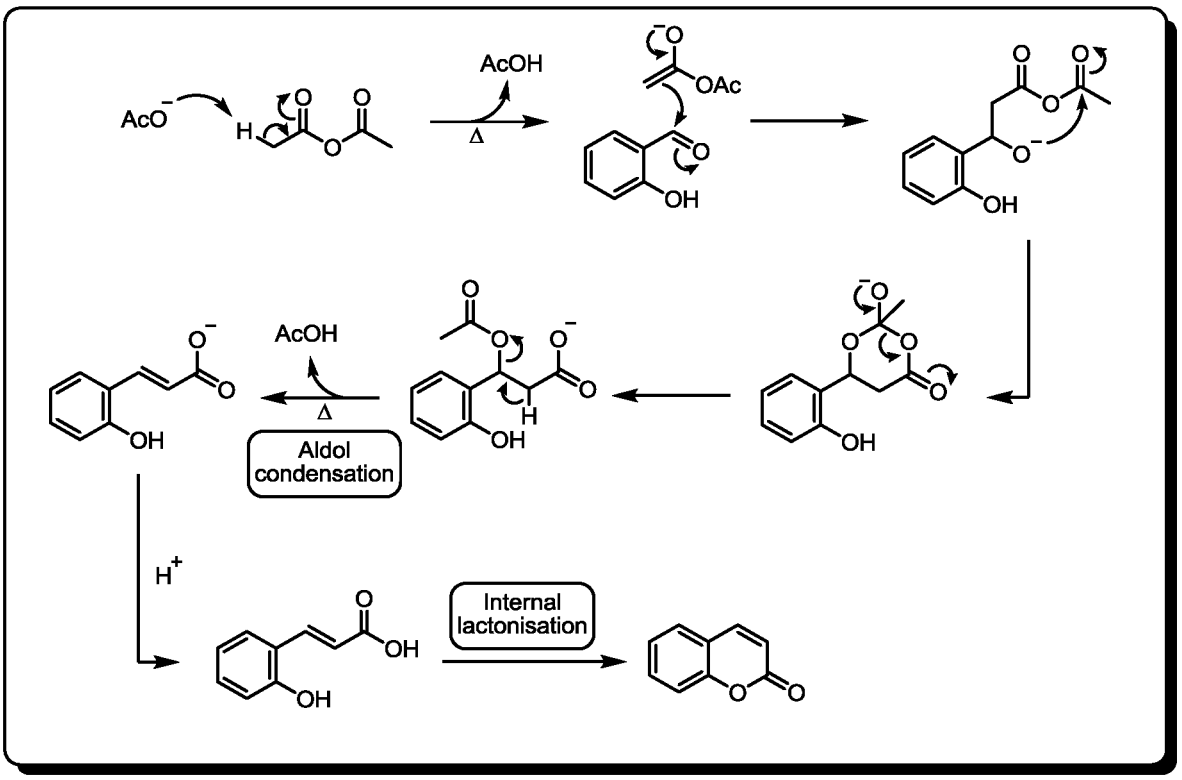

Scheme 2.5: Intermolecular Perkin reaction mechanism.[21-23]

Though this is a universally accepted mechanism for Perkin condensation, it is contested by the intramolecular proposition which contends that internal lactonisation of the *trans*-cinnamic acid intermediate is unlikely to occur under the reaction conditions used due to its *trans*-configuration.[23] The intramolecular approach proposes that aldol condensation is preceded by intramolecular lactonisation (ring closure) of an *o*-acetyl salicylaldehyde intermediate which forms during the reaction.[23, 24]

Just like the Knoevenagel condensation, the Perkin reaction requires a hydroxyl group on C-2 of the benzaldeyde substrate. Although an effective method, this requirement somewhat limits the substrate scope of the reaction. Also, the low yields and harsh reaction conditions are among other limitations of this procedure. There are numerous attempts described in literature to improve the reaction conditions and substrate scope of the Perkin reaction.[25] These variations share similarities with the Knoevenagel reaction: they require an activated methylene in addition to salicyadehyde as substrates and yield 3-substituted coumarins.[25] They have been widely applied for synthesis of 3-aminocoumarins and derivatives.[26] In this work, a variation of the Perkin condensation was employed for synthesis of the coumarin core of the Nb analogues using 4-hydroxysalicylaldehydes and an acetyl-activated methylene, *N*-acetyl glycine.

2.2. SYNTHESIS OF NOVOBIOCIN ANALOGUES

In line with the aims and objectives of the project, the overall study commenced with the synthesis of Nb analogues. In the proposed target analogues, the noviose sugar appendage on C-7 of the coumarin core was replaced with simplified cyclic substituents: phenyl and piperidinyl rings, yielding 7-*O*-phenyl (phenylated) and 7-*O*-piperidinyl (piperidinyl) Nb analogues, respectively. Fc and the previously reported biphenyl **A**, were appended in place of benzamide chain of Nb. The design of the Nb analogues pursued in this study is highlighted in **Scheme 2.5** in light of the SAR data of the Nb analogues investigated in literature.[27-29]

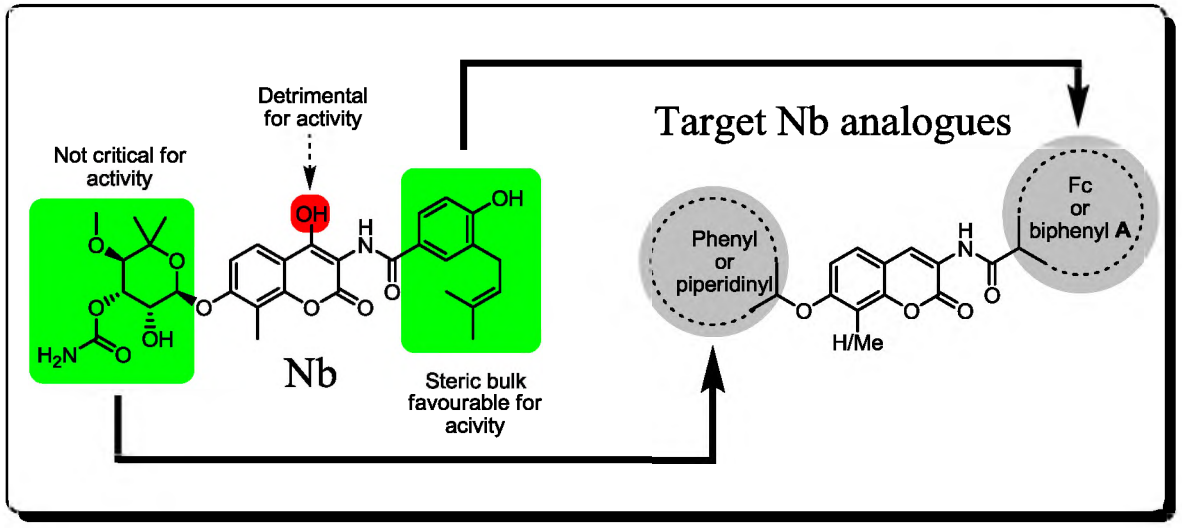

Scheme 2.6: Design of Nb analogues pursued in this study.

Syntheses of both phenylated and piperidinyl analogues were initiated by preparation of the coumarin nucleus via Perkin condensation. Both types of analogues were synthesised starting from the coumarin core prepared by the Perkin methodology. The desired structural moieties (phenyl, piperidinyl, Fc, and biphenyl **A**) were successively appended to produce their corresponding target Nb analogues (**Scheme 2.7**).

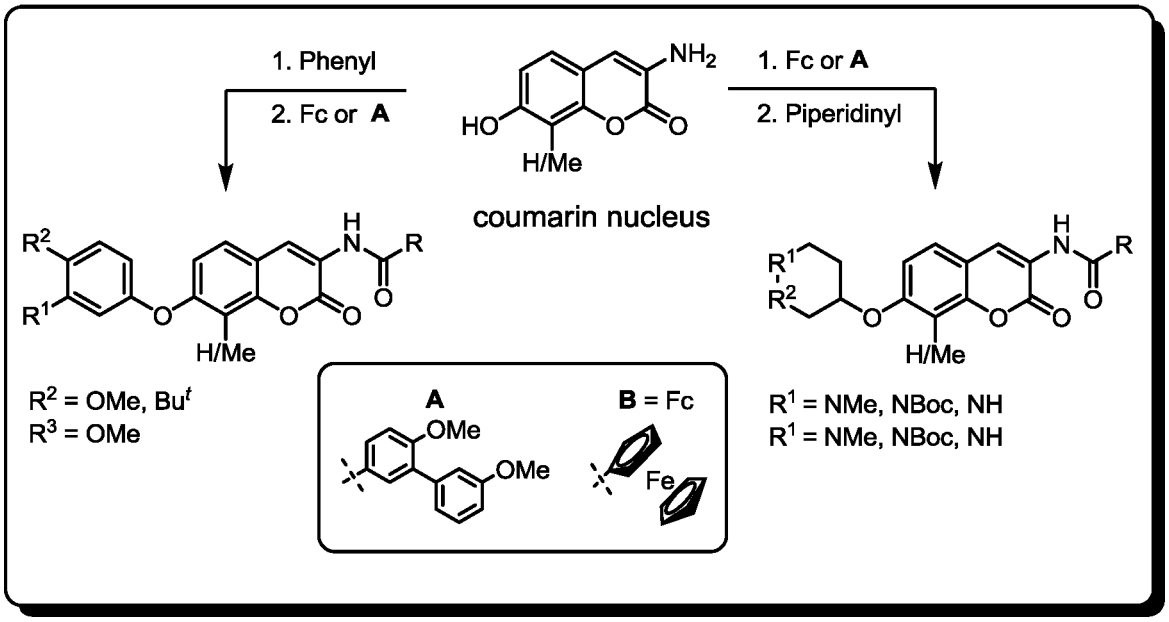

Scheme 2.7: Outline for synthesis of Nb analogues.

2.2.1. Preparation of the coumarin nucleus of Nb analogues

As important substrates of the Perkin methodology for coumarin synthesis, the salicylaldehydes **2.2a-b** were prepared by formylation of resorcinols **2.1a-b** under Vilsmeier-Haack conditions (**Scheme 2.8**).[30]

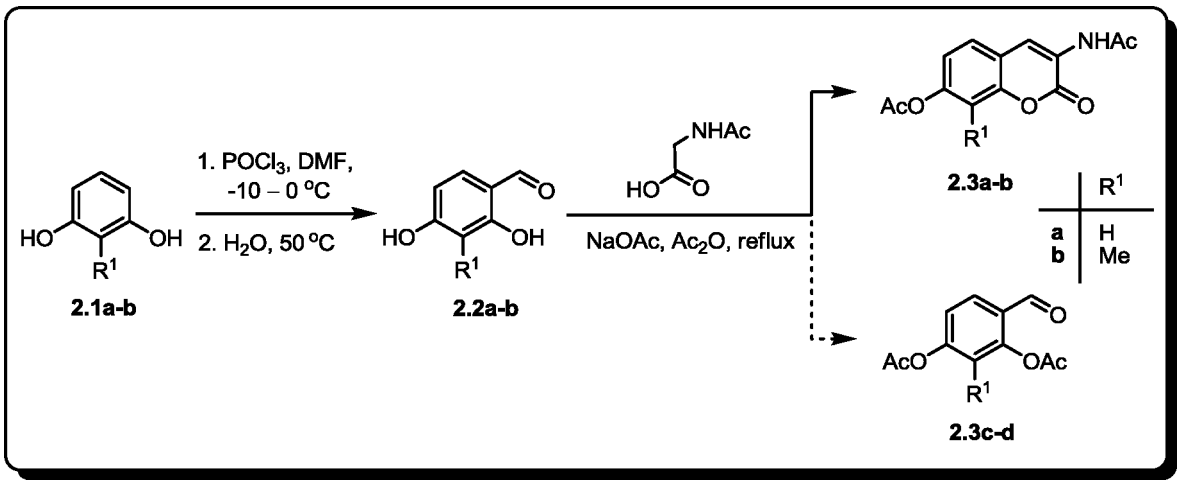

Scheme 2.8: Formation of coumarins **2.3a-b** and their presumed side products **2.4a-b** under Perkin conditions.

The reaction entailed treating anhydrous dimethyl formamide (DMF) under stirring with phosphorus oxychloride ($POCl_3$) added dropwise at 18 – 25 °C in acetonitrile in a water bath for an hour to form the Vilsmeier-Haack reagent, which was subsequently reacted with resorcinols **2.1a-b** *in situ* at a temperatures between –10 and 0 °C. The resulting yellow

precipitate, which is a precursor of the formylation product, was hydrolysed with H_2O at 50 °C to effect salicylaldehydes **2.2a-b** in good yields, 60 and 66%, respectively.

The structures of the products were confirmed by proton and carbon-13 nuclear magnetic resonance spectroscopy techniques (^{1}H NMR and ^{13}C NMR, respectively). The signals observed for both salicylaldehydes resonated with the ones reported in literature for these compounds.[30] For ^{1}H NMR, the aldehyde proton appeared just above δ 9 ppm, whilst the hydroxyl groups were observed as broad signals above δ 10 ppm. **Figure 2.1** shows assignment of protons in the ^{1}H NMR spectrum of compound **2.2a** as an example. Appearance of a signal in the carbonyl region of the ^{13}C NMR spectrum of the products further confirmed successful formylation of resorcinols **2.1a-b** to salicylaldehydes **2.2a-b**.

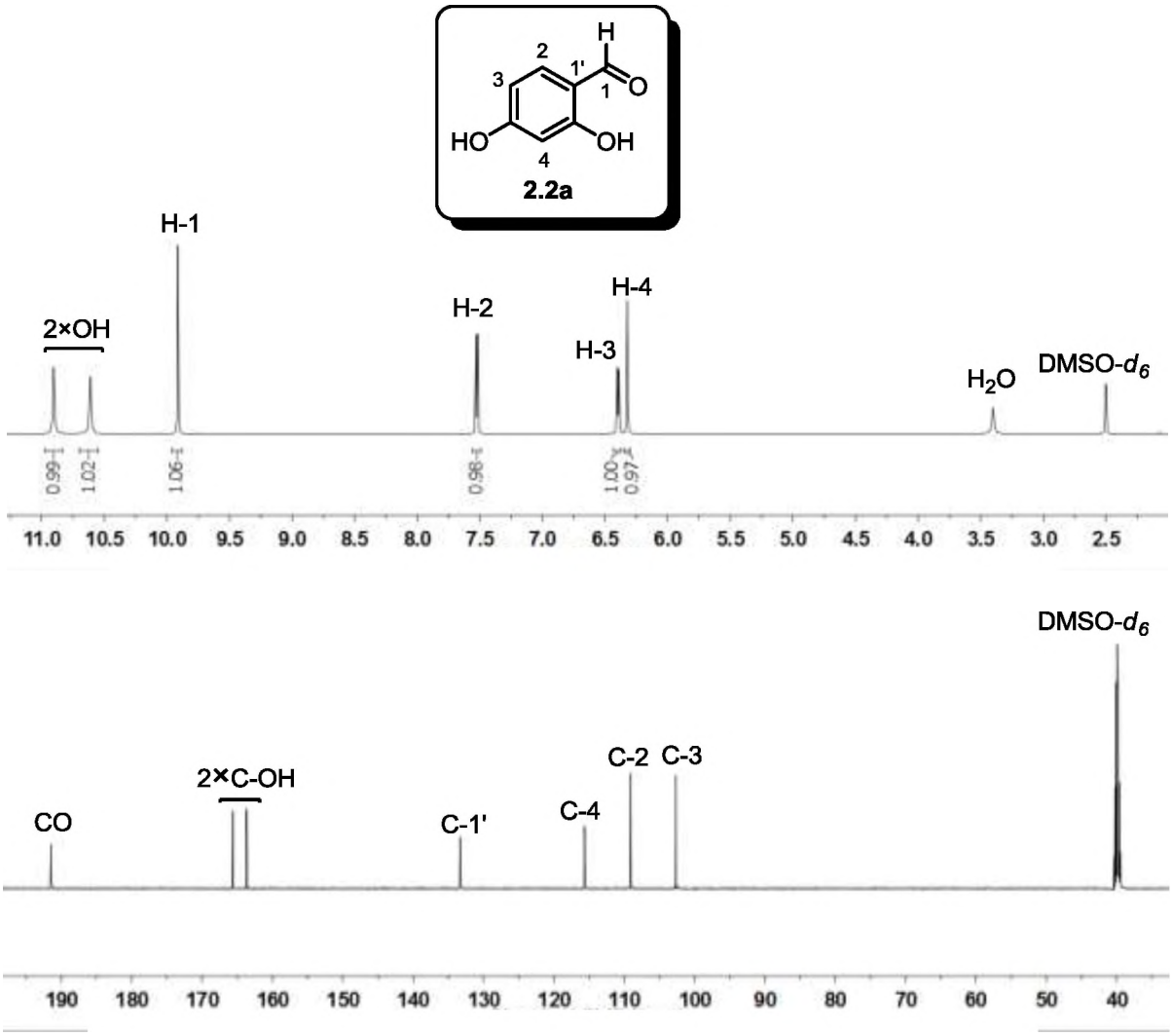

Figure 2.2: ^{1}H and ^{13}C NMR spectrum of **2.2a**.

Following successful formylation of resorcinols, the parental coumarin nucleus which constitutes the core of Nb was attained via a modified Perkin condensation[26] of salicylaldehydes **2.2a-b** with *N*-acetyl glycine in the presence of anhydrous NaOAc as a base in excess Ac_2O to effect 7-acetoxy-3-acetamidocoumarins **2.3a-b** in relatively low yields: 38 and 33%, respectively (**Scheme 2.8**). The progress of the reaction was monitored by thin-layer chromatography (TLC), which revealed many side products. Though known for effecting low product yields, this modification has proved useful and effective for accessing particularly 3-aminocoumarins as it provides the simplest and most direct route.[26, 31] It was for these reasons that it was chosen over other known procedures for coumarin synthesis.

Low yields the coumarin products could be attributed to the harsh reaction conditions employed (highly acidic medium and elevated temperatures) and the resultant tedious workup, which involved washing the pasty crude product successively with distilled water and EtOAc. Besides, the hydroxyl group on C-4 of the salicylaldehyde ring is known to cause the salicylaldehyde to react sluggishly under Perkin conditions due to its electron-donating nature.[21, 26, 32] In our case, the low-yielding effects of the electron-donating groups (EDGs) are further illustrated by the fact that the 8-methyl (8-Me) coumarin, **2.3b**, was attained in the lowest yield (33%) whilst coumarin **2.3a**, containing a lesser electron-donating hydrogen atom at C-8, was accessed in a slightly higher yield (38%).

It is also noteworthy that the same *p*-hydroxyl concomitantly undergoes acetylation under the Perkin conditions used, forming 7-acetoxy-3-acetamidocoumarin, since the reaction medium has high levels of the acetate ion (NaOAc and Ac_2O). This would suggest the *o*-hydroxyl of the salicylaldehyde substrate also experiences acetylation to some extent. This could provide further explanation for the low yields of the reaction since two competing pathways will now be effected: one leading to formation of the desired products **2.3a-b** and the other to formation of the acetylated side products, 2,4-diacetoxybenzaldehydes **2.3c-d** (**Scheme 2.8**). Although these presumed side products were not isolated during workup, there is evidence in literature for acetylation of *o*-hydroxyl of salicylaldehyde in the presence of Ac_2O and a strong base.[23, 24]

As with salicylaldehydes, the structures of acetylated coumarins **2.3a-b** were confirmed by ^1H and ^{13}C NMR spectroscopy. **Figure 2.3** illustrates ^1H and ^{13}C NMR spectra of **2.3a**, highlighting the important structural features of this compound. The signals observed in both ^1H and ^{13}C NMR spectra of **2.3a-b** were consistent with the signals reported in literature for

these products.[26] For ^{1}H NMR, the protons on the benzene ring of the coumarin core were observed between δ 7.0 and 8.6 ppm, which is slightly downfield compared to the salicylaldehyde substrates (**Figure 2.2**). This phenomenon is indicative of successful cyclisation.[26] Most important was the appearance of a singlet proton at δ 8.60 and 8.61 ppm, respectively, in ^{1}H NMR spectra of **2.3a** and **2.3b**, which is characteristic of the coumarin ring.[26] Formation of the coumarin ring was further suggested by the appearance of the lactone carbonyl signal around δ 157.3 ppm in ^{13}C NMR spectra of both coumarin products.

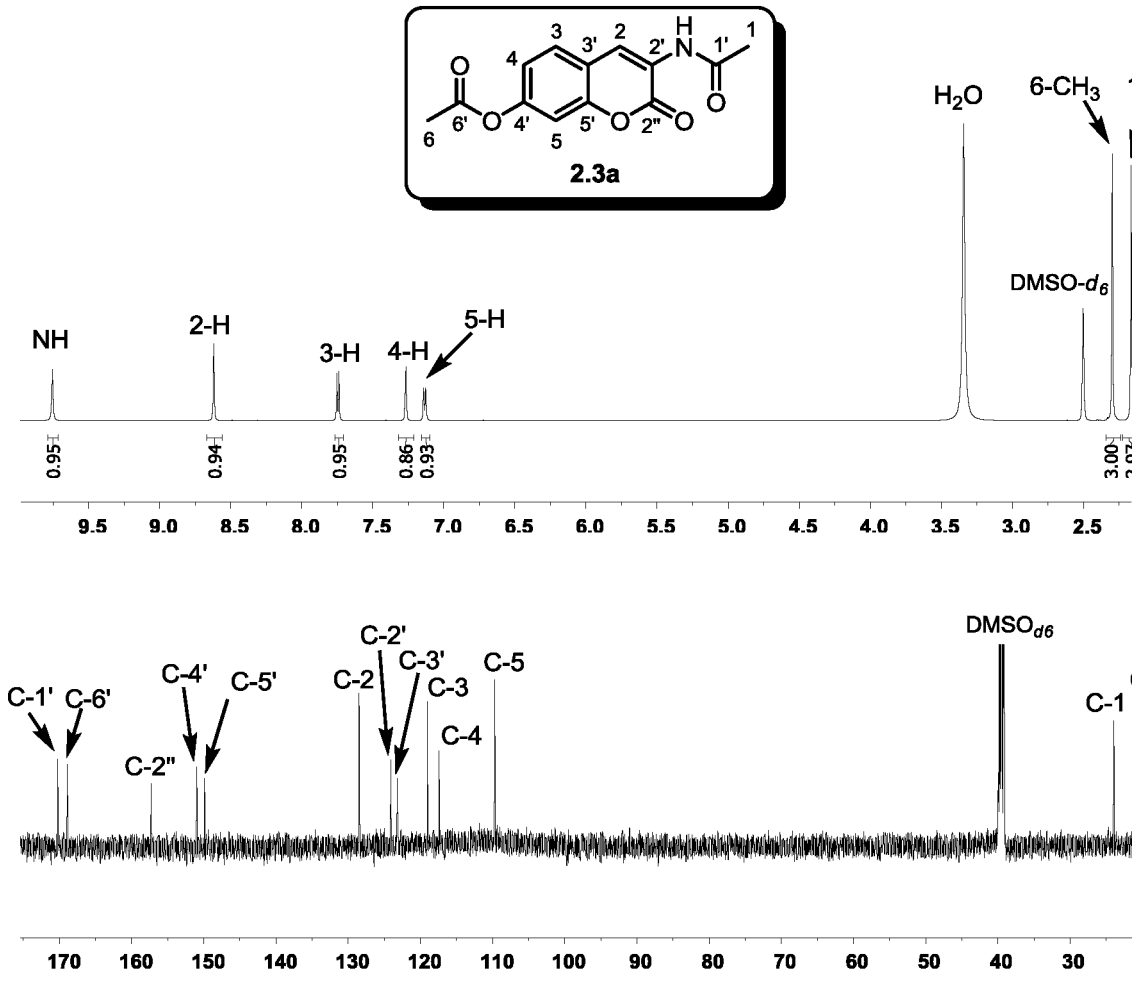

Figure 2.3: ^{1}H and ^{13}C NMR spectra of **2.3a**.

After successful preparation of *N*-acetyl 7-acetyloxy-3-aminocoumarins, **2.3a-b**, it was imperative to deacetylate either at position 3 (for attaching Fc and biphenyl **A**) or position 7 (for phenyl and piperidinyl) of the coumarin nucleus to allow coupling of these structural motifs required for target compounds. There is a plethora of deacetylation procedures in literature for both esters and amides.[33-35] Since the functional groups that are effected following deacetylation of **2.3a-b**, i.e. hydroxyl and amine, are labile and elicit similar reactivities, we

wanted a procedure that would selectively deacetylate one group whilst leaving the other still protected. This was achieved by employing a two-step, one-pot procedure developed by Burk and Allen for facile conversion of *N*-acetamides into *N*-*tert*-butoxycarbamates.[36] The procedure utilizes an amidation reaction between a secondary *N*-acetamide and di-*tert*-butyldicarbonate (Boc_2O) catalyzed by 4-dimethylaminopyridine (DMAP) to displace the hydrogen atom on the nitrogen of the acetamide. This gives a tertiary amide intermediate, which is subsequently deacetylated in the second step via base-catalyzed hydrolysis to yield solely an *N*Boc-protected product.

In our case, the first step of the Allen and Burk procedure was envisaged to exchange the acetyl in position 3 of the coumarin ring for the Boc group, whilst the deacetylation step was envisaged to effectively hydrolyze the 7-acetoxy moiety to effect *N*-Boc 7-hydroxy-3-aminocoumarins. The acetylated aminocoumarins, **2.3a-b**, and catalytic amounts of DMAP were stirred together with excess Boc_2O at ambient temperature in tetrahydrofuran (THF) as reported by Kudale *et al.*[26] As before, the progress of the reaction was monitored by TLC. Both acetyl coumarins **2.3a** and **2.3b** were completely consumed under these reaction conditions after an hour. The resultant clear brown solution, presumably containing a tertiary amide intermediate, turned orange upon successive addition of hydrazine monohydrate ($NH_2H_2 \bullet H_2O$) and methanol, and was stirred for 20 minutes. Addition of $NH_2H_2 \bullet H_2O$, simultaneously deacetylated the acetoxy at C-7 of the coumarin reactants (**2.3a-b**), yielding *N*-Boc 7-hydroxy-3-aminocoumarins, **2.4a-b** (**Scheme 2.9**. The products were purified by silica gel column chromatography following a laborious reaction workup that involved removal of excess hydrazine by successively washing the reaction solution in dichloromethane (DCM) with 1 M HCl, $CuSO_4$, and $NaHCO_3$ solutions. Compound **2.4a** was obtained in 81% yield as a white solid, whereas **2.4b** was attained as a pale-yellow solid in 66%.

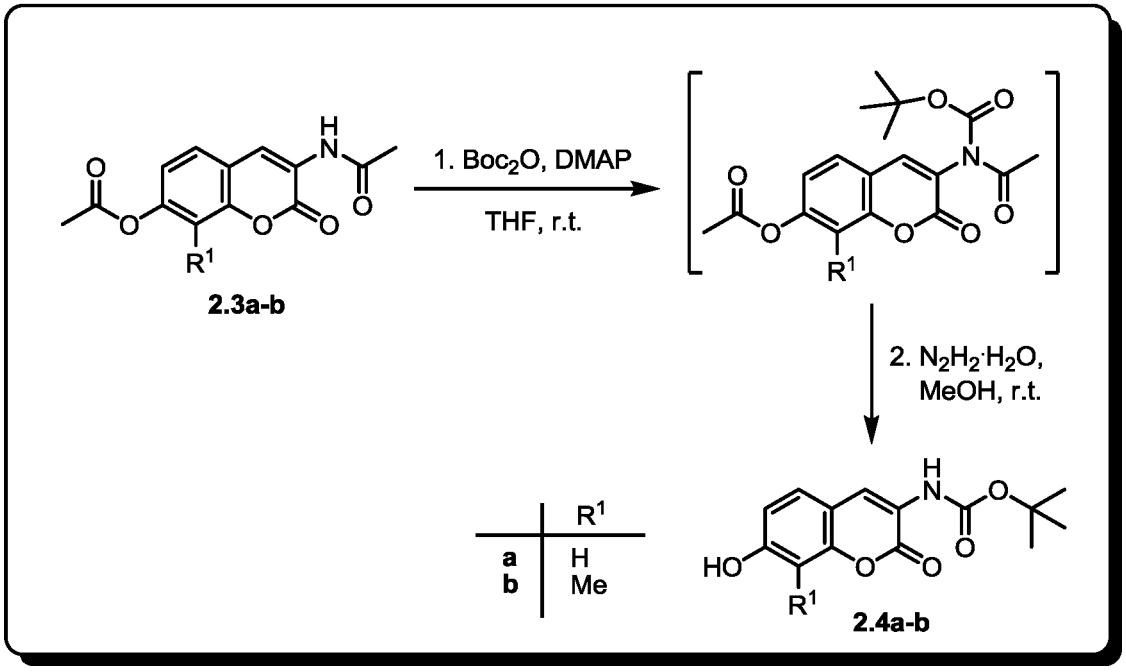

Scheme 2.9: Hydrolysis of *N*-acetyl 7-acetoxy-3-aminocoumarins **2.3a-b**.

Like before, the hydrolysis products were characterised by NMR spectroscopy techniques. **Figure 2.4** shows the ^{1}H NMR spectrum of compound **2.4b** as a representation of ^{1}H NMR spectra of the hydrolysis products. The coumarin signals remained almost unchanged in ^{1}H NMR spectra of both products relative to their corresponding starting materials, **2.3a-b**. Most significant was the disappearance of both acetyl signals in the aliphatic region and the appearance of a broad signal below δ 10 ppm, which is characteristic of the OH group (**Figure 2.3**). An intense singlet, indicative of the Boc group, was also observed in the aliphatic region around δ 1.45 ppm. Disappearance of acetate signals was also observed in ^{13}C NMR spectra of these compounds, further confirming successful deacetylation of compounds **2.3a-b** (**Figure 2.3**). The signals of the Boc group resonated at δ 158.3 – 159.4 ppm (C=O), 80.1 – 80.2 ppm (quaternary C) and 27.92 – 28.01 ppm (3×Me) as reported in literature.[26]

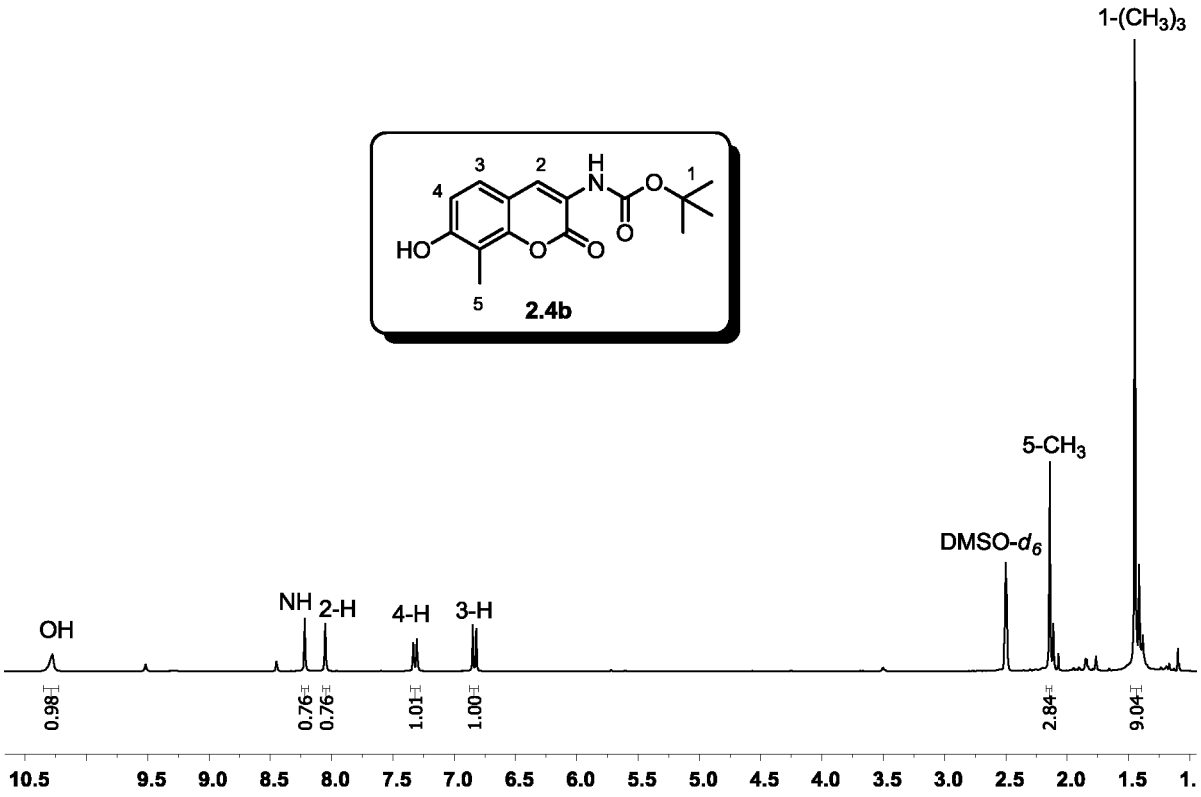

Figure 2.4: ^{1}H NMR spectrum of **2.4b**.

2.2.2. Synthesis of 7-*O*-phenyl Nb analogues

The hydrolysis of acetylated coumarins (**2.3a-b**) afforded products, **2.4a-b**, bearing a hydroxyl group on C-7 of the coumarin nucleus. The hydroxyl functional group elicits a wide variety of reactivities, from simple reactions, like S_N2 substitutions to more involved transformations such as etheration and hydroboration. In line with the aims and objectives of the present study, the substituted phenyl moieties were appended at position 7 of the coumarin nucleus via the Chan-Lam coupling protocol.[37]

In Nb and most analogues reported in literature, position 7 is occupied by the stereochemically complex noviose sugar. Like most sugars, noviose exhibits both R- and S-configurations, and thus has D- and L-enantiomers, respectively. Synthesis of the noviose is far from trivial.[38] Although there have been a variety of protocols developed for synthesis of noviose, there has not been one that is more direct and can be performed in less than 10 steps.[38]

In light of the SAR data of Nb analogues for cancer, through Hsp90 inhibition, the noviose sugar is known to impart high activity into Nb analogues.[1-3, 39] However, it has been reported that activity can still be retained by appending other structural motifs, both cyclic and acyclic,

in lieu of the noviose moiety.[27, 29] In our case, the phenyl rings bearing substituents: methoxy (OMe) in positions 3' and 4', and *tert*-butyl (Bu^t) in position 4' were selected for investigation, and have also been explored as noviose replacements in literature.[29]

2.2.2.1. Synthesis of *N*-Boc 7-phenyloxy-3-aminocoumarins (2.6a-f)

Using commercially available boronic acid derivatives of the substituted phenyls selected for investigation, the Chan-Lam coupling protocol was employed to couple these moieties to position 7 of *N*-Boc 7-hydroxy-3-aminocoumarins, **2.4a-b**. The Chan-Lam protocol is a copper-promoted etherification procedure that involves cross-coupling of phenols with aryl boronic acids.[40] This procedure has many benefits compared to other classical etherification protocols such as Ullman-Goldberg and Buchwald-Hartwig reactions.[40] Among other benefits are the milder reaction conditions (low temperatures and weak bases) and general affordability due to use the of inexpensive copper(II) salts.[40]

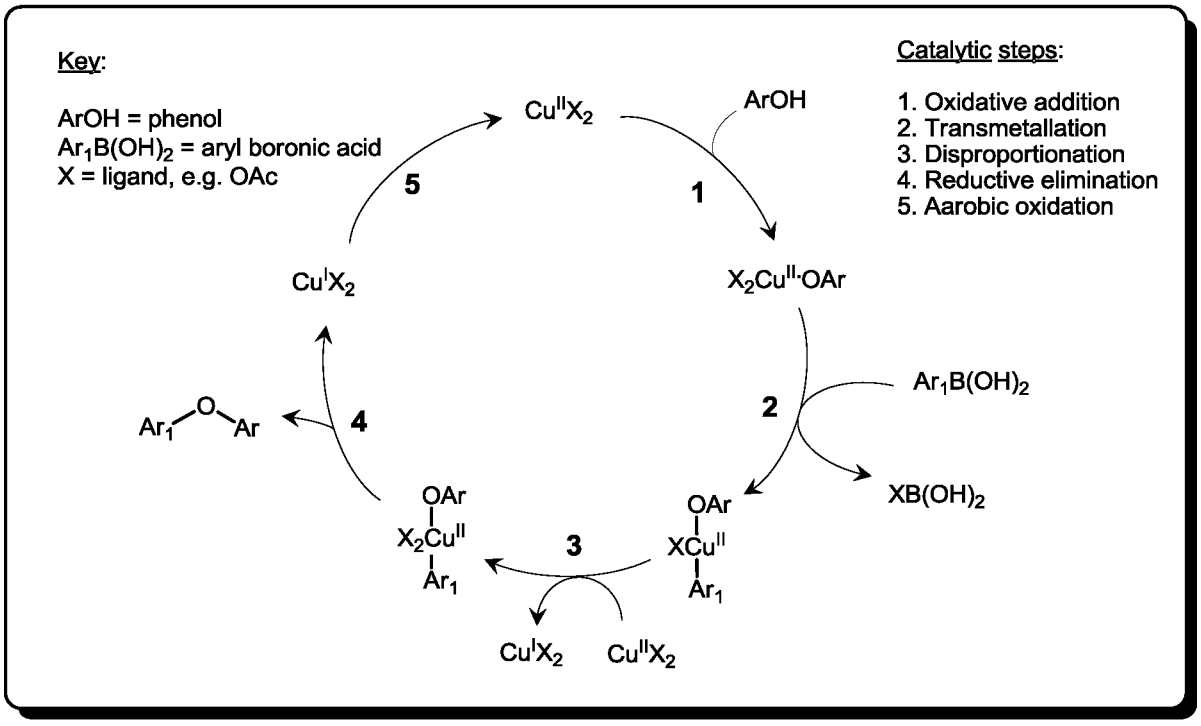

Scheme 2.10: Proposed reaction mechanism of Chan-Lam coupling.[40]

Although there are still many unanswered questions, the proposed mechanism of Chan-Lam etheration is supposed to proceed via a typical redox, organometatalic catalysis (**Scheme 2.10**).[40] The reaction is initiated by oxidative addition of the phenol substrate to the copper(II) salt ($Cu^{II}X_2$) followed by transfer of the aryl of the boronic acid via transmetalation (**Scheme 2.10**). The resultant Cu(II) intermediate undergoes disproportionation by another $Cu^{II}X_2$

equivalent. Reductive elimination of the resultant quaternary intermediate gives the final ether product. The $Cu^{II}X_2$ catalyst gets restored by aerobic oxidation of $Cu^{I}X_2$ from reductive elimination (**Scheme 2.10**).

Etheration of compounds **2.4a-b** was effected using Chan-Lam coupling procedure as reported by Medda *et al.*, which is specific for etheration of hydroxycoumarins.[37] As highlighted in **Scheme 2.11**, compounds **2.4a-b** (1 eq.) were suspended in DCM together with appropriate phenylboronic acids **2.5a-c** (2 eq.) and copper acetate monohydrate ($Cu(OAc)_2 \cdot H_2O$) (1 eq.). Treatment of the suspension with 5 equivalents of triethylamine (Et_3N) resulted in a dark-green solution into which activated powdered 4 Å molecular sieves were immediately added. The reaction solution was stirred under N_2 atmosphere.

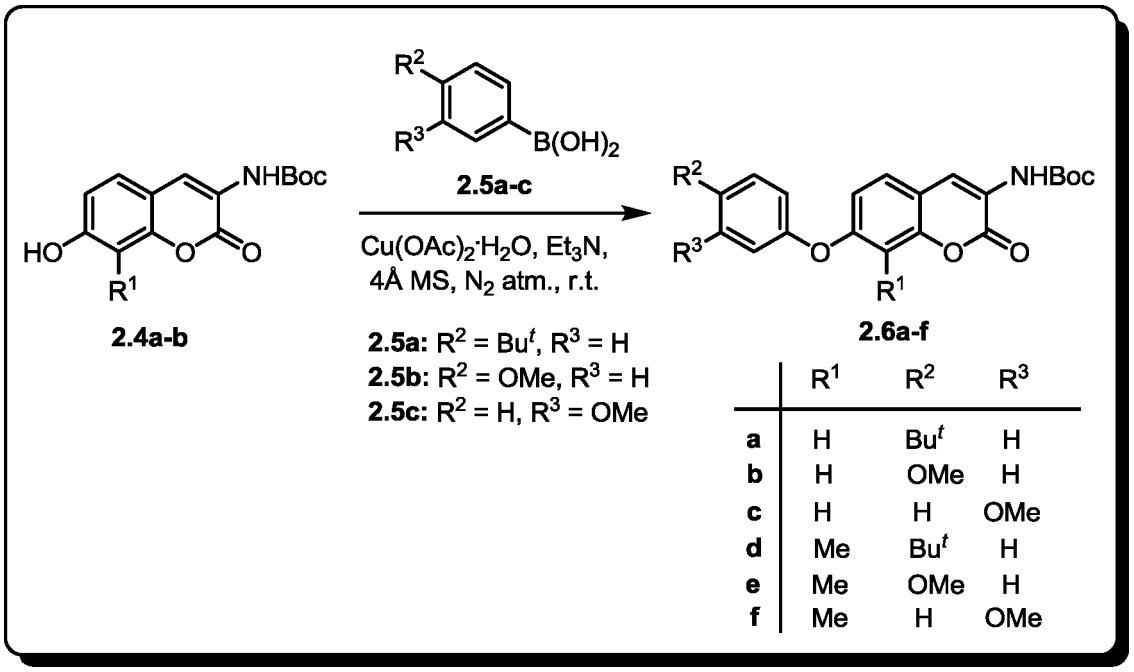

	R^1	R^2	R^3
a	H	Bu^t	H
b	H	OMe	H
c	H	H	OMe
d	Me	Bu^t	H
e	Me	OMe	H
f	Me	H	OMe

Scheme 2.10: Etheration of 7-hydroxycoumarins **2.4a-b** with phenylboronic acids **2.5a-b**.

Whilst all the phenolic starting material had been completely consumed for most boronic acids after 48 hours, as monitored by TLC, the reaction of compound **2.4b** with 4-*tert*-butylphenylboronic acid (**2.5a**) did not go into completion even after 3 days of stirring. This reflected in the product yield since the corresponding phenylated product (**2.6d**) was attained in the lowest yield of 11%. Following purification by silica gel column chromatography, the phenylated products were achieved as white solids in low to moderate yields: 11 – 45% (**Table 2.1**).

Table 2.1: Product yields of Chan-Lam etherification.

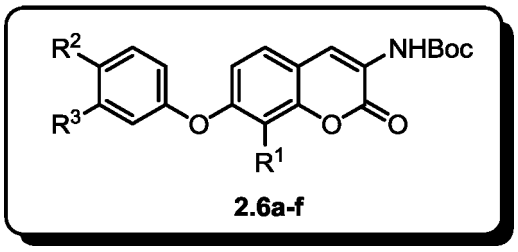

2.6a-f

Entry	Compound	R^1	R^2	R^3	%Yield
1	**2.6a**	H	Bu^t	H	29
2	**2.6b**	H	OMe	H	33
3	**2.6c**	H	H	OMe	23
4	**2.6d**	Me	Bu^t	H	11[a]
5	**2.6e**	Me	OMe	H	38
6	**2.6f**	Me	H	OMe	45

[a]Reaction did not go into completion.

The diminished yields were not a surprise since many side products were noticed upon monitoring the progress of the reaction by TLC. Medda *et al.* also experienced the same issue in their study during the development of this procedure.[37] They further identified phenolic and diaryl ether derivatives of the boronic acid substrates as the major side products. From a mechanistic view-point, the low yields could also be explained by employment of an inert atmosphere, which was necessitated by the sensitivity of the reaction. The catalytic cycle of Chan-Lam coupling involves anaerobic oxidation for the recovery of the active Cu(II) catalyst, i.e. $Cu^{II}(OAc)_2$ (**Scheme 2.10**). Use of an inert atmosphere would imply absent anaerobic oxidation, which would hinder the recovery of $Cu^{II}(OAc)_2$, and thus limit further catalysis of the substrates to form products.

The structures of the phenylated products (**2.6a-f**) were confirmed by ^1H and ^{13}C NMR spectroscopy. Signals of the coumarin nucleus remained unchanged relative to the hydroxycoumarin reactants, **2.4a-b**, in both ^1H and ^{13}C NMR spectra of all products. The broad singlet of the OH group, which resonated below δ 10.00 ppm in ^1H NMR spectra of compounds **2.4a-b**, was not observed in the ^1H NMR spectra of the phenylated products. In addition, appearance of extra signals observed in the aromatic region and intense singlets in the aliphatic region, corresponding to OMe and Bu^t groups, further confirmed successful coupling of the phenyl moieties to the coumarin core at C-7. **Figure 2.5** illustrates the observed signals discussed above.

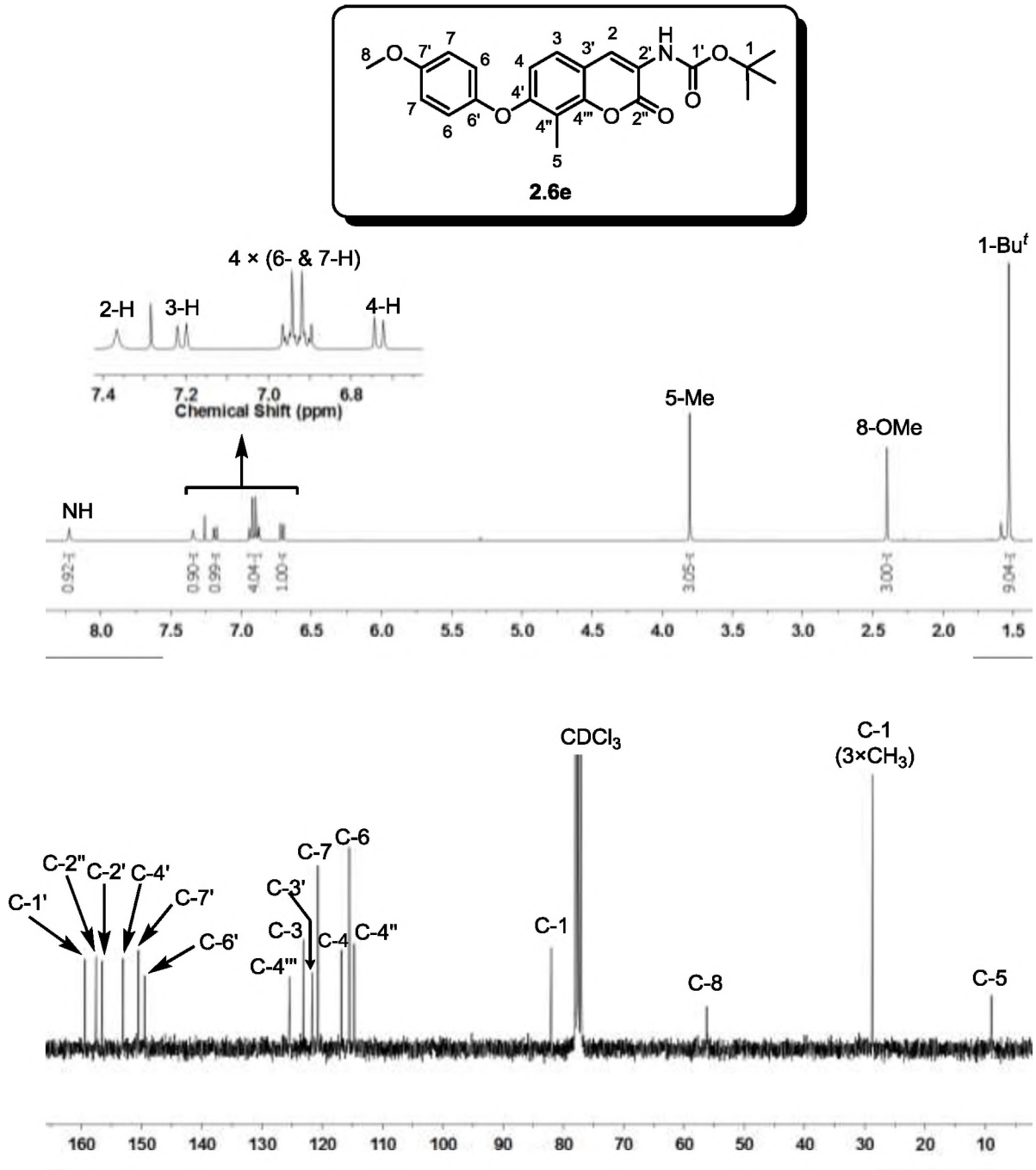

Figure 2.5: ^{1}H and ^{13}C NMR spectra of **2.6e**.

2.2.2.2. *N*Boc-deprotection of phenylated 3-aminocoumarins

The *N*Boc-protected 7-phenyloxy-3-aminocoumarins, **2.6a-f**, were subjected to acidic Boc-deprotection conditions to liberate the amine at C-3 of the coumarin ring. This was achieved facilely by treating compounds **2.6a-f** with commercially available 4M HCl in dioxane solution, and the resulting suspension was stirred at room temperature for 12 hours. As usual,

the progress of the reaction was monitored by TLC. The disappearance of compounds **2.6a-f** on the TLC plate marked complete hydrolysis of the Boc group. Following complete hydrolysis, the thick, milky suspension that resulted was cautiously treated with a small amount of perchloric acid ($HClO_4$) to completely dissolve it. Addition of saturated $NaHCO_3$ solution effected neutralisation of the reaction solution. The products were extracted with DCM, dried over magnesium sulphate ($MgSO_4$) and obtained in good to excellent yields (55 – 99%) as yellow solids after removal of the solvent under reduced pressure (**Table 2.2**). The free 3-aminocoumarins, **2.7d-f**, carrying the methyl group at C-8 (R^1 = Me) were obtained in higher yields than their hydrogen-containing variants, **2.7a-c**. For both 8-H and 8-Me variants, the OMe group of the phenyl ring seemed to effect higher yields than the Bu^t (**Table 2.2**).

Table 2.2: Yields of 7-phenyloxy-3-amicomarins **2.7a-f**.

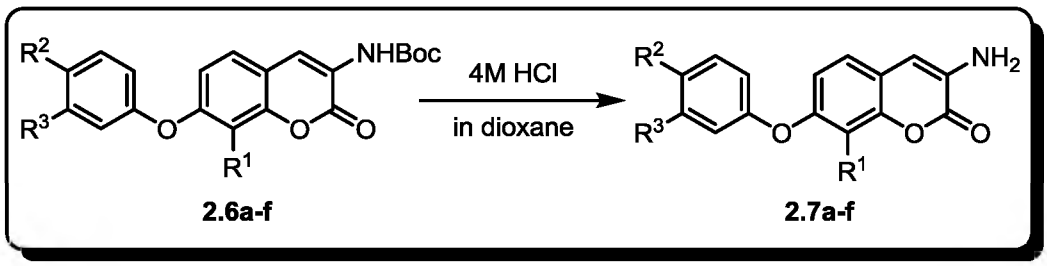

2.6a-f **2.7a-f**

Entry	Compound	R^1	R^2	R^3	%Yield
1	**2.7a**	H	Bu^t	H	53
2	**2.7b**	H	OMe	H	66
3	**2.7c**	H	H	OMe	66
4	**2.7d**	Me	Bu^t	H	76
5	**2.7e**	Me	OMe	H	95
6	**2.7f**	Me	H	OMe	99

Regarding characterisation of the products, successful Boc-deprotection was confirmed by the disappearance of the Boc signals between δ 1.47 and 1.53 ppm of ^1H NMR spectra of products, and appearance of broad singlets indicative of the free amine (NH_2), which resonated at δ 3.80 – 4.20 ppm. The region where the NH_2 group was observed is characteristic of free 3-aminocoumarins as has been observed in literature for this class of compounds.[26, 31]

2.2.2.3. Preparation of biphenyl A

As discussed in the in **Section 1.3** and **Section 1.5**, the biphenyl **A** moiety enhances the anticancer activity of Nb analogues through Hsp90 inhibition. This moiety was included in the current study to produce organic counterparts of the phenylated, novel ferrocenyl Nb analogues

for comparison purposes. These organic derivatives have been previously synthesised and investigated for anticancer activity.[29]

Having successfully coupled the phenyl moieties to position 7 of the coumarin core (required for target analogues) and liberated the 3-NH_2 group of compounds **2.6a-f** in satisfactory yields, the resultant free 7-phenyloxy-3-aminocoumarins (**2.7a-f**) were now ready for coupling with carboxylic acids of Fc and biphenyl **A** via amidation. Before such coupling, biphenyl **A** had to be prepared since it is not commercially available, unlike Fc. This moiety was assembled by employing the palladium-promoted Suzuki coupling method, which is a C–C bond-forming protocol. The synthesis was initiated by ester-protection of the carboxylic acid OH of the commercially available precursor, 3-iodo-3-metoxybenzoic acid **2.8** (**Scheme 2.12**).

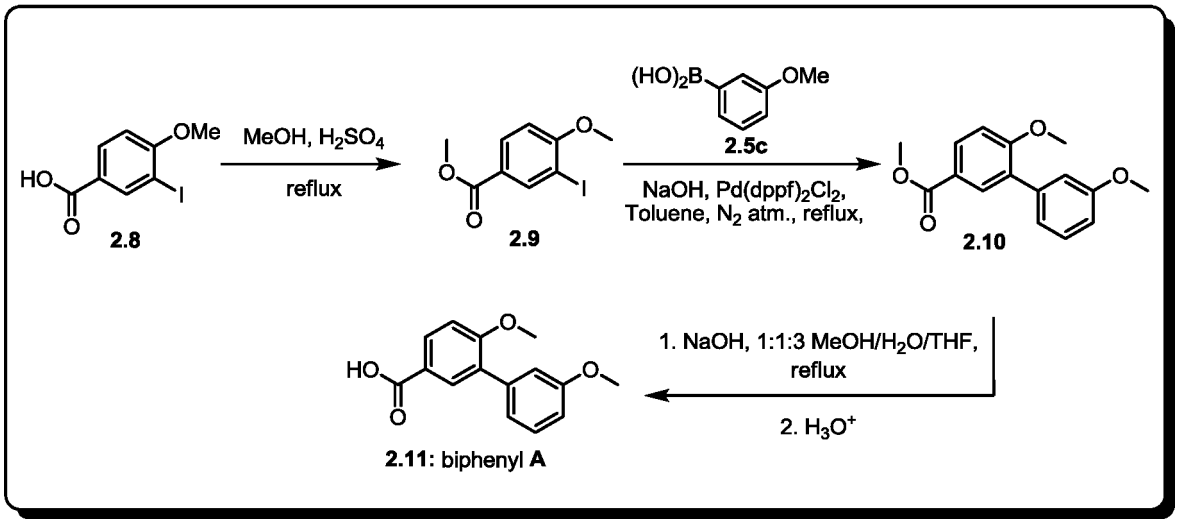

Scheme 2.12: Synthetic route to biphenyl **A**.

Esterification of **2.8** was achieved by conventional acid-catalysed esterification with excess methanol under reflux for 12 hours. The product was attained as an off-white solid after extraction with ethyl acetate (EtOAc) and removal of the solvent, yield: 85%. **Figure 2.6** shows full assignment of proton signals in ^{1}H NMR spectrum of the ester product, **2.9**.

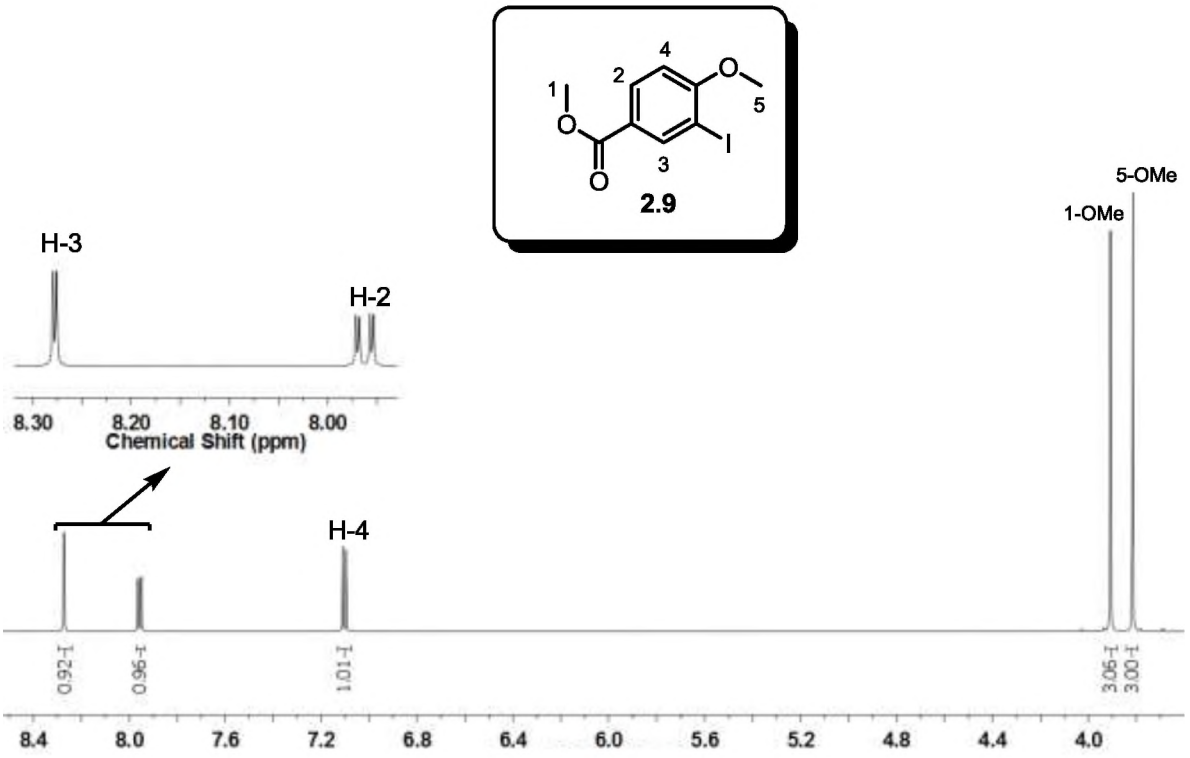

Figure 2.6: ^{1}H NMR spectrum of **2.9**.

Suzuki cross-coupling of ester **2.9** (1 eq.) with boronic acid **2.5c** (3 eq.) was achieved thermally by reflux under N_2 atmosphere to access the biphenyl ester **2.10** in the presence of a palladium catalyst: [1,1'-Bis(diphenylphosphino)ferrocene]dichloropalladium(II), i.e. $Pd(dppf)_2Cl_2$. After 24 hours, complete conversion of **2.9** was noted by its disappearance and formation of a new spot upon monitoring the progress of the reaction by TLC. The product was isolated as a colourless oil in 90% yield after purification by silica gel column chromatography. The most significant features of the ^{1}H NMR spectrum of **2.10** are the appearances of a new methoxy signal at δ 3.82 ppm and new aromatic signals, *viz.*: a triplet (1H) and two multiplets (3H) at δ 7.34 and 6.92 – 7.04 ppm, respectively, which were consistent with the structure of the compound, suggesting successful C–C coupling of **2.5c** with **2.9** (**Figure 2.7**).

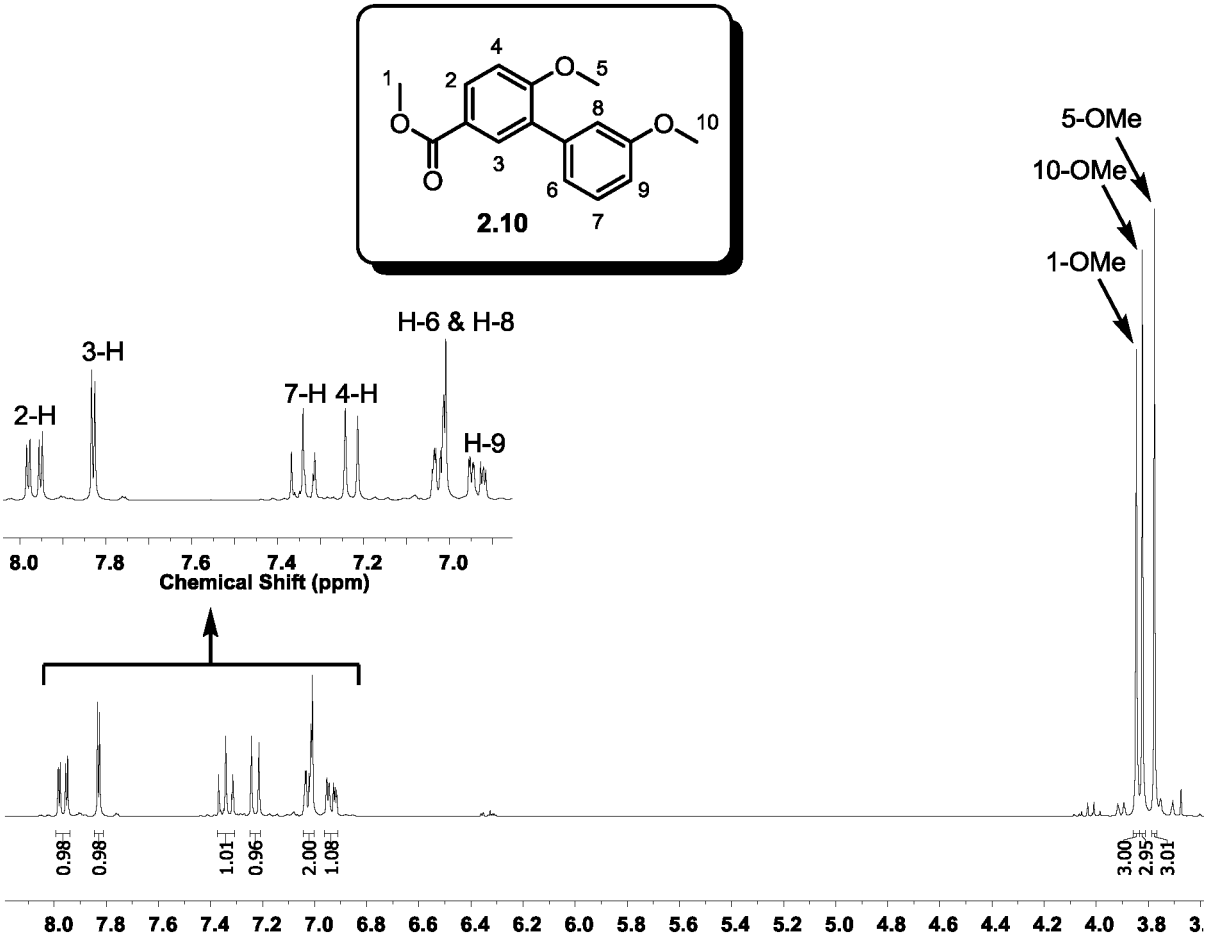

Figure 2.7: ^{1}H NMR spectrum of **2.10**.

The carboxylic acid functionality was recovered by sodium hydroxide (NaOH) hydrolysis of **2.10** in 1:1:3 MeOH/H_2O/THF solvent mixture followed by an acidic workup with HCl solution to give biphenyl carboxylic acid **2.11** in a yield of 89%. The disappearance of the third methoxy signal in the aliphatic region and appearance of the carboxylic acid OH group at δ 12.73 ppm of the ^{1}H NMR spectrum of **2.9** confirmed successful recovery of the carboxylic acid functionality.

2.2.2.4. Synthesis of target phenylated Nb analogues (2.113a-f and 2.14a-f)

With both the carboxylic acids of biphenyl **A** and Fc, and the free 7-phenyloxy-3-aminocoumarins (**2.7a-f**) at hand, the synthesis of target 7-*O*-phenyl Nb analogues (i.e. phenylated analogues) was performed by coupling the respective precursors via amidation (**Scheme 2.13**). The amide bond spans a wide region of the chemical spectrum, from complex macromolecules such as proteins to simple pharmaceutical drugs. It is reported that over 25% of all known drugs approved by the FDA in the United States contain at least one amide bond.[41]

In the context SAR data, the amide functionality is known to be critical for anticancer activity of Nb analogues through Hsp90 inhibition.[28]

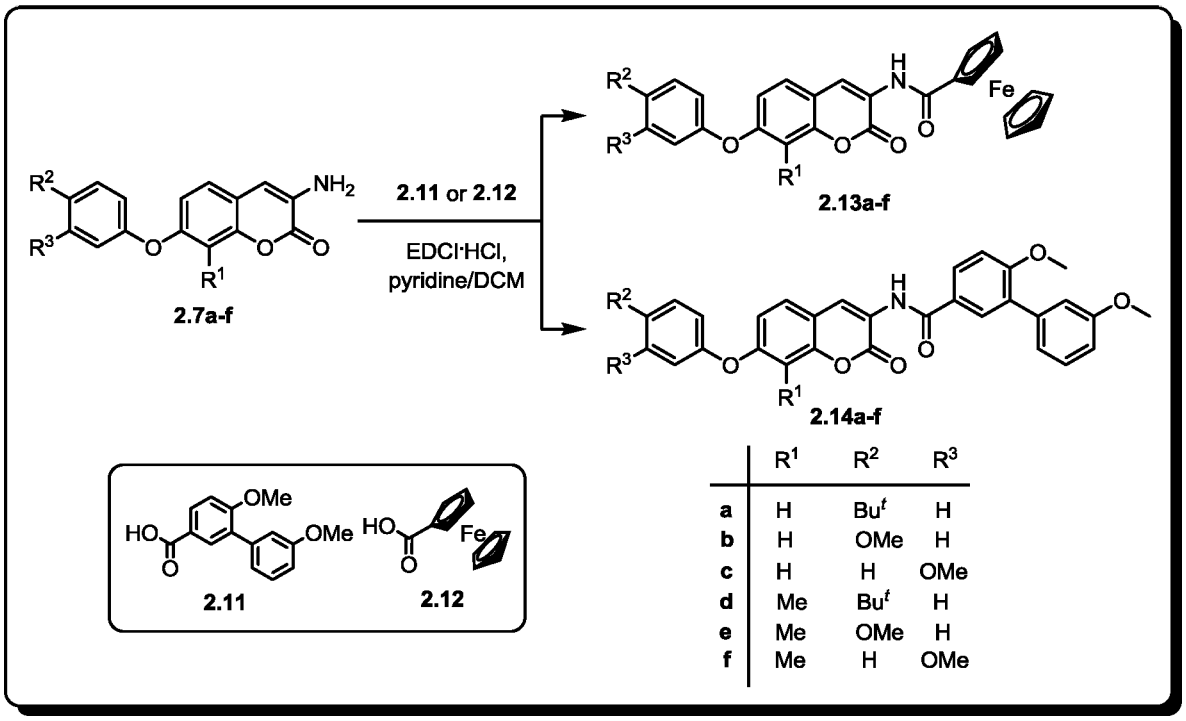

Scheme 2.13: Synthesis of target ferrocenyl (**2.13a-f**) and organic (**2.14a-f**) 7-*O*-phenyl Nb analogues.

Successful preparation of target analogues was effected by EDCI amidation (**Scheme 2.13**).[1] The reaction entailed treating the free 3-aminocoumarins **2.7a-f** with 30% pyridine/DCM solution at room temperature for 10 minutes, followed by addition of 2 equivalents of a relevant diaryl carboxylic acid, biphenyl **A** acid (**2.11**) or ferrocene carboxylic acid (**2.12**), and 3 equivalents of EDC•HCl. Pre-treatment of aminocoumarins with pyridine was necessary to activate the 3-NH_2 of the coumarin substrates. The reaction was further stirred for 1 to 3 days depending on the carboxylic acid used.

The progress of the reaction was monitored by TLC. The formation of ferrocenyl analogues (**2.13a-f**) was terminated after 1 day of stirring as TLC did not indicate any further consumption of the aminocoumarin reactants after 12 hours of stirring. The ferrocenyl analogues were purified by silica gel column chromatography using 10% EtOAc/Hex solvent system after the removal of solvents under reduced pressure. The yields of these analogues ranged between 13 and 45% (**Table 2.3**). Except for **2.13e**, the 8-Me analogues (**2.13d** and **2.13f**) were obtained in higher yields than their respective hydrogen counterparts, i.e. 8-H analogues (**2.13a** and **2.13c**). This could be explained by the influence of the electronic effects of the methyl and

hydrogen groups at C-8 on the reactivity of 3-NH_2 in the coumarin reactants. The methyl being a better electron-releasing group donates higher electron density to the coumarin ring than the hydrogen, and thus activates the 3-NH_2 of 8-Me aminocoumarins (**2.7d-f**) for amidation.

Table 2.3: Yields of phenylated ferrocenyl analogues.

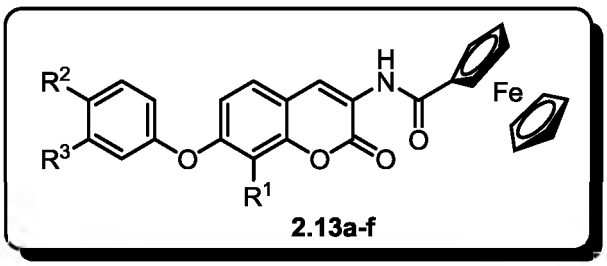

2.13a-f

Entry	Compound	R^1	R^2	R^3	%Yield
1	**2.13a**	H	Bu^t	H	28
2	**2.13b**	H	OMe	H	52
3	**2.13c**	H	H	OMe	41
4	**2.13d**	Me	Bu^t	H	45
5	**2.13e**	Me	OMe	H	19
6	**2.13f**	Me	H	OMe	45

The structures of the products **2.13a-f** were confirmed by the spectroscopic techniques: NMR (^{1}H and ^{13}C NMR), infra-red (IR) and high-resolution mass spectroscopy (HRMS) in addition to CHNS micro-analysis. ^{1}H NMR spectra of **2.13a-f** revealed the characteristic proton signals due to the Fc moiety as two triplets and one singlet between δ 4.26 and 4.87 ppm. The amide NH resonated around δ 8.70 ppm, and was observed at ν 3400 – 3396 cm^{-1} in the IR spectra of the compounds. In ^{13}C NMR spectra, the carbon signals of the cyclopentadienyl (Cp) rings appeared in the range δ 68.5 – 75.2 ppm. The region where the Fc signals were observed for these compounds was concurrent with that of other biologically important ferrocenyl compounds reported in literature for both ^{1}H and ^{13}C NMR spectra.[42, 43] There were no significant changes in the signals of the coumarin and phenyl moieties with respect to the phenylated free 3-aminocoumarin substrates (**2.7a-b**). Representative ^{1}H and ^{13}C NMR spectra of Fc analogues are illustrated by those of **2.13d** in **Figure 2.8** below.

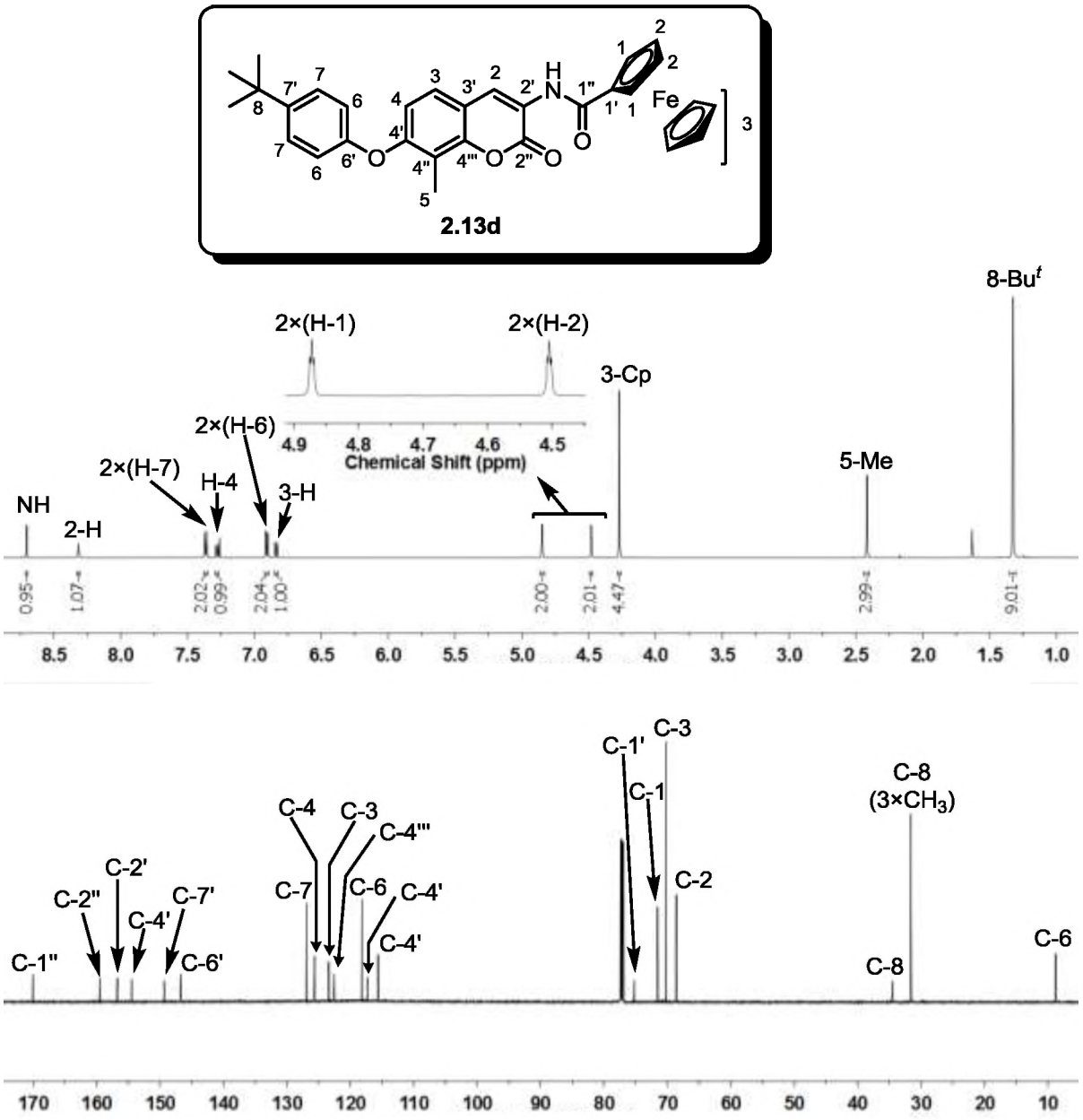

Figure 2.8: ^{1}H and ^{13}C NMR spectra of **2.13d** in $CDCl_3$.

HRMS spectra of the compounds revealed intense signals of the molecular ion peaks $[M+H]^+$ at *m/z*: 522.1381(**2.13a**), 496.0851 (**2.13b**), 496.0835 (**12.13c**), 536.1520 (**2.13d**) and 510.1004 (**2.13e**), which were consistent with the respective structures of the compounds. The computed values of carbon, nitrogen and hydrogen percentage composition of compounds **2.13a-f** for CHNS micro-analysis were in agreement with the observed values (**Table 2.4**).

Table 2.4: Elemental analysis results of phenylated ferrocenyl analogues.

Entry	Compound	Calculated			Found		
		C	H	N	C	H	N
1	**2.13a**	69.11	5.22	2.69	68.23	6.03	2.27
2	**2.13b**	65.47	4.27	2.83	65.54	4.95	2.74
3	**2.13c**	65.47	4.27	2.83	65.88	4.97	2.27
4	**2.13d**	69.54	5.46	2.62	70.23	3.92	2.72
5	**2.13e**	66.03	4.55	2.27	66.77	4.59	2.66
6	**2.13f**	66.03	4.55	2.75	66.46	4.61	2.66

Now turning attention to organic Nb analogues (**2.14a-f**), the conversion of aminocoumarin reactants (**2.7a-f**) was only discernible after 24 hours of stirring as indicated by TLC. The reaction was terminated after 3 days when TLC showed no change in the reaction progress. The crude products obtained after the removal of solvents were purified by preparative TLC. DCM was used as an eluent to develop the preparative TLC plates spotted with the crude products (reconstituted in THF). The bands of the products were collected and recovered with DCM to yield the desired compounds as off-white and yellow solids in modest to average yields (**Table 2.5**). As with Fc analogues, the organic 8-Me analogues (**2.14d-f**) were effected in higher yields than their 8-H derivatives (**2.14a-c**), possibly for the same reasons.

Table 2.5: Yields of phenylated organic analogues.

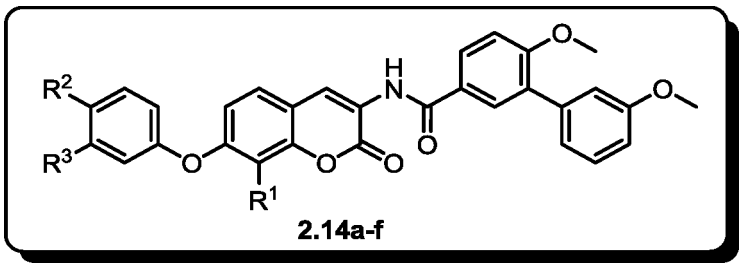

2.14a-f

Entry	Compound	R^1	R^2	R^3	%Yield
1	**2.14a**	H	Bu^t	H	37
2	**2.14b**	H	OMe	H	13
3	**2.14c**	H	H	OMe	27
4	**2.14d**	Me	Bu^t	H	55
5	**2.14e**	Me	OMe	H	71
6	**2.14f**	Me	H	OMe	45

The organic novobiocins (**2.14a-f**) were characterized in a similar manner as the ferrocenyl analogues (**2.13a-f**). Successful amide coupling was confirmed by the appearance of the amide NH signal around δ 8.20 ppm in the ^{1}H NMR spectra of these compounds. Analysis of the IR spectra of each compound revealed a sharp band in the range *v* 3366 – 3405 cm^{-1}, which is characteristic of the amide N-H stretch. The proton signals of the biphenyl **A** moiety overlapped with those of the coumarin nucleus and phenyl units in the aromatic region of both ^{1}H and ^{13}C NMR spectra of the products as exemplified in **Figure 2.9**.

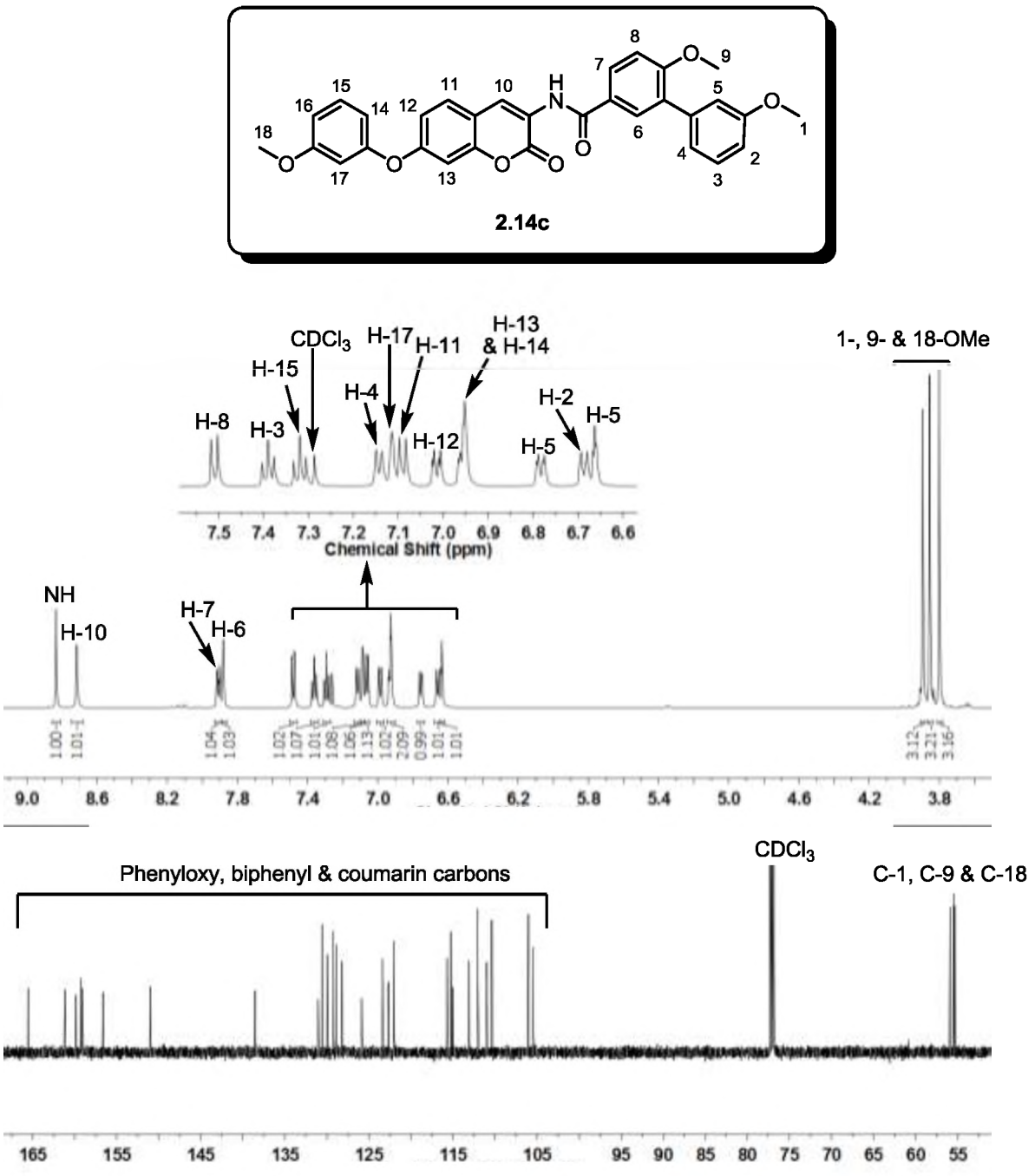

Figure 2.9: ^{1}H and ^{13}C NMR spectra of **2.14a**.

The observed elemental analysis values of the organic Nb analogues were consistent with the calculated values (**Table 2.6**). The base peaks were observed as intense signals at *m/z*: 550.2216 (**2.14a**), 524.1700 (**2.14b**), 524.1714 (**2.14c**), 564.2377 (**2.14d**), 538.1881 (**2.14e**) and 538.1852 (**2.14f**), respectively, in HRMS spectra of **2.14a-f**. These were coherent with the structures of these compounds.

Table 2.6: CHNS micro-analysis data of organic Nb analogues.

Entry	Compound	Calculated			Found		
		C	H	N	C	H	N
1	**2.14a**	74.30	5.69	2.55	74.63	5.95	2.66
2	**2.14b**	71.12	4.81	2.68	70.44	4.84	2.27
3	**2.14c**	71.12	4.81	2.68	71.62	5.25	2.53
4	**2.14d**	74.58	5.90	2.46	74.07	4.95	2.61
5	**2.14e**	71.50	5.06	2.61	70.14	4.61	2.60
6	**2.14f**	71.50	5.06	2.61	70.17	5.19	2.61

2.2.2.5. Attempted amidation procedures

Before successful amidation with EDCI via the method employed above, various amidation protocols had been attempted to access the target analogues. Among such attempts was amidation with activated acyl derivatives of carboxylic acids **2.11** and **2.12** (**Scheme 2.14**).

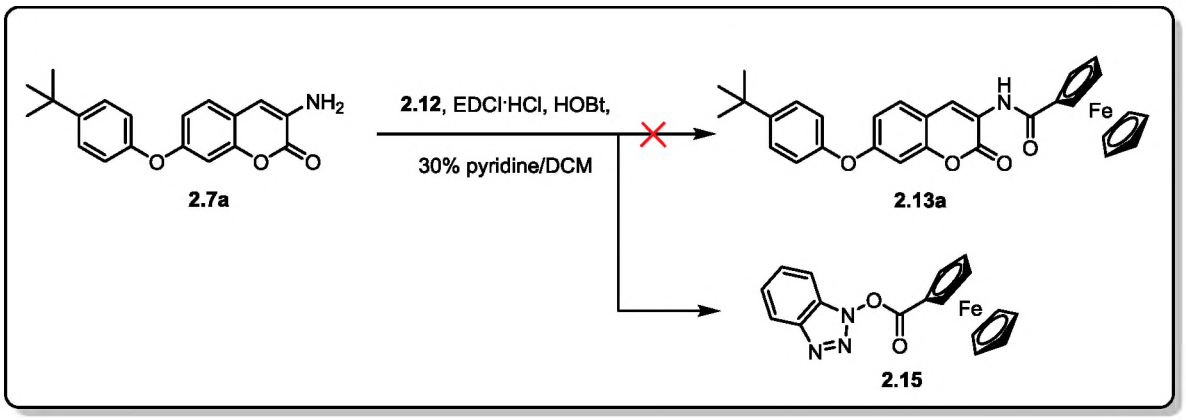

Scheme 2.14: Attempted amidation of **2.7a** with **2.11** by acyl activation with HOBt.

Amidation by acyl chloride activation of biphenyl **A** acid **2.12** for coupling with free 3-aminocoumarin derivatives for preparation of a different library of Nb analogues investigated for anticancer activity was reported by Zhao *et al.*[44] Though the procedure for activation of the acid was not fully disclosed, it was reported to have been effected with thionyl chloride

($SOCl_2$). In our case, conversion of both acid **2.11** and **2.12** was attempted by refluxing them with excess $SOCl_2$ or in equimolar ratios in DCM. However, the products could not be isolated since they turned into insoluble pasty materials upon removal of the solvents. Formation of the acyl chloride *in situ* by stirring the free amines **2.7a-f** with the resultant pasty materials (reconstituted in 50% pyridine/DCM solution) did not give the desired amide products either. Attempted amidation with HOBt exclusively yielded the activated acid derivatives instead of the desired products even after two days of stirring with the aminocoumarin substrates (**2.7a-f**). **Figure 2.6** shows the ^{1}H NMR spectrum of an HOBt-activated Fc acid, **2.15**.

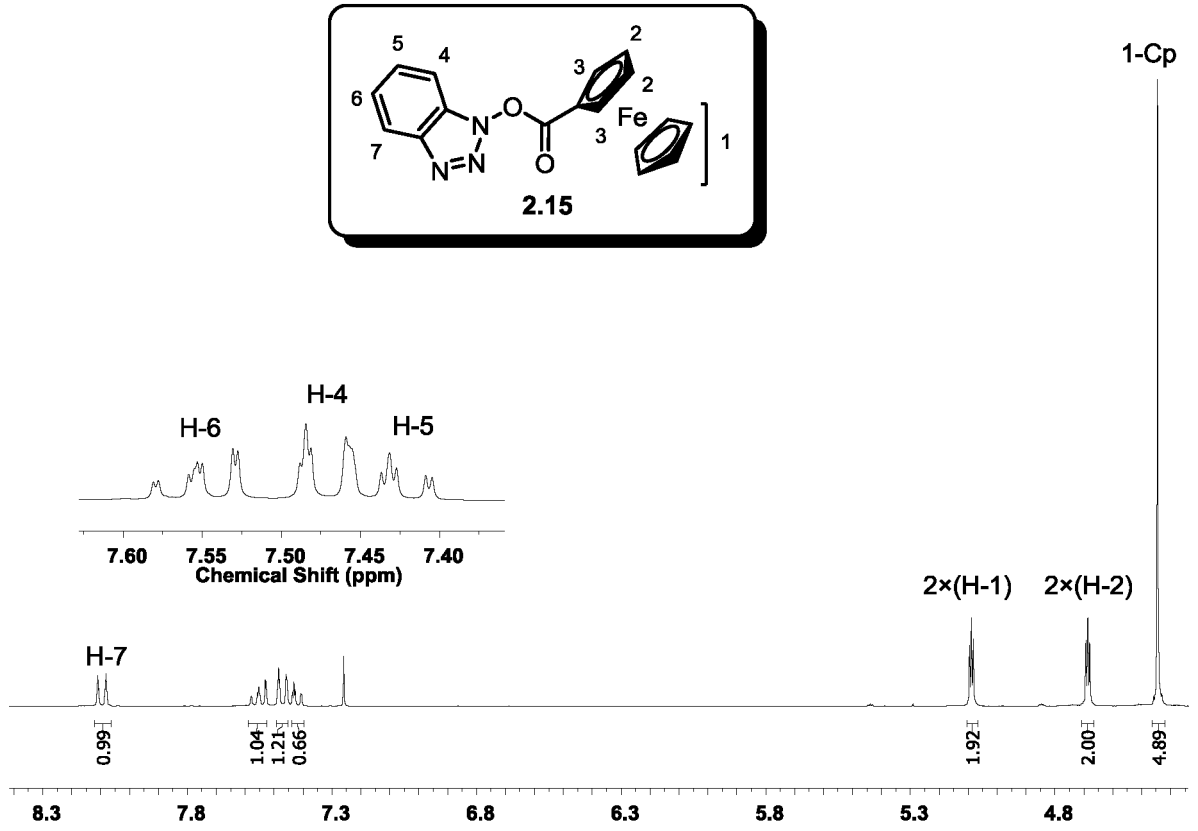

Figure 2.10: ^{1}H NMR of HOBt-activated Fc carboxylic acid, **2.15**.

2.2.3. Synthesis of target piperidinyl Nb analogues

Upon biological screening of the phenylated Nb analogues (**2.13a-f** and **2.14a-f**), it was discovered that these compounds were only sparingly soluble in DMSO, which was used as a solvent in the bioassays. It was postulated that the observed poor aqueous solubility could have been an effect of the hydrophobic phenyl moieties appended at C-7 of the analogues, and somewhat limited their biological activity. Based on this, we envisaged displacing the phenyl moieties with more hydrophilic motifs for better aqueous solubility and improved biological activity (presumably) whilst retaining the steric bulk in position 7.

To realize this, 3'- and 4'-*N*-methyl or -*N*Boc or -NH substituted piperidinols (**2.15a-d**) were selected as replacements of the phenyl motifs since they are both cyclic (for steric bulk) and contain polar NMe and NH groups that participate in H-bonding and are known to be favourable for aqueous solubility (**Figure 2.11**). The *N*Boc-protected piperidinols (**2.15e-f**) were prepared from commercially available NH-containing piperidinols (**2.15c-d**) using the first step of the procedure described for the synthesis of *N*-Boc 7-hydroxy-3-aminocoumarins (**2.4a-b**) (**Section 2.2.1**). It is also noteworthy that these motifs have been shown to retain the efficacy of Nb analogues against cancer cell lines through Hsp90 inhibition as noted in **Section 1.3**.[27, 28]

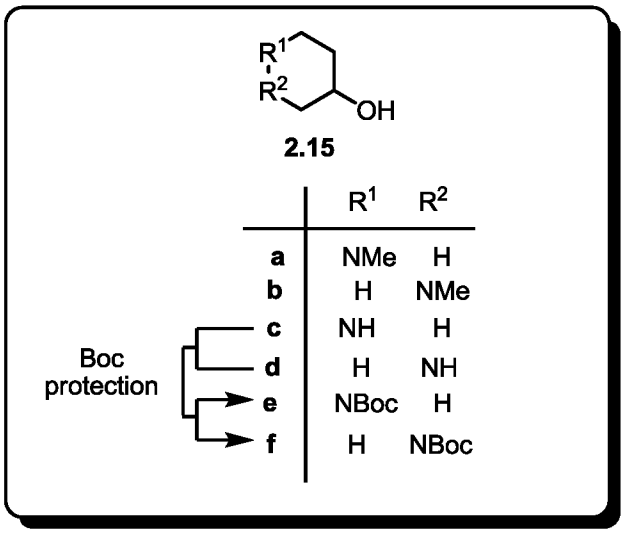

Figure 2.11: Piperidinols selected as replacements of phenyl moieties.

The synthesis of target piperidinyl analogues was envisaged as highlighted in **Scheme 2.15**, commencing with the benzylation of *N*-Boc 7-hydroxy-3-aminocoumarins, **2.4a-b**. This route involved protection of the hydroxyl at C-7, which would later be recovered for coupling of the desired pipiridinyl moieties after attachment of the diaryl units (Fc and biphenyl **A**).

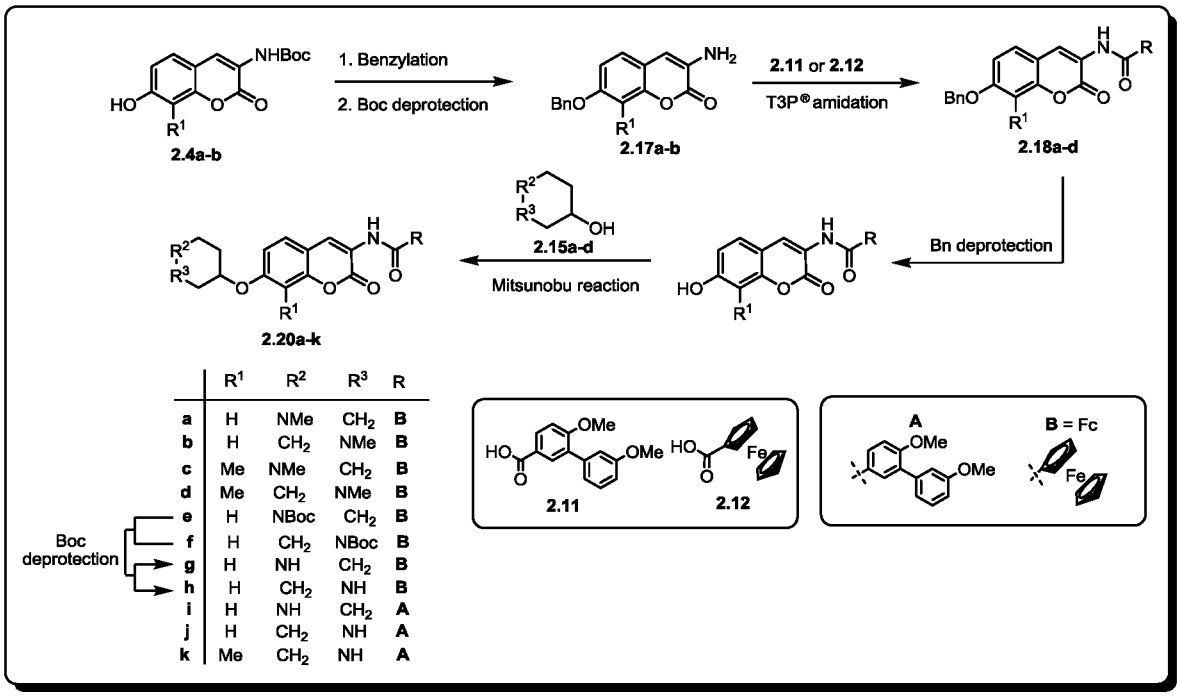

	R^1	R^2	R^3	R
a	H	NMe	CH_2	B
b	H	CH_2	NMe	B
c	Me	NMe	CH_2	B
d	Me	CH_2	NMe	B
e	H	NBoc	CH_2	B
f	H	CH_2	NBoc	B
g	H	NH	CH_2	B
h	H	CH_2	NH	B
i	H	NH	CH_2	A
j	H	CH_2	NH	A
k	Me	CH_2	NH	A

Scheme 2.15: Synthetic route to target piperidinyl Nb analogues, **2.19a-k**.

2.2.3.1. Preparation of benzyl-protected 3-aminocoumains (2.16a-b)

The benzylation reaction was performed conventionally by refluxing equimolar amounts of **2.4a-b** and benzylbromide in acetone in the presence of excess potassium carbonate (K_2CO_3) (4.0 eq.). Purification of the crude products by silica gel column chromatography yielded the pure compounds **2.16a-b** (not shown in **Scheme 2.15**) in excellent yields: 88 – 93%, as white solids. ^{1}H NMR spectra of the benzylation products revealed five extra aromatic proton signals in the aromatic region overlapping with the coumarin protons, and the methylene group (CH_2) resonating around δ 5.00 ppm. This confirmed successful benzylation of the phenolic coumarins as exemplified by **Figure 2.12**.

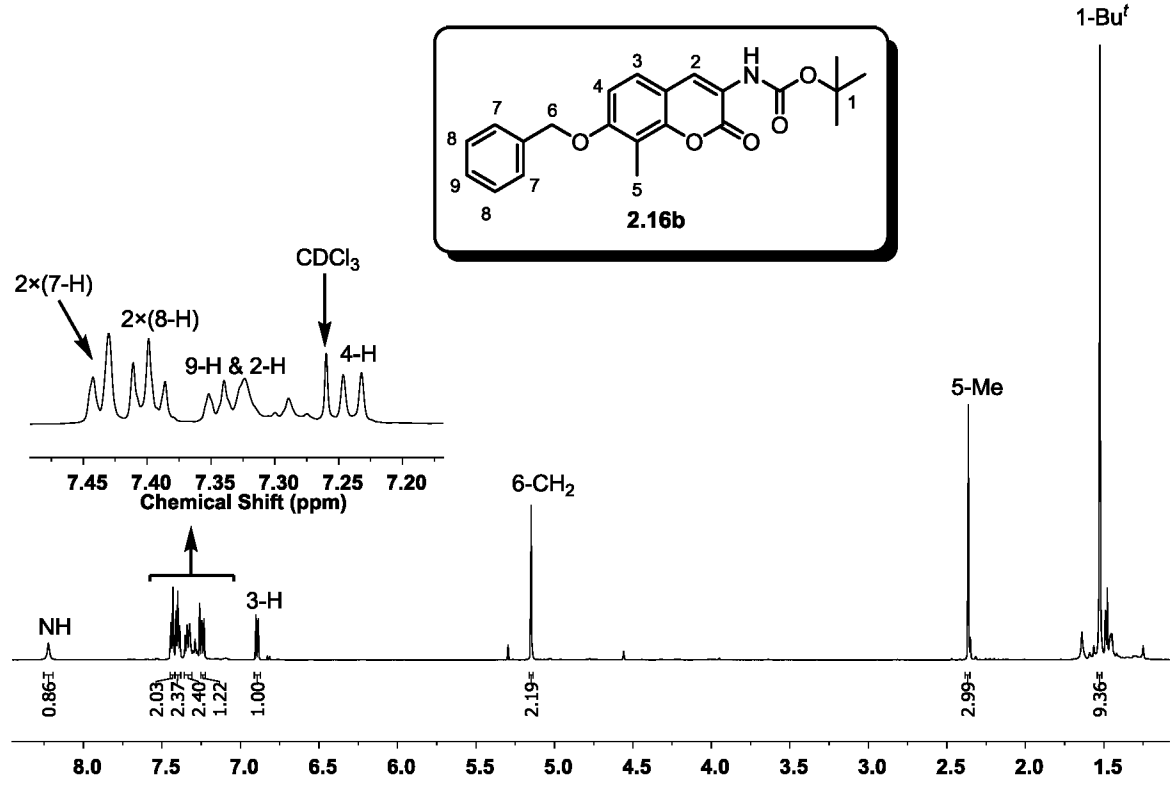

Figure 2.12: ^{1}H NMR spectrum of **2.16b**.

Before coupling of the Fc and biaryl **A** moieties, compounds **2.16a-b** were Boc-deprotected as previously highlighted for preparation of free 7-phenyloxy-3-aminocoumarins (**2.17a-b**) in the synthesis of phenylated Nb analogues (**Section 2.2.2.2**). Successful removal of the Boc group was confirmed by the disappearance of the Boc-signals in both ^{1}H and ^{13}C NMR spectra of the products (**2.17a-b**), which were accessed as yellow solids in good to excellent yields. Whilst the reaction of **2.16a** proceeded smoothly and exclusively afforded **2.17a** (as monitored by TLC) in high purity and yield (93%), conversion of **2.16b** was achieved with some difficulty and required warming the suspension in a water bath (at ~50 °C) for an hour. Formation of side products was also observed on the TLC plate for this conversion. Hence, the product **2.17b** was purified by silica gel flash column chromatography and accessed in a lower yield of 71%.

Following liberation of 3-NH_2, the diaryl acids (**2.11** and **2.12**) had to be appended on the benzamide side (RHS) of the coumarin core for preparation of target analogues. Unlike the synthesis of the phenylated analogues (**2.13a-f** and **2.14a-f**), which was achieved in one step via EDCI amidation (in low yields) after liberation of 3-NH_2, the synthetic route envisaged for preparation of the piperidinyl analogues required 2 – 3 steps after amidation to access the target compounds (**2.20a-k**) (**Scheme 2.15**). For this reason, EDCI coupling could not be employed

since it would afford the amidation products (**2.18a-d**) in low yields and would further diminish the amounts of products as substrates in the succeeding steps leading to the final Nb analogues (**2.20a-k**). As a result, a better-yielding amidation protocol using a peptide coupling reagent, *n*-propylphosphonic anhydride (T3P®), was employed and it is discussed below.

2.2.3.2. Amidation with *n*-propylphosphonic acid (T3P®)

As the name suggests, *n*-propylphosphonic anhydride is the anhydride derivative of propylphosphonic acid under the trade name T3P® (**Figure 2.13**). It was developed in 1980s exclusively for peptide synthesis, but over the years it has found application in other areas of chemistry including dehydration chemistry and synthesis of functionalised heterocycles.[25, 45] T3P® amidation offers many benefits such as low toxicity, milder reaction conditions, lack of shock sensitivity, and wide substrate applicability (including epimerization-prone substrates) and offering high product yields.[25, 45] It was selected in this study for the amide-coupling of free 7-*O*-benzyl-3-aminocoumarins (**2.17a-d**) with acids **2.11** and **2.12** mainly because of its high-yielding quality.

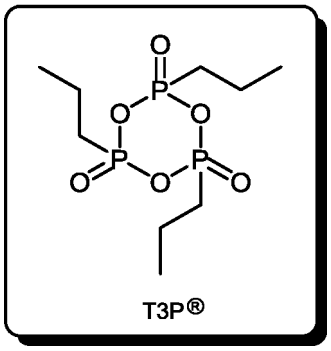

Figure 2.13: Structure of *n*-propylphosphonic anhydride (T3P®).

T3P® amidation was initially carried out by suspending stoichiometric amounts of free 3-aminocoumarin **2.17a** and acids **2.12** in 1:2 pyridine/EtOAc solvent mixture on ice followed by the addition of commercially available 50% T3P®/EtOAc solution (2.0 eq.), which were stirred at 0 °C for 24 hours as reported by Dunetz *et al.* for amidation of epimerization-prone substrates.[45] As in the previous cases, the reaction progress was monitored by TLC. After 24-hour stirring, TLC indicated no consumption of substrates nor formation of the products.

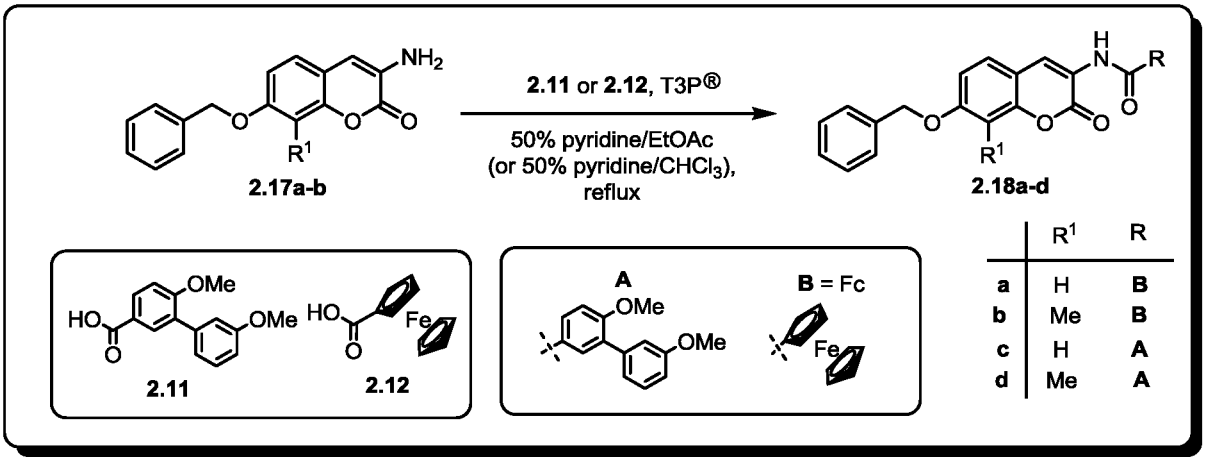

Scheme 2.16: T3P® amidation of **2.18a-d**.

This problem was solved by refluxing the reaction mixture at 75 °C, still following the reaction progress with TLC (**Scheme 2.16**). Transformation of the substrates to the amide products was noticed after 12 hours of stirring as spots of the substrates became faint and a new spot visible. The reaction was terminated after 24 hours and the solvents were removed *in vacuo* to give the crude products. Purification of the crude products by silica gel column chromatography afforded compound **2.18a** as an orange solid in moderate yield of 50% (nearly unsatisfactory). The yield was improved by changing the major solvent from EtOAc to chloroform (**Scheme 2.16**), which gave **2.18a** in 80% yield. This modification was employed for synthesis of the remaining amides **2.18b-d**, including the organic derivatives (**Table 2.7**).

Table 2.7: Product yields of T3P® amidation.

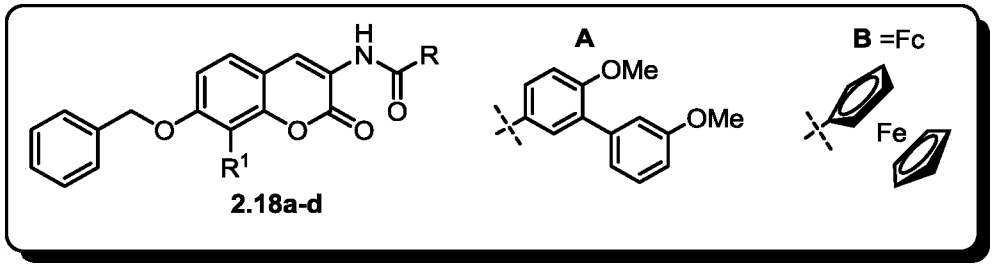

Entry	Compound	R^1	R	%Yield
1	**2.18a**	H	B	80
2	**2.18b**	Me	B	68
3	**2.18c**	H	A	50
4	**2.18d**	Me	A	42

The ferrocenyl amides, **2.18a-b**, were obtained in higher yields than their organic derivatives, **2.18c-d**. Interestingly, the 8-H variants (containing a lesser EDG) were effected in better yields than their respective 8-Me counterparts. This was contrary to the observation made for the amidation with EDCI for preparation of phenylated Nb analogues (**2.13a-f** and **2.14a-f**) in **Section 2.2.2.4**.

The structures of the products (**2.18a-d**) were confirmed as was done for phenylated Nb analogues. The ferrocene signals were observed in the same region in the ^{1}H and ^{13}C NMR spectra of **2.18a-b**, as exemplified in **Figure 2.10**, confirming successful coupling of acid **2.11** to free 3-aminocoumarins (**2.17a-b**). The organic derivatives (**2.18c-d**) revealed signals of the biphenyl moiety as was observed for the organic, phenylated Nb analogues (**Section 2.2.4**). Except for **2.18a**, the base peaks in HRMS spectra of compounds **2.18c-d** were observed as intense signals at *m/z*: 494.1056 (**2.18b**), 507.1682 (**2.18c**) and 521.1838 (**2.18d**), which was consistent with their molecular masses $[M+H]^{+}$. Although **2.18a** had a base peak with only ~5% peak intensity at *m/z* 480.0905, its fragmentation pattern (removal of the benzyloxy group at C-7) corresponded with the signal observed at *m/z* 373.1766, thus confirming its structure.

2.2.3.3. Synthesis of 7-hydroxy Nb analogues (2.19a-d)

To couple the piperidinols (**2.15a-d**) to C-7 of the coumarin ring for synthesis of target analogues, the benzyl group of the benzylated Nb analogues (**2.18a-d**) was removed by facile palladium-promoted hydrogenolysis using 10% mol palladium on carbon (Pd/C) as a catalyst. After stirring compounds **2.18a-d** with 10% mol Pd/C in THF for 12 hours at room temperature (monitored by TLC), the products were filtered through a small pad of silica gel and eluted with EtOAc to remove Pd/C. The collected filtrates were concentrated *in vacuo* to the give the 7-hydroxy Nb analogues (**2.19a-d**) in yields of: 93% (**2.19a**), 33% (**2.19b**), 70% (**2.19c**) and 40 % (**2.19d**). Successful de-benzylation was indicated by the disappearance of the benzyl signals in both ^{1}H and ^{13}C NMR spectra of the resulting compounds (**2.19a-d**) in the aromatic and methylene regions. A broad band was also observed in the IR spectra of these compounds at ν 3228 – 3258cm^{-1}, indicating presence of the hydroxyl group (**Figure 2.14**).

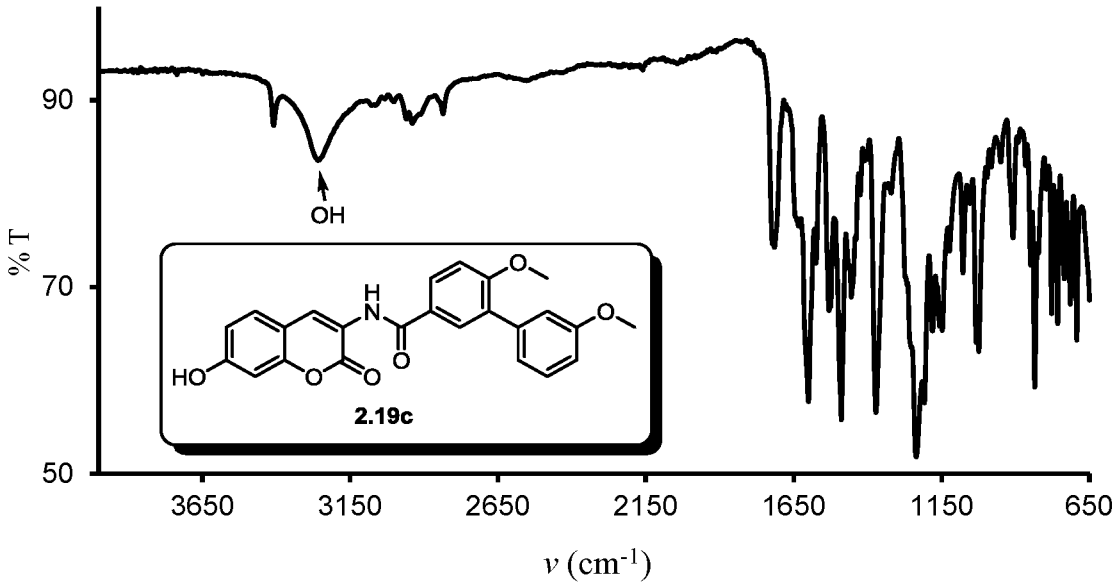

Figure 2.14: IR spectrum of **2.19c**.

Except for **2.19b** whose structure was confirmed by analysis of its fragmentation pattern, the HRMS data of the other compounds (**2.19a** and **2.19c-d**) revealed base peaks which were consistent with their proposed structures as shown in **Table 2.8**.

Table 2.8: HRMS data of 7-hydroxy Nb analogues.

Entry	Compound	Expected (M)	Found $[M+H]^+$
1	**2.19a**	389.0351	390.0392
2	**2.19b**	403.0507	413.2609[a]
3	**2.19c**	417.1212	418.1270
4	**2.19d**	431.1369	432.1434

[a]Confirmed by analysis of compound's fragmentation pattern.

2.2.3.4. Synthesis of target piperidinyl Nb analogues (2.20a-k)

Having successfully acquired the 7-hydroxy Nb analogues, **2.19a-d**, in satisfactory yields (33 – 93%), piperididinols (**2.15a-d**) were coupled to C-7 via Mitsunobu etheration. The Mitsunobu reaction was originally developed for the coupling of primary and secondary alcohols with aldehydes to form esters in the presence of azodicarboxylates, *viz.*: diethyl azodicarboxylate (DEAD) and diisopropyl azodicarboxylate (DIAD), and triphenyl phosphine (PPh_3) (**Scheme 2.16**).[46] Over the years, the application of the reaction has been expanded to include preparation of ethers, thioethers and amines from compounds with active protons like phenols and carboxylic acids.[46]

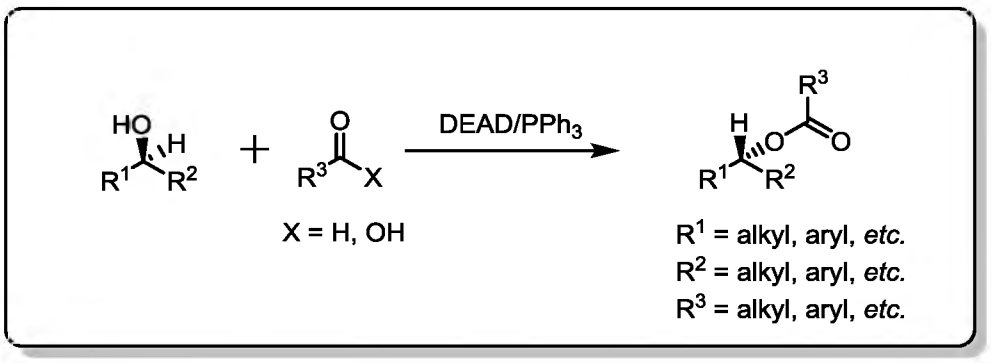

Scheme 2.17: Mitsunobu esterification.

In our case, the Mitsunobu reaction was employed to append piperidinols (**2.15a-d**) to C-7 of the phenolic 7-hydroxy Nb analogues, **2.19a-d**, using DIAD and PPh_3 to effect the final piperidinyl Nb analogues (**Scheme 2.17**). The synthesis of 3'- and 4'-*N*-methyl analogues was achieved in a single step, whereas that of NH-containing analogues required an additional *N*Boc-deprotection step. The reaction was performed by stirring a suspension of equimolar amounts of the phenolic substrates (**2.19a-d**) and 3'- or 4'-*N*-methyl or -*N*Boc piperidinols (**2.15a-c** and **2.15e-f**), and PPh_3 (2.0 eq.) in anhydrous THF in an ice-bath following addition of DIAD (2.0 eq.). The course of the reaction was monitored by TLC. Following termination of the reaction after 5 hours, the reaction mixture was concentrated under reduced pressure and the resulting residue resolved by silica gel column chromatography or preparative TLC.

The 3'- and 4'-NMe or -*N*Boc piperidinyl ferrocenyl Nb analogues (**2.20a-f**) were purified by column chromatography (5% MeOH/DCM) and obtained as orange and red solids in very low to modest yields (**Table 2.9**). These compounds were characterized similarly to the benzyloxy (OBn) and hydroxyl (OH) Nb analogues (**2.18a-d** and **2.19a-d**).

Table 2.9: Isolated yields of 3'- and 4'-*N*-methyl and -*N*Boc Fc-Nb analogues (**2.20a-f**).

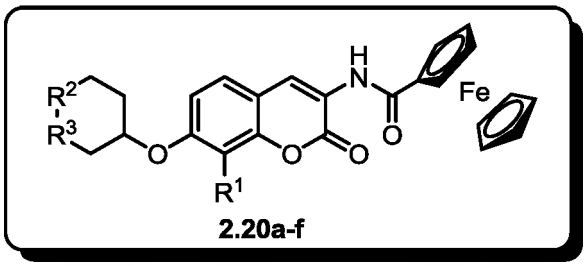

2.20a-f

Entry	Compound	R^1	R^2	R^3	%Yield
1	**2.20a**	H	NMe	H	41
2	**2.20b**	H	H	NMe	37
3	**2.20c**	Me	NMe	H	22
4	**2.20d**	Me	H	NMe	38
5	**2.20e**	H	*N*Boc	H	37
6	**2.20f**	H	H	*N*Boc	41

Successful etheration was indicated by the disappearance of the broad band in the IR spectra of products, which had been observed at ν 3228 – 3258 cm^{-1} for the phenolic reactants (**2.19a-b**) (**Figure 2.15**). This indicated the hydroxyl group was no longer present in the products.

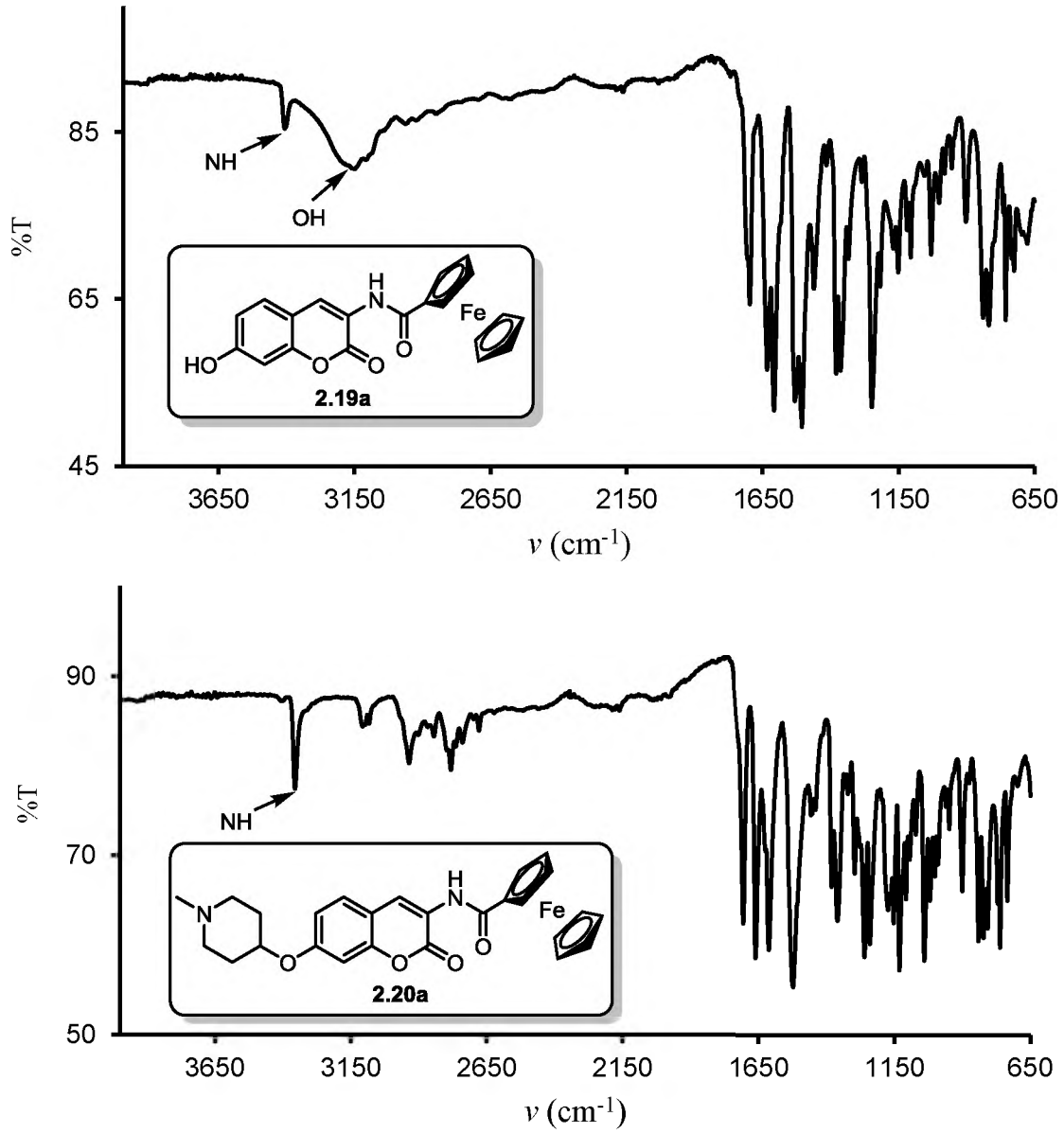

Figure 2.15: IR spectra of **2.19a** and **2.20a**.

Furthermore, ^{1}H and ^{13}C NMR spectra of the products revealed the piperinyl CH_2 peaks in the aliphatic region similarly to other piperidinyl Nb analogues reported in literature, therefore confirming successful attachment of the piperidinyl moieties.[27, 28] For the 4'-substituted piperidinyl analogues (**2.20a**, **2.20c** and **2.20e**), the cyclic CH_2 protons resonated at δ 1.77 – 2.75 ppm as broad multiplets, each integrating to 2 hydrogens. Multiplets of protons of the CH_2s attached to the nitrogen were slightly de-shielded (δ 3.35 – 3.73 ppm) for the 4'-*N*Boc derivative (**2.20e**) as has been observed in literature (**Figure 2.16**).[27] This de-shielding was possibly due to the presence of the amide functionality which draws electron density away from the CH_2s, causing them to resonate at higher chemical shifts (**Figure 2.16**).[27] The

piperidinyloxy CH resonated in the ferrocene region between δ 4.40 and 4.57 ppm as indicated in the ^{1}H NMR spectrum of compound **20.20e**. This was not the case with the 3'-*N*Boc derivative (**2.20f**).

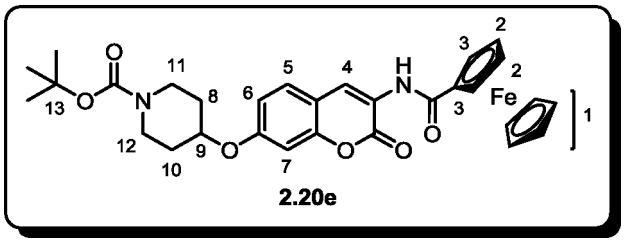

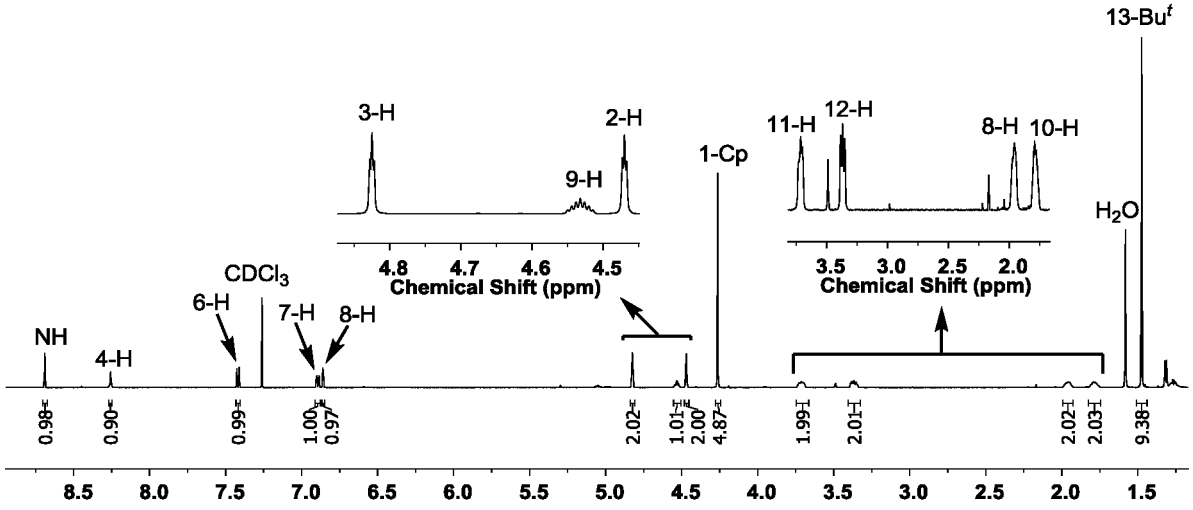

Figure 2.16: ^{1}H NMR spectrum of **2.20e**.

The 3'- and 4'-*N*Boc piperidinyl Fc analogues, **2.20e-f**, were further subjected to Boc-deprotection with 10% TFA/DCM solution to afford their corresponding 3'- and 4'-NH piperidinyl products (**2.20g-h**) in high purity and yields (95 – 97%). **Figure 2.17** shows ^{1}H NMR spectrum of **2.20h**, highlighting successful removal of the Boc group as indicated by the appearance of a multiplet at δ 5.84 ppm (corresponding to the NH) and disappearance of the Boc signals in the aliphatic region. These observations were consistent with the spectra of other 3'- and 4'-NH piperidinyl Nb analogues reported in literature.[27]

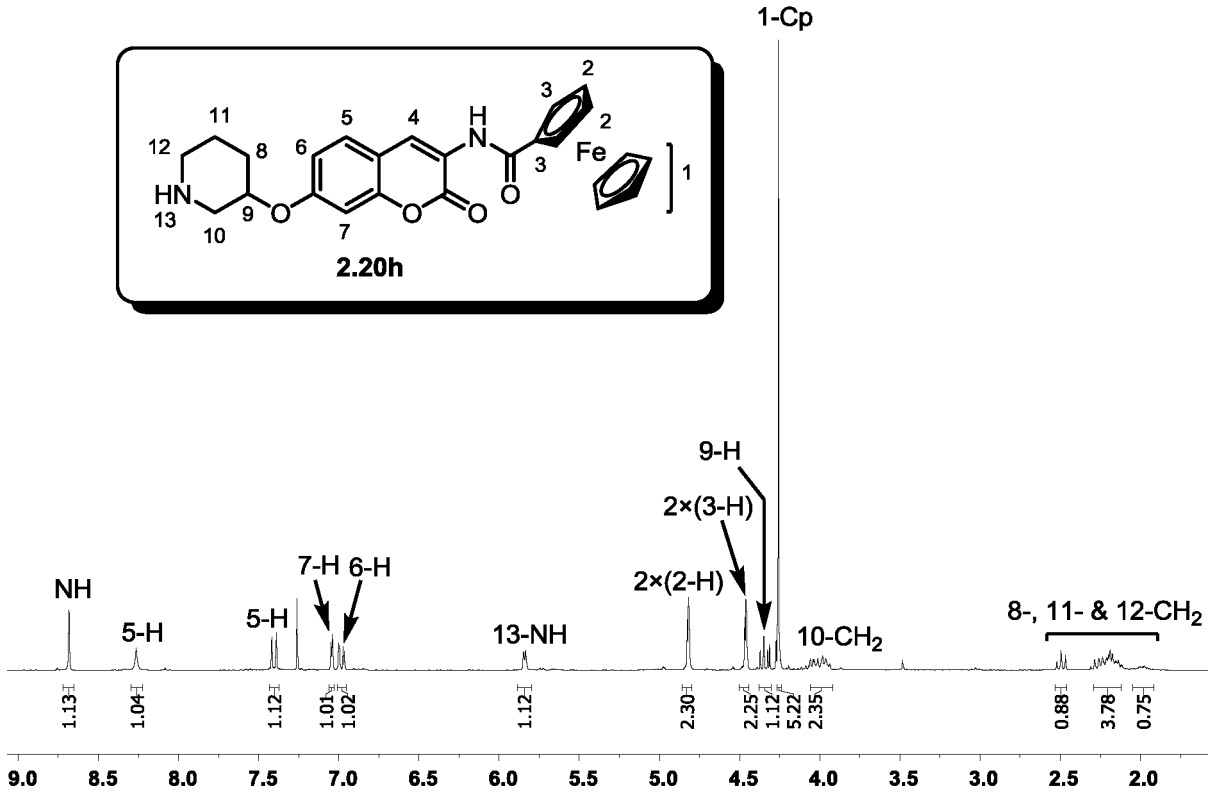

Figure 2.17: ^{1}H NMR spectrum of **2.20h**.

For organic compounds, analogues containing 3'- and 4'-NH piperidinyl units were synthesized as the reference compounds, i.e. **2.20i-k**. They were prepared by subjecting 3'- and 4'-*N*Boc piperidinols (**2.15c-d**) and relevant 7-hydroxy Nb analogues (**2.19c-d**) to produce their corresponding 3'- and 4'-*N*Boc Nb analogues. The reaction progress was monitored by TLC like before. Attempted purification of these products could not be successfully achieved with either silica gel column chromatography or preparative TLC due to the formation of many side products, which had similar retention factor (R_f) values to the desired products, as indicated by TLC. This problem was solved by subjecting the crude products to the *N*Boc-deprotecting conditions with 10% TFA/DCM solution, which resolved the spots by lowering the R_f values of the desired products. Preparative TLC purification of the resultant residues, using DCM as an eluent, afforded 3'- and 4'-NH piperidinyl Nb analogues (**2.20i-k**) as white solids in low yields of 9 – 16%.

The organic analogues (**2.20i-k**) were characterized in the same manner as the Fc analogues (**2.20a-h**). The piperidinyl ring was observed in the aliphatic region of both ^{1}H and ^{13}C NMR spectra of the compounds, similarly to 3'- and 4'-NH piperidinyl Fc analogues (**2.20g-h**). The

piperidinyl NH group was observed around δ 5.85 ppm, and it was confirmed by performing a deuterium (D_2O) wash experiment on compound **2.20j** as illustrated below (**Figure 2.18**).

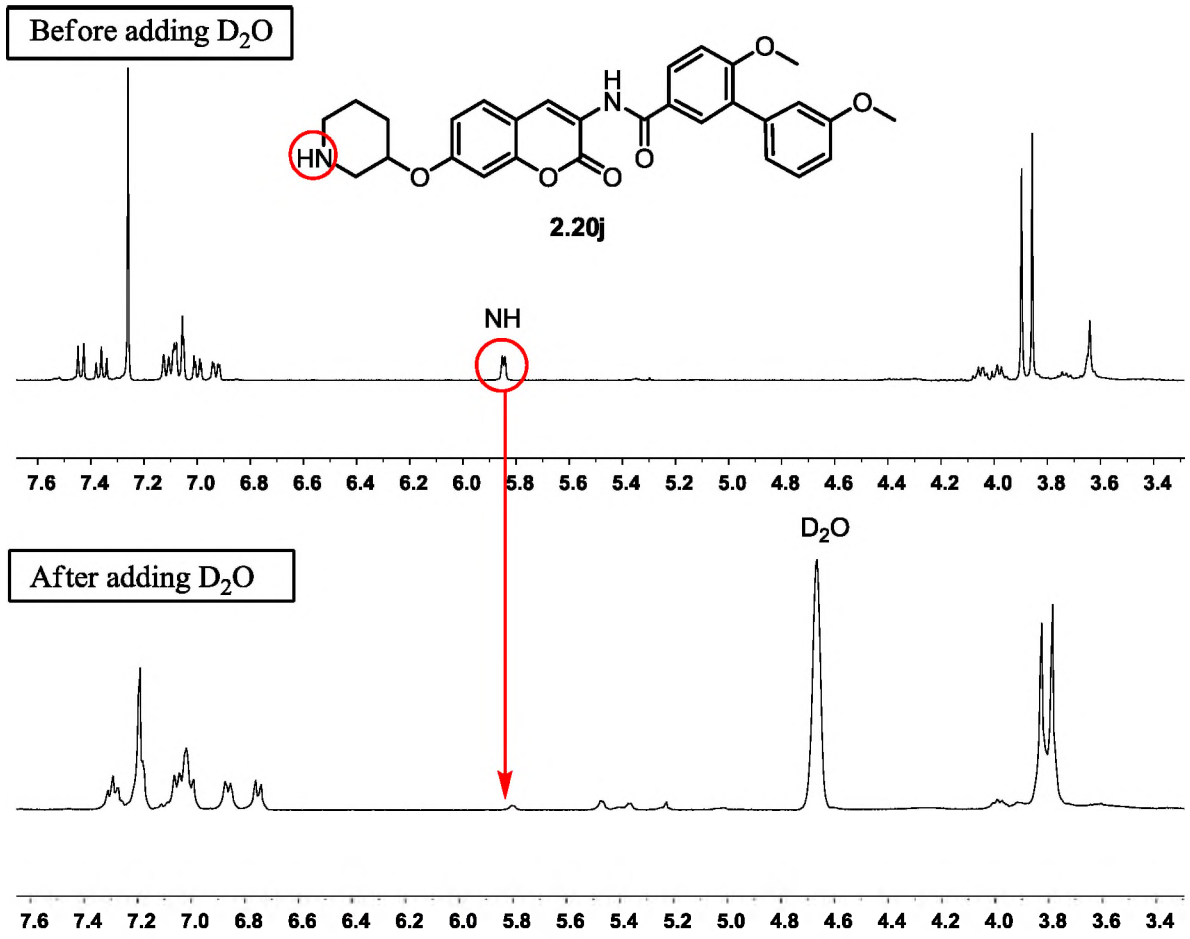

Figure 2.18: Deuterium wash experiment on **2.20j**.

On performing the deuterium wash experiment, the ^1H NMR spectrum of compound **2.20j** was initially recorded normally in deuterated chloroform ($CDCl_3$). Upon adding a drop of deuterium oxide (D_2O) into the same NMR sample containing **2.20j** and then acquiring the spectrum, the signal corresponding to NH resonating around δ 5.85 ppm disappeared since the hydrogen carried is exchangeable, and was presumably exchanged for deuterium atoms (from D_2O) which are not visible in NMR (**Figure 2.18**).

As with the phenylated analogues (**2.13a-f** and **2.14a-f**), the structures of both Fc and organic piperidinyl analogues were further confirmed with HRMS in a similar manner. Except for analogues **2.20e-f** and **2.20k** which were confirmed by fragmentation analysis of their structures, the base peaks of all the other compounds (**2.20a-d** and **2.20g-j**), corresponding to their molecular masses, were observed in their respective HRMS spectra (**Table 2.10**).

Table 2.10: HRMS data of piperidinyl Nb analogues **2.20a-d** and **2.20g-j**.

Entry	Compound	Calculated (M)	Observed $[M+H]^+/M^+$
1	**2.20a**	486.1242	487.1318
2	**2.20b**	486.1242	487.1328
3	**2.20c**	500.1398	501.1471
4	**2.20d**	500.1398	500.1398
5	**2.20g**	472.1085	473.1156
6	**2.20h**	472.1085	473.3104
7	**2.20i**	500.1947	501.3754
8	**2.20j**	500.1947	500.3809

Analysis of the fragmentation patterns of compounds **2.20e** and **2.20k**, in light of their respective HRMS spectra, revealed peaks corresponding to their fragments as shown in **Figure 2.19** and **Figure 2.20**.

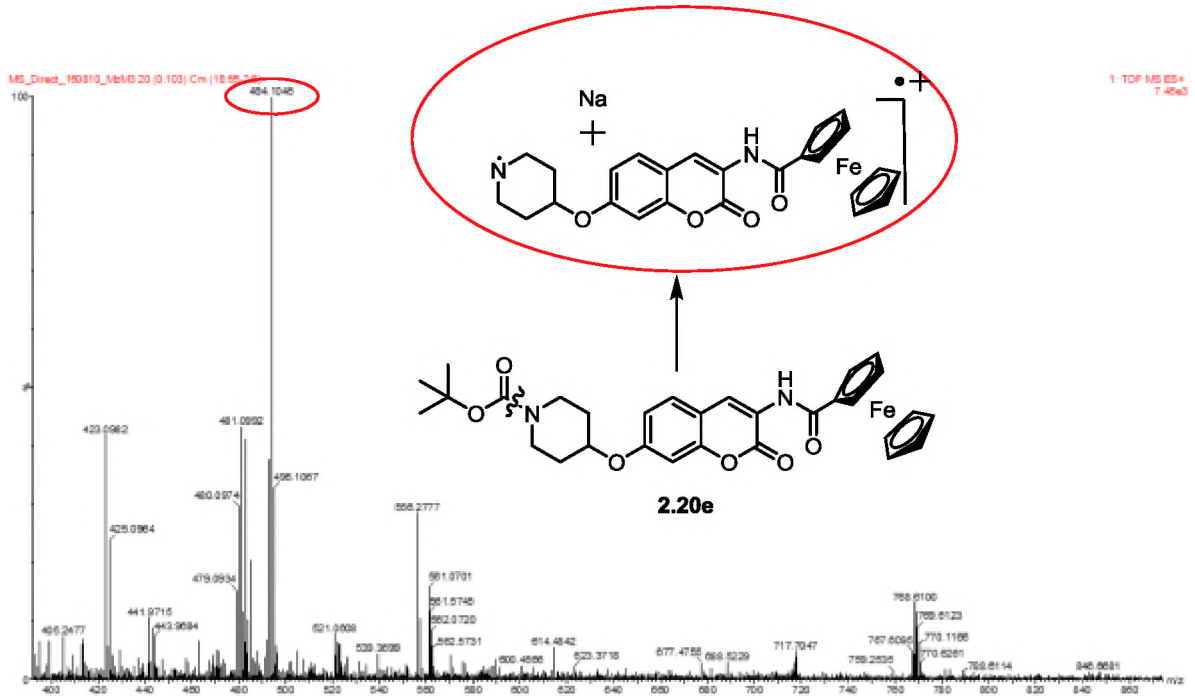

Figure 2.19: Fragmentation and HRMS analysis of **2.20e**.

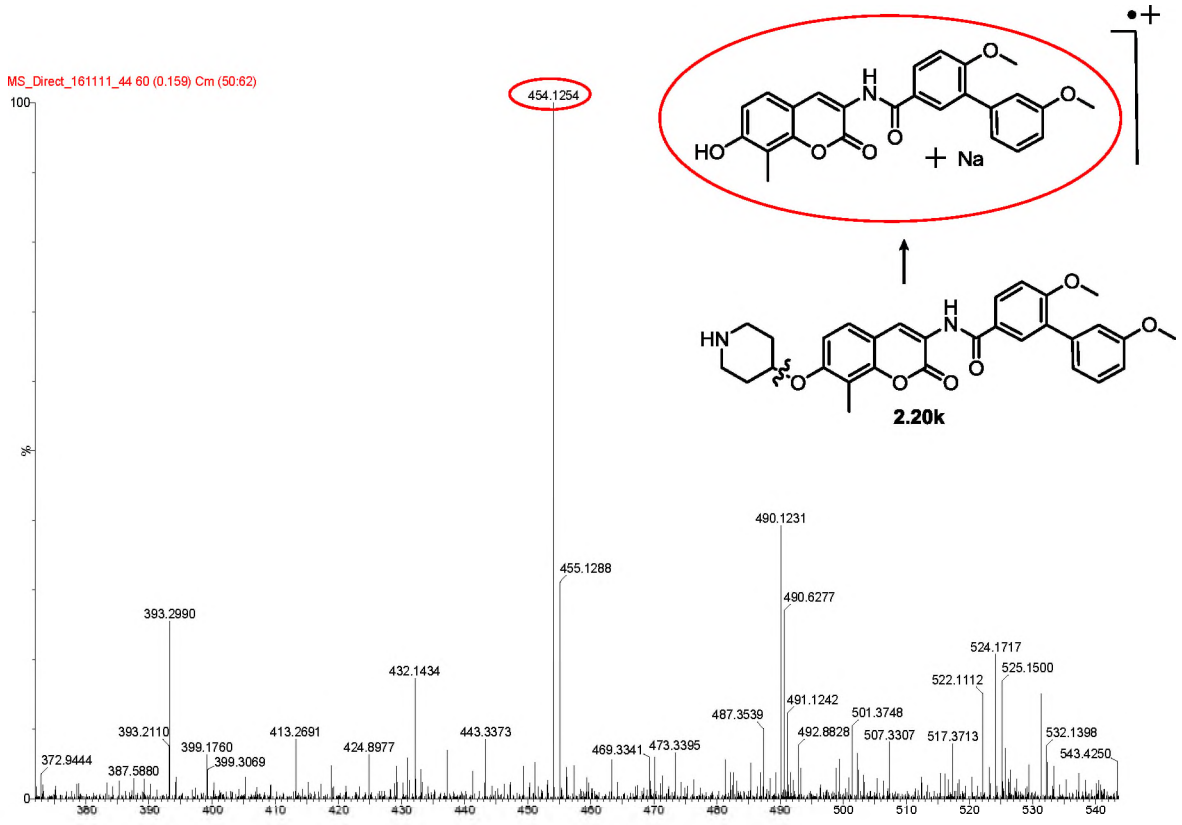

Figure 2.20: Fragmentation and HRMS analysis of **2.20k**.

2.3. CONCLUSIONS AND FUTURE WORK

In this part of the study, a modified Perkin condensation methodology which makes use of salicylaldehydes and *N*-acetyl glycine was employed to assemble the coumarin nucleus to which the structural units of interest were appended to produce the desired ferrocenyl and organic Nb analogues. The phenylated Nb analogues, **2.13a-f** and **2.14a-f**, were achieved in modest to good yields (13 – 71%) via Chan-Lam *O*-coupling and EDCI amidation. To improve the observed poor aqueous solubility of these analogues which was perceived during biological screening of the compounds, the piperidinyl moieties were envisaged as replacements of the phenyl moieties. The targerted piperidinyl analogues (**2.20a-k**) were accessed through T3P® amidation and Mitsunobu coupling in low, but adequate yields. All the Nb analogues synthesized were characterised by spectroscopic techniques: 1D NMR (^{1}H and ^{13}C NMR), HRMS and IR. The structures of phenylated analogues were further confirmed by CHNS microanalysis.

It is obvious from these results that part of the objectives of the overall study have been achieved, i.e. ferrocenyl Nb analogues and some of their corresponding organic variants

bearing biphenyl **A** have been successfully synthesized and their structures confirmed. Future investigations and/or extension of this work with regard to synthesis would entail the following:

1. Optimizing the reaction conditions for both EDCI and T3P® amidation for better product yields of Nb analogues.
2. Expanding the piperidinyl Nb series, which could not be pursued further due to time constraints and scope of the project.
3. Expanding the library of Nb analogues with improved aqueous solubility by incorporating various other structural motifs known to be favourable for aqueous solubility.

REREFENCES

1. J. A. Burlison, C. Avila, G. Vielhauer, D. J. Lubbers, J. Holzbeierlein and B. S. Blagg, *J. Org. Chem.*, **2008**, *73*, 2130-2137.
2. X. M. Yu, G. Shen, L. Neckers, H. Blake, J. Holzbeierlein, B. Cronk and B. S. Blagg, *J. Am. Chem. Soc.*, **2005**, *127*, 12778-12779.
3. J. A. Burlison, L. Neckers, A. B. Smith, A. Maxwell and B. S. Blagg, *J. Am. Chem. Soc.*, **2006**, *128*, 15529-15536.
4. G. Le Bras, C. Radanyi, J.-F. Peyrat, J.-D. Brion, M. Alami, V. Marsaud, B. Stella and J.-M. Renoir, *J. Med. Chem.*, **2007**, *50*, 6189-6200.
5. G. K. B. Gunaherath, M. T. Marron, E. K. Wijeratne, L. Whitesell and A. L. Gunatilaka, *Bioorg. Med. Chem.*, **2013**, *21*, 5118-5129.
6. S. Sethna and R. Phadke, *Org. React.*, **1953**, 1-25.
7. S. Sethna, N. Shah and R. Shah, *J. Chem. Soc.*, **1938**, 228-232.
8. H. Valizadeh and A. Shockravi, *Tetrahedron Lett.*, **2005**, *46*, 3501-3503.
9. D. S. Bose, A. Rudradas and M. H. Babu, *Tetrahedron Lett.*, **2002**, *43*, 9195-9197.
10. M. K. Potdar, S. S. Mohile and M. M. Salunkhe, *Tetrahedron Lett.*, **2001**, *42*, 9285-9287.
11. M. K. Potdar, M. S. Rasalkar, S. S. Mohile and M. M. Salunkhe, *J. Mol. Catal. A: Chem.*, **2005**, *235*, 249-252.
12. V. Singh, J. Singh, K. P. Kaur and L. Goverdhan, *J. Chem. Res., Synop* . **1997**, 58-59.
13. M. S. Manhas, S. N. Ganguly, S. Mukherjee, A. K. Jain and A. K. Bose, *Tetrahedron Lett.*, **2006**, *47*, 2423-2425.
14. D. Sharma, S. Kumar and J. Makrandi, *Green Chem. Lett. Rev.*, **2011**, *4*, 127-129.
15. R. H. Vekariya and H. D. Patel, *Synth. Commun.*, **2014**, *44*, 2756-2788.
16. S. S. Al-Shihry, *Molecules*, **2004**, *9*, 658-665.
17. F. Fringuelli, O. Piermatti and F. Pizzo, *J. Chem. Educ.*, **2004**, *81*, 874.
18. T. Harayama, K. Katsuno, H. Nishioka, M. Fujii, Y. Nishita, H. Ishii and Y. Kaneko, *Heterocycles*, **1994**, *2*, 613-622.
19. I. Yavari, R. Hekmat-Shoar and A. Zonouzi, *Tetrahedron Lett.*, **1998**, *39*, 2391-2392.
20. S. M. Sethna and N. M. Shah, *Chem. Rev.*, **1945**, *36*, 1-62.
21. Y. Ogata and M. Tsuchida, *J. Org. Chem.*, **1959**, *24*, 78-83.
22. W. Perkin, *J. Chem. Soc.*, **1868**, *21*, 181-186.

23. P. Majumder and S. Majumder, *Eur. J. Med. Chem.*, **1993**, *28*, 572-578.
24. M. Crawford and J. Shaw, *J. Chem. Soc.*, **1953**, 3435-3439.
25. J. K. Augustine, A. Bombrun, B. Ramappa and C. Boodappa, *Tetrahedron Lett.*, **2012**, *53*, 4422-4425.
26. A. A. Kudale, J. Kendall, C. C. Warford, N. D. Wilkins and G. J. Bodwell, *Tetrahedron Lett.*, **2007**, *48*, 5077-5080.
27. H. Zhao, B. Reddy Kusuma and B. S. Blagg, *ACS Med. Chem. Lett.*, **2010**, *1*, 311-315.
28. H. Zhao, E. Moroni, B. Yan, G. Colombo and B. S. Blagg, *ACS Med. Chem. Lett.*, **2012**, *4*, 57-62.
29. B. R. Kusuma, A. S. Duerfeldt and B. S. J. Blagg, *Bioorg. Med. Chem. Lett.*, **2011**, *21*, 7170-7171.
30. W. L. Mendelson and S. Hayden, *Synth. Commun.*, **1996**, *26*, 603-610.
31. D. K. Das, S. Sarkar, M. Khan, M. Belal and A. T. Khan, *Tetrahedron Lett.*, **2014**, *55*, 4869-4874.
32. A. A. de Marchi, M. S. Castilho, P. G. Nascimento, F. C. Archanjo, G. del Ponte, G. Oliva and M. T. Pupo, *Bioorg. Med. Chem.*, **2004**, *12*, 4823-4833.
33. G.-B. Wang, L.-F. Wang, C.-Z. Li, J. Sun, G.-M. Zhou and D.-C. Yang, *Res. Chem. Intermed.*, **2012**, *38*, 77-89.
34. A. R. Katritzky, Z. Wang, M. Wang, C. R. Wilkerson, C. D. Hall and N. G. Akhmedov, *J. Org. Chem.*, **2004**, *69*, 6617-6622.
35. R. S. Varma, M. Varma and A. K. Chatterjee, *J. Chem. Soc., Perkin Trans. 1*, **1993**, 999-1000.
36. M. J. Burk and J. G. Allen, *J. Org. Chem.*, **1997**, *62*, 7054-7057.
37. A. Medda, G. Pal, R. Singha, T. Hossain, A. Saha and A. R. Das, *Synth. Commun.*, **2013**, *43*, 169-181.
38. X. M. Yu, G. Shen and B. S. Blagg, *J. Org. Chem.*, **2004**, *69*, 7375-7378.
39. K. Sidera and E. Patsavoudi, *Recent Pat. Anticancer Drug Discov.*, **2014**, *9*, 1-20.
40. J. X. Qiao and P. Y. Lam, *Synthesis*, **2011**, *2011*, 829-856.
41. C. A. Montalbetti and V. Falque, *Tetrahedron*, **2005**, *61*, 10827-10852.
42. R. Raj, A. Saini, J. Gut, P. J. Rosenthal and V. Kumar, *Eur. J. Med. Chem.*, **2015**, *95*, 230-239.

43. G. M. Maguene, J.-B. Lekana-Douki, E. Mouray, T. Bousquet, P. Grellier, S. Pellegrini, F. S. T. Ndouo, J. Lebibi and L. Pélinski, *Eur. J. Med. Chem.*, **2015**, *90*, 519-525.

44. H. Zhao, A. C. Donnelly, B. R. Kusuma, G. E. Brandt, D. Brown, R. A. Rajewski, G. Vielhauer, J. Holzbeierlein, M. S. Cohen and B. S. Blagg, *J. Med. Chem.*, **2011**, *54*, 3839-3853.

45. J. R. Dunetz, Y. Xiang, A. Baldwin and J. Ringling, *Org. Lett.*, **2011**, *13*, 5048-5051.

46. Z. Wang, *Comprehensive Organic Name Reactions and Reagents*, John Wiley & Sons, Inc: Hoboken, **2009**.

3. BIOLOGICAL EVALUATION STUDIES

This chapter presents the biological investigation of the synthesised Nb analogues. The anticancer and antiplasmodial activities of these compounds are discussed in **Section 3.1** and **Section 3.3**, respectively. The results of the cytotoxicity (**Section 3.2**) and Hsp90 inhibition studies (**Section 3.4**) are also discussed before drawing the general conclusions (**Section 3.5**) of the chapter.

3.1. ANTICANCER ACTIVITY OF TARGET NOVOBIOCIN ANALOGUES

Both the phenylated (**2.13a-f** and **2.14a-f**) and piperidinyl (**2.20a-k**) Nb analogues were evaluated for *in vitro* anticancer activity against one of the most aggressive cancer cell lines, HCC38 triple negative breast cancer cell line.[1] The assays were performed in collaboration with the lab of Assoc. Prof. A.L. Edkins (Biochemistry and Microbiology Department, Rhodes University). In all cases, the compounds were dissolved in dimethylsulfoxide (DMSO). Paclitaxel, a known anticancer drug, was used as a positive control, whilst Nb was used as a reference compound in the assays. The activity of each compound against the cell line is presented as a concentration of the compound that suppressed viability of the cells to half of the initial population, i.e. half-maximal inhibitory concentration (IC_{50}) value.

3.1.1. Anticancer activity of phenylated Nb analogues (2.13a-f and 2.14a-f)

The *in vitro* anticancer activity of the phenylated Nb analogues (**2.13a-f** and **2.14a-f**) is shown in **Table 3.1**. At first glance, the general pattern that emerged from the results is that the Fc-containing derivatives (**2.13a-f**) showed higher potency compared to their non-Fc derivatives (**2.14a-f**) with the exception of **2.14c** and **2.14e**, which displayed highest activity in the whole library. For example, compound **2.13a** showed ~10-fold increased activity compared to its non-ferrocenyl counterpart, **2.14a**, and parental Nb. Similarly, compound **2.13d** showed higher activity compared to its congener compound **2.14d** with ~26-fold improvement. Although compound **2.13c** displayed reduced activity than the parental compound Nb, its organic variant (**2.14c**) was inactive against the cell line (**Table 3.1**).

Table 3.1: Anticancer activity of phenylated Nb analogues against HCC38 cancer cell line.

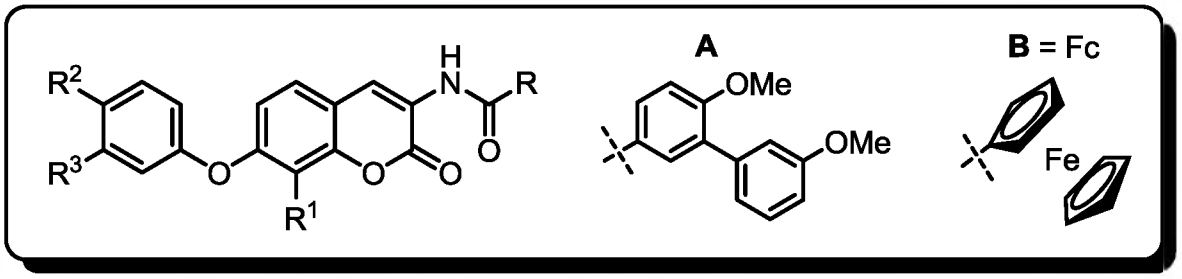

Entry	Compound	R	R^1	R^2	R^3	IC_{50} (μM)
1	**2.13a**	B	H	Bu^t	H	20.7
2	**2.13b**	B	H	OMe	H	13.2
3	**2.13c**	B	H	H	OMe	261.5
4	**2.13d**	B	Me	Bu^t	H	8.7
5	**2.13e**	B	Me	OMe	H	1.1
6	**2.13f**	B	Me	H	OMe	8.0
7	**2.14a**	A	H	Bu^t	H	197.4
8	**2.14b**	A	H	OMe	H	0.36
9	**2.14c**	A	H	H	OMe	N.A.
10	**2.14d**	A	Me	Bu^t	H	223.1
11	**2.14e**	A	Me	OMe	H	2.1
12	**2.14f**	A	Me	H	OMe	>1000
13	**Nb**	–	–	–	–	205.1
14	**Paclitaxel**	–	–	–	–	0.029

N.A.: not active.

The lack of activity observed for most of the organic derivatives (**2.14a-f**), excluding **2.14b** and **2.14e**, against the cell line in this study appeared to be in agreement with the findings by Kusuma and co-workers who had also synthesized and demonstrated poor anti-proliferative effects of these compounds against SkBr3 and MCF7 breast cell lines (**Table 3.1**).[2] Despite being active against HCC38 in the current study, both compounds **2.14b** and **2.14e** were inactive against SkBR3 and MCF7 breast cancer lines.[2] The lower activity of the Fc compound **2.13b** with respect to its organic derivative (**2.14b**), amongst other reasons, could be attributed

to its observed poor aqueous solubility. Generally, all the ferrocenyl derivatives (**2.13a-f**) were only sparingly soluble in DMSO compared to the organic analogues (**2.14a-f**) during the assays.

Since we limited our study to specific simplified novobiocin-like compounds with phenyl moieties at position 7 of the coumarin core bearing the ferrocene unit, a realistic structure-activity relationship (SAR) trend could not be clearly defined for this series of compounds. Nevertheless, the general trends observed with respect to the effects of functional groups on the activity of compounds screened was as follows:

1. The presence of the methyl group at position 8 of the coumarin framework seemed to favour enhanced activity for the Fc analogues (**2.13a-c**) more than the hydrogen (**2.13d-f**), whereas the opposite was observed for organic analogues (**2.14a-f**). Increase in activity by methylation at C-8 was also observed by Burlison *et al.* for a different class of organic Nb analogues.[3]
2. The 4'-OMe of the phenyl moiety at C-7 was better tolerated for activity than 4'-Bu^t and 3'-OMe for both Fc and organic Nb analogues.

3.1.2. Anticancer activity of OBn/OH and piperidinyl Nb analogues (2.18a-d/2.19a-d and 2.20a-k)

As highlighted in **Section 2.2.3**, the piperidinyl Nb analogues were designed and synthesised with an effort to improve the aqueous solubility of the phenylated Nb analogues and, thus, presumably enhance their anticancer activity. The 7-benzyloxy (OBn) and 7-hydroxy (OH) Nb analogues (**2.18a-d** and **2.19a-d**, respectively) were also evaluated for anticancer activity against the same cell line as phenylated Nb analogues in **Section 3.1.1**, i.e. HCC38, as they resemble the analogues designed for this study. The anti-proliferative activity of these analogues is presented in **Table 3.2**.

Table 3.2: IC_{50} values of 7-OBn and 7-OH Nb analogues against HCC38 cancer cell line.

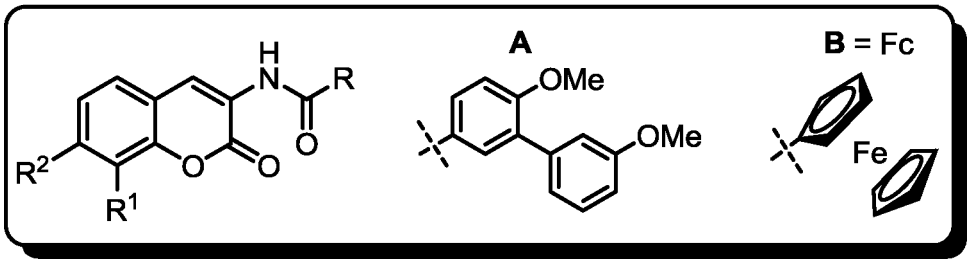

Entry	Compound	R	R^1	R^2	IC_{50} (μM)
1	**2.18a**	B	H	OBn	182.9
2	**2.18b**	B	H	OBn	41.1
3	**2.18c**	A	Me	OBn	47.6
4	**2.18d**	A	Me	OBn	5.0
5	**2.19a**	B	H	OH	11.7
6	**2.19b**	B	H	OH	29.3
7	**2.19c**	A	Me	OH	2.2
8	**2.19d**	A	Me	OH	N.D.

N.D.: not determined

Whilst the 7-OH analogues (**2.19a-d**) dissolved readily in DMSO, the OBn variants (**2.18a-d**) required longer periods of shaking and heating to dissolve, even more than the phenylated analogues (**2.18a-f** and **2.20a-f**). Compound **2.19d** was evaluated not for anticancer activity since its colour interfered with the assay. From the biological results in **Table 3.2**, compound **2.19c** bearing biphenyl **A** and containing the OH group was the most potent in the whole OBn/OH series. Contrary to the previous findings made for the phenylated analogues (**Section 3.1.1**), compounds bearing biphenyl **A** (**2.18c-d** and **2.19c-d**) were generally more efficacious than their Fc counterparts (**2.18a-b** and **2.19a-b**). Within the OBn series, the 8-Me analogues (**2.18c-d**) appeared to be more potent than their 8-H derivatives (**2.18a-b**) (**Table 3.2**). There was no discernible relationship between 8-Me and 8-H derivatives in the OH series, i.e. compounds **2.19a-d**. The compounds in the OH series (**2.19a-d**) had superior activity than their OBn variants (**2.18a-d**). This observation seemed to consistent with the supposition that aqueous solubility of Nb analogues influences their biological activity (**Section 2.2.3**) since the OBn group (H-bond acceptor) retards aqueous solubility of a compound more than the OH group, which is both a H-bond donor and acceptor. Nevertheless, both OH and OBn analogues

were comparable in activity to the phenylated analogues, **2.13a-f** and **2.14a-f** (**Table 3.1**) with IC_{50} values in the low to mid μM range.

Having evaluated both OBn and OH analogues, the pieridinyl Nb analogues (**2.20a-k**) were subjected to the same assay, i.e. screening for anti-proliferative activity against the HCC38 breast cancer cell line. The results are presented in **Table 3.3**.

Table 3.3: IC_{50} values of piperidinyl Nb analogues against HCC38 cancer cell line.

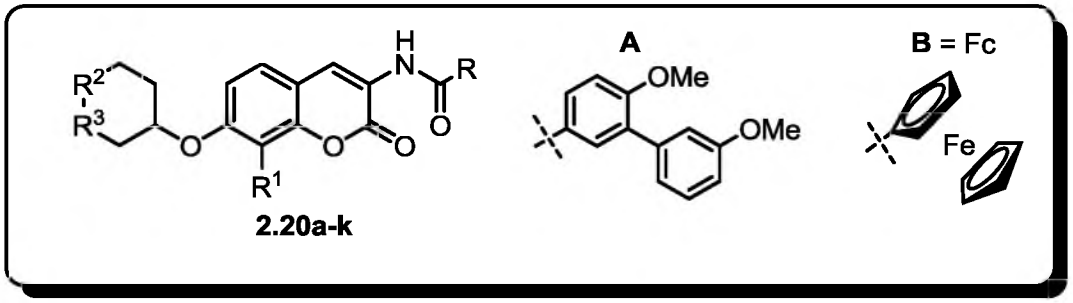

Entry	Compound	R	R^1	R^2	R^3	IC_{50} (μM)
1	**2.20a**	B	H	NMe	CH_2	51.4
2	**2.20b**	B	H	CH_2	NMe	47.9
3	**2.20c**	B	Me	NMe	CH_2	36.8
4	**2.20d**	B	Me	CH_2	NMe	13.8
5	**2.20e**	B	H	*N*Boc	CH_2	29.8
6	**2.20f**	B	H	CH_2	*N*Boc	30.0
7	**2.20g**	B	H	NH	CH_2	11.8
8	**2.20h**	B	H	CH_2	NH	108.9
9	**2.20i**	A	H	NH	CH_2	19.5
10	**2.20j**	A	H	CH_2	NH	69.4
11	**2.20k**	A	Me	CH_{2C}	NH	38.0

As with the phenylated analogues (**Table 3.1**), the activity of analogues bearing the Fc unit in the piperidinyl series (**2.20a-h**) was generally superior to that of organic analogues (**2.20i-k**) (**Table 3.3**). However, the piperidinyl analogues still did not significantly impart superior activity to the phenylated analogues (**Table 3.1**) despite their improved solubility in DMSO observed during the assay. Compared to the phenylated analogues, only fewer compounds in

this series had IC_{50} values in the low micromolar region. Regardless, the activities were still similar.

The 3'-*N*-methyl analogues (**2.20b** and **2.20d**) were almost twice as efficacious as the 4' variants (**2.20a** and **2.20c**), whilst the *N*Boc derivatives (**2.20e** and **2.20f**) exhibited comparable activities: 29.8 and 30.0 μM, respectively (**Table 3.3**). Zhao *et al.* made the same observations for organic Nb analogues bearing the benzamide chain of Nb (**Figure 2.1**), which were tested for anti-proliferative activity against SKBr3 and MCF-7 cancer cell lines.[4] Within the NH series (**2.20g-k**), the 4'-substituted derivatives possessed higher efficacy than their 3'-substituted counterparts by ~5-fold increase (**Table 3.3**). There was no discernible trend in activity between 8-H and 8-Me analogues. Overall, the NH functionality (H-bond donor and acceptor) was generally more tolerated for activity than both NMe and *N*Boc groups (H-bond acceptors) in the piperidinyl series (**Table 3.3**). This observation was also made by Zhao *et al.*[4] and is consistent with the previous findings made for the OBn and OH candidates (**Table 3.2**): hydrophilic groups appear to favour the biological activity of Nb analogues.

3.1.3. Summary of anticancer activity studies

All the synthesised target Nb analogues were evaluated for *in vitro* anticancer activity against the HCC38 breast cancer cell line using DMSO. Although only sparingly soluble in DMSO, the phenylated Nb analogues (**2.13a-f** and **2.14a-f**) generally exhibited comparable activities to both the 7-OBn/OH (**2.18a-d** and **2.19a-d**) and 7-piperidinyl Nb analogues (**2.20a-k**). Within the OBn/OH and piperidinyl series, the OH and NH groups, which are capable of participating in hydrogen-bonding as both H-bond donors and acceptors, were more favoured for activity than the OBn, NMe and *N*Boc groups which are only H-bond acceptors. Although analogues bearing groups that favour aqueous solubility of a compound (i.e. OH and NH) were somewhat inferior in activity compared to the phenylated analogues, they were generally more potent than their variants with functional groups possessing lesser capacity to favour aqueous solubility (i.e. OBn, NMe and *N*Boc). Nevertheless, this latter observation seems to support the presumption that poor aqueous solubility limits the activity of the Nb analogues.

3.2. HeLa CELL TOXICITY ASSAY STUDIES

As a practice by the collaborators that performed the assays, compounds that are to be screened for antiplasmodial activity are tested for their relative human cell cytotoxicity effects using HeLa cells prior to conducting the antiplasmodial assays. This is done to test if any of the activity that might be observed for the compounds to be screened is specific for the *Plasmodium*

parasitic cells and not the human cells. In this study, the Nb analogues were screened for cytotoxicity effects at a single point concentration of 20 μM in duplicates. These assays were conducted in collaboration with Mrs. M. Isaacs (Centre for Chemico- and Biomedicinal Research Unit, Rhodes University).

All the phenylated analogues (**2.13a-f** and **2.14a-f**) showed no significant decrease in percentage viability of the HeLa cells (>50%) as shown in **Figure 3.1**. In the context of anticancer assay results of these compounds in **Section 3.1.1.**, these data suggested that the observed *in vitro* anticancer activity of these compounds was selective for the HCC38 breast cancer cell line (**Table 3.1**) employed in the assay and not for the HeLa cells which are also cancerous (cervical origin). It is also important to note that the single-point concentration assay used in the cytotoxicity study is less accurate than the IC_{50} determination, hence the interpretation made here is done so with reservations.

Figure 3.1: The *in vitro* cell toxicity (HeLa cells) results of phenylated Nb analogues.

The OBn/OH (**2.18a-d** and **2.19a-d**) and piperidinyl analogues (**2.20a-k**) were subjected to the same assay. Whilst a majority of the compounds did not suppress the population of the HeLa cells to less than 50%, the organic analogues: 7-OH analogues (**2.19c-d**) and 3'-NH analogues (**2.20j-k**), significantly reduced the viability of the cells to less than 50%, implying high potency of the compounds against the HeLa cells (**Figure 3.2**). Therefore, these compounds appeared to possess *in vitro* anticancer activity against both breast and cervical cancer cell

lines, HCC38 and HeLa cells, respectively. This interpretation is made with the same reservations as the phenylated Nb analogues in the context of anticancer activity as previously discussed.

Figure 3.2: The *in vitro* cell toxicity (HeLa cells) results of OBn/OH and piperidinyl Nb analogues.

3.3. ANTIPLASMOIAL ACTIVITY OF TARGET NOVOBIOCIN ANALOGUES

The antiplasmodial activity of the target analogues was investigated against the chloroquine-sensitive *P. falciparum* strain, 3D7. The samples of the compounds were prepared as was done for anticancer assays. Chloroquine (CQ) was used as a control drug in the assays and Nb as a reference compound. As a standard practice, the antiplasmodial screening study commenced with the single-point concentration assay of the compounds against the 3D7 strain at 20 μM concentration. Compounds showing promising activity (i.e. those that effect less than 25% cell viability of the parasite) were evaluated at different concentration values to determine their IC_{50} values.

3.3.1. Antiplasmodial activity of phenylated Nb analogues (2.13a-f and 2.14a-f)

The single-point concentration evaluation of phenylated Nb analogues (**2.13a-f** and **2.14a-f**) revealed the Fc derivatives **2.13a** and **2.13c** as the most promising (**Figure 3.3**). None of the organic derivatives (**2.14a-f**) showed any promising anti-proliferative effects against the

parasite (**Figure 3.3**) at the tested concentration. Thus, compounds **2.13a** and **2.13c** were subjected to further tests at different concentrations for IC_{50} determination. The IC_{50} values of these compounds are illustrated in **Figure 3.4**. Compound **2.13a** was the most active in the phenylated series with percentage viability and IC_{50} values of 7.59% and 9.47 μM, respectively.

Figure 3.3: Antiplasmodial activity of phenylated Nb analogues against 3D7 *P. falciparum* strain plotted in parallel with their cytotoxicity results against HeLa cells at 20 μM.

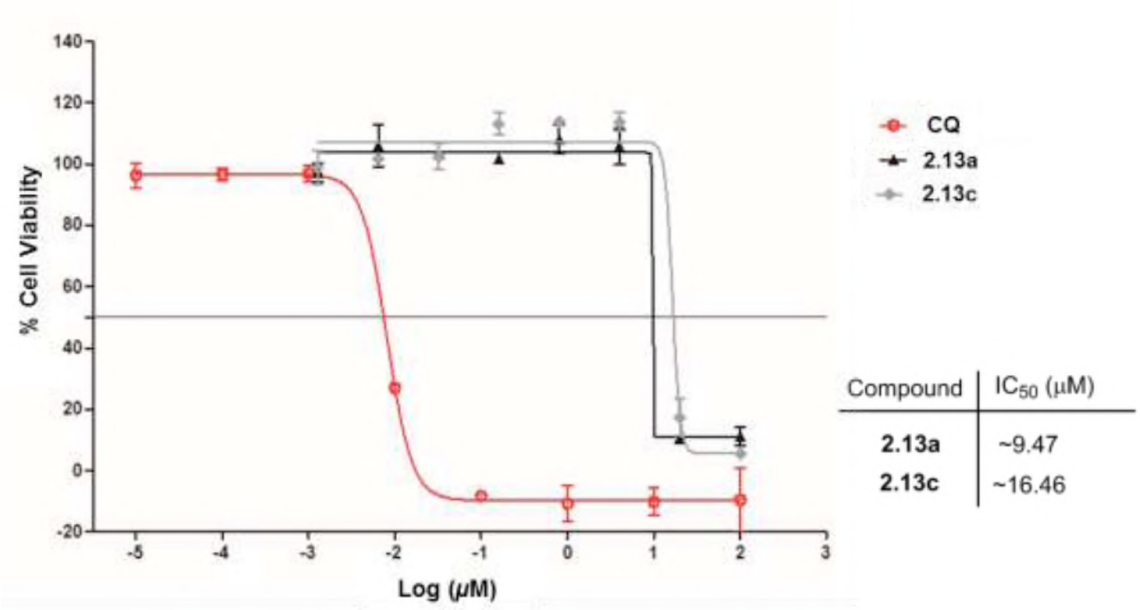

Figure 3.4: Percentage viability of the 3D7 *P. falciparum* parasite at different concentrations and related IC_{50} values of **2.13a** and **2.13c**.

3.3.2. Antiplasmodial activity of OBn/OH and piperidinyl Nb analogues

In the OBn/OH series, only the organic analogues carrying the OH at C-7 (i.e. **2.19c-d**) showed the most promising antiplasmodial activity (**Figure 3.5**). However, since these were deemed toxic against the HeLa cell line in **Section 3.2** (**Figure 3.2**), they were not subjected to further assays for determining their IC_{50} values as their activity might have been a result of general cytotoxicity effects. Although the 3'-NH substituted organic analogues, **2.20j-k**, in the piperidinyl series showed promising activity, they were also not subjected to further tests for the same reasons as compounds **2.19c-d**.

Figure 3.5: Antiplasmodial activity of piperidinyl Nb analogues against 3D7 *P. falciparum* strains plotted in parallel with their cytotoxicity results against HeLa cells at 20 μM.

Three Fc analogues, **2.20a-c**, all with *N*-methyl substituents exhibited favourable antiplasmodial activity against the 3D7 strain, whereas only one in the organic series, **2.20i**, possessed promising activity (**Figure 3.5**). Highest activity was observed for analogue **2.20c** with a percentage cell viability value of 1.94%. These data suggested the Fc moiety was more favourable for antiplasmodial activity than the biphenyl **A** motif. Also, the *N*-methyl group seemed to be well-tolerated for antiplasmodial activity since all three Fc analogues (**2.20a-c**) exhibiting promising activity had the same group in common. Compounds **2.20a-c** and **2.20i** were subjected to further assays to determine their IC_{50} values at the time the current thesis was compiled, but these assays were not yet concluded due to time constraints. Hence, no direct comparison in antiplasmodial activity could be made between these analogues (**2.20a-c** and **2.20i**) and the phenylated analogues (**2.13a** and **2.13c)** in terms of IC_{50} values.

3.3.3. Summary of antiplasmodial activity studies

As with the anticancer study, a comprehensive SAR profile of the target Nb analogues could not be generated. Generally, the Fc moiety seemed to be more favourable for antiplasmodial activity than biphenyl **A** for all analogues investigated. Although some organic analogues (**2.19c-d** and **2.20k**) showed significant inhibition of the 3D7 parasite, they were toxic against

the HeLa cell line, hence their activity was deemed non-specific for the *Plasmodium* parasite. Unlike the observations made for anticancer activity, the observed solubility of the analogues in DMSO did not seem to have any effect on their antiplasmodial activity.

3.4. HSP90 INHIBITION STUDIES

In line with the aims and objectives of the project, the target Nb analogues were designed for potential anticancer and antiplasmodial activity presumably through inhibition of Hsp90. Having evaluated the compounds for both anticancer and antiplasmodial activities, we sought to prove that the observed activities were, in fact, a result of Hsp90 inhibition for both pathogens. To realize this, different *Saccharomyces cerevisiae* (yeast) strains expressing different Hsp90 isoforms were employed in the assays to probe Hsp90 inhibitory activity of the compounds showing the most promising anticancer and antiplasmodial activities. The Hsp90 inhibition assays were done in collaboration with the lab of Assoc. Prof. A.L. Edkins (Rhodes University).

The yeast strains used were DP552 (expressing parental yeast Hsp90), DP553 (expressing *P. falciparum* Hsp90), DP555 (expressing human Hsp90α) and DP584 (expressing human Hsp90β).[5] Compounds **2.13a** and **2.20c** were chosen as representative compounds from both phenyl and piperidinyl series and used in the assays as they demonstrated high efficacy for both anticancer and antiplasmodial activities. The assay, which was performed for the first time, entailed incubating 50 μM (in DMSO) of each compound with the appropriate yeast cell culture and spectrophometrically monitoring the population of the yeast cells over a period of two days at 6, 16, 24, 30 and 40-hour intervals. DMSO was used a negative control in the assays. Due to availability of resources and time constraints of the project, a positive control (i.e. an effective, known Hsp90 inhibitor) was not included in the assay. Surprisingly, the growth of the yeast cells incubated with the compounds (**2.13a** and **2.20c**) was identical to that of the cells incubated with the negative control (DMSO) despite the presence of the compounds. The results are illustrated in **Figure 3.6**.

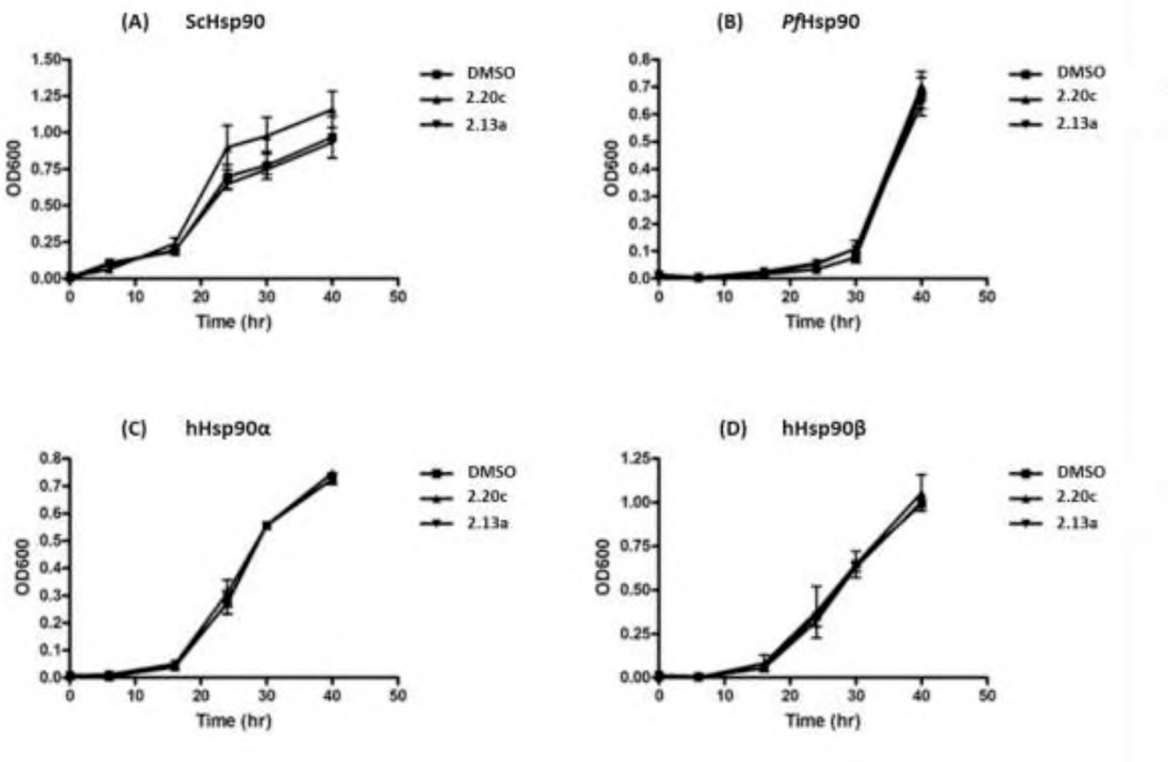

Figure 3.6: Hsp90 inhibition study of compounds **2.13a** and **2.20c** against: **A** – yeast Hsp90, **B** – *Pf*Hsp90, **C** – hHs90α and **D** – Hsp90β.

These results suggested that the observed anticancer and antiplasmodial potencies of the compounds tested was independent of Hsp90 inhibition. However, the assay was performed for the first time and a number of important assay parameters were not optimised, and could have been the reason why the assay did not work as expected. Such factors include: cell wall permeability of the yeast cells, use of a positive control (i.e. known Hsp90 inhibitor), testing different concentrations of the compounds instead of a fixed concentration (i.e. 50 μM) and optimising the temperature conditions of the assay.

In conclusion, although the obtained data suggested no direct correlation between the observed anticancer and antimalarial activities of the analogues and Hsp90 inhibition, this observation remains to be confirmed due to the conditions of the assay used. Optimisation studies of the assay conditions were underway at the time this thesis was compiled, but could not be included due to time constraints of the project.

3.5. CONCLUSIONS AND FUTURE WORK

In this part of the study, compounds bearing the Nb scaffold were investigated for anticancer and antiplasmodial activity, respectively, against the triple negative HCC38 breast cancer cell line and 3D7 *P. falciparum* strain. In all cases, the Fc analogues generally exhibited superior anticancer and antimalarial activities to the organic analogues. The phenylated analogues showed similar *in vitro* anticancer activities to both OBn/OH and piperidinyl analogues with IC_{50} values in the low to mid micromolar range despite their observed modest solubility in DMSO. There seemed to be a correlation between the observed solubility of the compounds in the OBn/OH and piperidinyl series and their *in vitro* anticancer activity. The cytotoxicity assay results suggested the observed antiplasmodial activity of the analogues for which the IC_{50} values were determined was specific for the *Plasmodium* parasite and not the human cells (HeLa cells). From the Hsp90 inhibition study using yeast strains expressing Hsp90 isoforms important for both cancer and the *Plasmodium* parasite, it was uncertain if the observed activities of the compounds was dependent of Hsp90 inhibition or not. Part of the aims and objectives of this project in the context of biological studies have been achieved. Future investigations of this work would encompass determining the IC_{50} values of the piperidinyl analogues with most promising antiplasmodial activity, optimising conditions of the Hsp90 assay and confirming the proposed target of the evaluated Nb analogues.

REFERENCES

1. A. Prat, O. Karginova, J. S. Parker, C. Fan, X. He, L. Bixby, J. C. Harrell, E. Roman, B. Adamo and M. Troester, *Breast Cancer Res. Treat.*, **2013**, *142*, 237-255.
2. B. R. Kusuma, A. S. Duerfeldt and B. S. J. Blagg, *Biorg. Med. Chem. Lett.*, **2011**, *21*, 7170-7171.
3. J. A. Burlison, C. Avila, G. Vielhauer, D. J. Lubbers, J. Holzbeierlein and B. S. Blagg, *J. Org. Chem.*, **2008**, *73*, 2130-2137.
4. H. Zhao, B. Reddy Kusuma and B. S. Blagg, *ACS Med. Chem. Lett.*, **2010**, *1*, 311-315.
5. D. Wilder, M.-P. Péli-Gull, P.-A. Briand, U. Tatu, and D. Picard, *Mol. Biochem. Parasitol.*, **2009**, *164*, 147-152.

4. EXPERIMENTAL

4.1. GENERAL DETAILS

All chemicals and solvents used in this study were sourced from Sigma-Aldrich (Pty) Ltd. and/or Merck (Pty) Ltd., and used without further purification. The progress of the reactions was monitored by analytical thin layer chromatography (TLC) using Merck F_{254} silica gel plates (supported on aluminium sheets) and the plates were visualised under ultraviolet (UV 254 and 366 nm) light and in iodine flask. Where necessary, the crude compounds were purified by silica gel column chromatography using Merck Kieselgel 60 Å: 70 – 230 (0.068 – 0.2 mm) silica gel mesh.

The ^{1}H and ^{13}C NMR spectra were recorded on Bruker Biospin 300, 400 or 600 MHz spectrometers, and were referenced internally using residual solvent signals of DMSO-d_6: 2.50 ppm for ^{1}H and 39.5 ppm for ^{13}C NMR, or $CDCl_3$: 7.26 ppm for ^{1}H and 77.2 ppm for ^{13}C NMR at room temperature. The spectra were processed using MestReNova software. The chemical shifts were recorded in parts per million (ppm) and the *J*-coupling constants in Herts (Hz). The abbreviations used to describe signal multiplicities are: s = singlet, br s = broad singlet, d = doublet, t = triplet, q = quartet, and m = multiplet. Elemental analysis was performed on Elementer Vario Microtube coupled to a thermal conductivity detector and a combustion tube at 1015 °C with reduction at 850 °C and pressures of Helium set at 1200 – 1350 millibars and oxygen at about 17 millibars. The high-resolution mass spectra (HRMS) were recorded on a Waters Synapt G2 Mass Spectrometer using electron impact (EI) ionization in the positive ionization mode, and the IR spectra were recorded on PerkinElmer Spectrum 100 FT-IR Spectrometer in the mid-IR range (640 – 4000 cm^{-1}). The melting points were determined using Reichert melting point apparatus.

4.2. SYNTHESIS OF TARGET NOVOBIOCIN ANALOGUES

This section highlights the synthetic procedures employed for the preparation of target Nb analogues and their intermediates. All the compounds were characterized by melting point, ^{1}H and ^{13}C NMR techniques. The chemical structures of target analogues were further confirmed by IR, HRMS, and CHNS microanalysis where relevant.

4.2.1. General procedure for synthesis of salicylaldehydes (2.2a-b)[1]

A solution of $POCl_3$ (1.2 eq.) in acetonitrile (20 mL) was added dropwise with stirring to a solution of DMF (1.4 eq.) in acetonitrile (20 mL) at 18 – 25 °C. The reaction solution was stirred at room temperature for 1 hour and then cooled to -10 °C in an ice bath. A solution of an appropriate resorcinol (1.0 eq.) in acetonitrile (20 mL) was added dropwise to the above solution, maintaining the temperature between –10 and 0 °C. A light yellow precipitate was observed during addition. The resulting yellow suspension was stirred at 0 °C for 30 minutes and then at 28 – 30 °C for 1 hour. The reaction solution was cooled to –5 – 0 °C for 30 minutes without stirring to form a precipitate. The acetonitrile layer was decanted and water (80 mL) was added to the precipitate. The resulting suspension was heated to 50 °C with stirring to obtain a clear light orange solution to which 0.1 M aqueous $Na_2S_2O_3$ solution (2 mL) was added. The resulting solution was cooled to –5 °C and stirred for 1 hour after which the solids were filtered off, washed with ice-cold water and air-dried to afford the respective product as a fluffy solid.

4-Hydroxysalicylaldehyde (2.2a)

$POCl_3$ (9.94 g, 64.8 mmol), DMF (5.56 g, 76.1 mmol) and resorcinol (6.21 g, 56.4 mmol) afforded **2.2a** as a pale pink solid (4.98 g, 60%). M.p.: 133-135 °C. (Lit.[1] 134-135 °C). ^{1}H NMR (600 MHz, DMSO-d_6): δ 10.90 (s, 1H, OH), 10.61 (s, 1H, OH), 9.91 (s, 1H, H_1), 7.52 (d, J = 8.5 Hz, 1H, H_4), 6.40 (dd, J = 8.6, 2.2 Hz, 1H, H_3), 6.32 (d, J = 2.3 Hz, 1H, H_2); ^{13}C NMR (150 MHz, DMSO): δ 191.0, 165.2, 163.3, 132.9, 115.2, 108.7, 102.2.

4-Hydroxy-3-methylsalicylaldehyde (2.2b)

$POCl_3$ (9.94 g, 64.8 mmol), DMF (5.56 g, 76.1 mmol) and 2-methylresorcinol (7.00 g, 56.4 mmol) afforded **2.2b** as an off-white fluffy solid (5.59 g, 66%). M.p.: 150-151 °C. ^{1}H NMR (300 MHz, DMSO): δ 11.53 (br s, 2H, 2×OH), 9.68 (s, 1H, H_1), 7.41 (d, J = 8.2 Hz, 1H, H_4), 6.56 (d, J = 8.5 Hz, 1H, H_3), 1.96 (s, 3H, H_2); ^{13}C NMR (75 MHz, DMSO): δ 195.1, 163.5, 161.3, 133.1, 114.1, 110.2, 108.2, 7.4.

4.2.2. General procedure for synthesis of acetamidocoumarins (2.3a-b)[2]

A mixture of a relevant salicylaldehyde **2.2a-b** (1.0 eq.), *N*-acetylglycine (1.0 eq.) and anhydrous sodium acetate (4.0 eq.) in acetic anhydride (25 mL) was heated at 110 – 120 °C with stirring for 4 hours. The resulting brown solution was allowed to cool to room temperature at which time it completely solidified. The solid was broken with a spatula, mixed with ice-cold water (30 mL) to give a light brown emulsion which was cooled in ice for 1 hour and then filtered to obtain a brown pasty residue. The residue was successively washed with ice-cold water
(3 × 10 mL) and ethyl acetate (3 × 10 mL), and air dried to give the relevant acetamidocoumarin **2.3a-b**.

7-Acetoxy-3-acetamidocoumarin (2.3a)

4-Hydroxysalicylaldehyde **2.2a** (5.00 g, 36.2 mmol), *N*-acetylglycine (4.24 g, 36.2 mmol) and anhydrous sodium acetate (11.88 g, 144.8 mmol) afforded **2.3a** as a pale yellow fluffy solid (3.6 g, 38%). M.p.: 184-187 °C, (Lit.[2] 234-236 °C). ^{1}H NMR (600 MHz, DMSO): δ 9.74 (s, 1H, H_2), 8.61 (s, 1H, H_3), 7.74 (d, J = 8.5 Hz, 1H, H_4), 7.26 (d, J = 1.7 Hz, 1H, H_6), 7.13 (dd, J = 8.4, 2.0 Hz, 1H, H_5), 2.30 (s, 3H, H_7), 2.16 (s, 3H, H_1); ^{13}C NMR (150 MHz, DMSO-d_6): δ 170.2, 168.9, 157.3, 151.0, 149.9, 128.5, 124.1, 123.2, 119.0, 117.4, 109.7, 23.9, 20.9.

7-Acetoxy-8-methyl-3-acetamidocoumarin (2.3b)

4-Hydroxy-3-methylsalicylaldehyde **2.2b** (5.00 g, 33.3 mmol), *N*-acetylglycine (3.90 g, 33.3 mmol) and anhydrous sodium acetate (10.93 g, 82.0 mmol) afforded **2.3b** as a pale yellow fluffy solid (3.10 g, 33%). M.p.: 258-260 °C. ^{1}H NMR (300 MHz, DMSO-d_6): δ 9.77 (s, 1H, H_2), 8.60 (s, 1H, H_3), 7.60 (d, J = 8.5 Hz, 1H, H_4), 7.10 (d, J = 8.5 Hz, 1H, H_5), 2.35 (s, 3H, H_6), 2.17 (s, 6H, H_1, H_7); ^{13}C NMR (75 MHz, DMSO): δ 170.2, 168.8, 157.3, 149.5, 148.4, 125.5, 123.8, 123.6, 119.1, 117.8, 117.3, 23.9, 20.5, 8.6.

4.2.3. General procedure for synthesis of *N*-Boc 7-hydroxy-3-aminocoumarins (2.4a-b)[2]

To a mixture of a relevant acetamidocoumarin **2.3a-b** (1.0 eq.) and DMAP (0.2 eq.) in THF (50 mL), Boc_2O (4.2 eq.) was added and reaction mixture stirred at room temperature for 1 hour. The initial yellow suspension became a clear brown solution. Hydrazine monohydrate (10.2 eq.) was then added to the reaction mixture followed by addition of methanol (50 mL). The reaction mixture was stirred for a further 30 minutes during which time it became a clear orange solution. The solvents were removed *in vacuo* and the resulting sticky yellow residue

was dissolved in DCM (50 mL) and successively washed with 1 M aqueous HCl solution (25 mL), 1 M aqueous $CuSO_4$ solution (25 mL), saturated aqueous $NaHCO_3$ solution (25 mL) and brine (25 mL). The organic layer was dried ($MgSO_4$), concentrated under reduced pressure to give a crude product which was purified by silica gel column chromatography (5% EtOAc/Hex) to give **2.4a-b**.

_N_-Boc 7-hydroxy-3-aminocoumarin (2.4a)

7-Acetoxy-3-acetamidocoumarin **2.3a** (3.00 g, 11.5 mmol), di-*tert*-butyldicarbonate (10.52 g, 48.2 mmol), DMAP (0.281 g, 2.3 mmol) and hydrazine monohydrate (5.57 g, 114.8 mmol) afforded **2.4a** as an off-white solid (2.26 g, 81%). Mp.: 189-190 °C (Lit.[2] 177-178 °C). ^{1}H NMR (600 MHz, DMSO-d_6): δ 10.33 (s, 1H, OH), 8.27 (s, 1H, H_2), 8.09 (s, 1H, H_3), 7.50 (d, J = 8.5 Hz, 1H, H_4), 6.78 (dd, J = 8.8, 2.5 Hz, 1H, H_5), 6.72 (d, J = 2.2 Hz, 1H, H_6), 1.46 (s, 9H, H_1); ^{13}C NMR (150 MHz, DMSO) δ 159.4, 158.0, 152.7, 151.4, 128.8, 125.2, 120.98, 113.5, 111.4, 101.9, 80.1, 27.9 (3C).

_N_-Boc 7-hydroxy-8-methyl-3-aminocoumarin (2.4b)

7-Acetoxy-8-methyl-3-acetamidocoumarin **2.3b** (3.00 g, 10.90 mmol), di-*tert*-butyldicarbonate (10.00 g, 45.8 mmol), DMAP (0.266 g, 2.2 mmol) and hydrazine monohydrate (5.57 g, 111.2 mmol) afforded **2.4b** as a pale yellow solid (2.02 g, 63%). Mp.: 110-113 °C. ^{1}H NMR (300 MHz, DMSO-d_6): δ 10.27 (s, 1H, OH), 8.21 (s, 1H, H_2), 8.05 (s, 1H, H_3), 7.32 (d, J = 8.5 Hz, 1H, H_4), 6.83 (d, J = 8.5 Hz, 1H, H_5), 2.14 (s, 3H, H_6), 1.45 (s, 9H, H_1); ^{13}C NMR (75 MHz, DMSO) δ 158.3, 157.3, 152.9, 149.6, 125.5, 120.7, 112.7, 111.5, 110.6, 80.2, 28.8, 28.0 (3C), 8.0.

4.2.4. General procedure for synthesis of *N*-Boc 7-phenyloxy-3-aminocoumarins (2.6a-f)[3]

An appropriate volume of Et_3N (5.0 eq.) was added to a mixture of **2.4a-b** (1.0 eq.), $Cu(OAc)_2•H_2O$ (1.0 eq.) or anhydrous $Cu(OAc)_2$ (1.0 eq.) and a relevant phenylboronic acid **2.5a-c** (2.0 eq.) in DCM (10 mL) followed by addition of freshly activated powdered 4 Å molecular sieves (ca. 920 mg). The resulting green suspension was stirred at room temperature for 48 hours under N_2 atmosphere after which the molecular sieves were removed through filtration over a small pad of silica gel (using DCM (50 mL) to recover product). The solvent was removed under reduced pressure and the resulting crude product was purified by silica gel chromatography (5% EtOAc/Hex) to afford the respective *N*-Boc 7-phenyl-*O*-3-aminocoumarins **2.6a-f**.

_N_-Boc 7-(4-*tert*-butylphenyl)-_O_-3-aminocoumarin (2.6a)

7-Hydroxy-3-acetamidocoumarin **2.4a** (0.500 g, 1.8 mmol), 4-*tert*-butylphenylboronic acid **2.5a** (0.642 g, 3.6 mmol), $Cu(OAc)_2•H_2O$ (0.360 g, 1.8 mmol) and Et_3N (0.913 g, 9.0 mmol) afforded **2.6a** as a white, fluffy solid (0.216 g, 29%). M.p.: 137-138 °C. ^{1}H NMR (400 MHz, DMSO): δ 8.45 (s, 1H, H_2), 8.19 (s, 1H, H_3), 7.69 (d, J = 8.4 Hz, 1H, H_4), 7.46 (d, J = 8.3 Hz, 2H, H_7), 7.04 (d, J = 8.4 Hz, 2H, H_8), 6.97 – 6.87 (m, 2H, H_5, H_6), 1.47 (s, 9H, H_1), 1.30 (s, 9H, H_{10}); ^{13}C NMR (100 MHz, $CDCl_3$) δ 159.6, 158.9, 153.3, 152.8, 150.8, 147.9, 128.4, 127.1 (2C), 123.0, 121.0, 119.8 (2C), 115.5 (3C), 115.0, 105.2, 81.8, 34.7, 31.7 (3C), 28.4 (3C).

_N_-Boc 7-(4-methoxyphenyl)-_O_-3-aminocoumarin (2.6b)

7-Hydroxy-3-acetamidocoumarin **2.4a** (0.500 g, 1.8 mmol), 4-methoxyphenylboronic acid **2.5b** (0.548 g, 3.6 mmol), Cu(OAc)2•H2O (0.360 g, 180.0 mmol) and Et_3N (0.913 g, 9.0 mmol) afforded **2.6b** as a white solid (0.200 g, 33%). M.p.: 74-75 °C. ^{1}H NMR (600 MHz, DMSO): δ 8.43 (s, 1H, H_2), 8.17 (s, 1H, H_3), 7.67 (d, J = 8.6 Hz, 1H, H_4), 7.09 (d, J = 9.0 Hz, 2H, H_7), 7.01 (d, J = 9.0 Hz, 2H, H_8), 6.90 (dd, J = 8.6, 2.3 Hz, 1H, H_5), 6.84 (d, J = 2.1 Hz, 1H, H_6), 3.77 (s, 3H, H_{10}); ^{13}C NMR (75 MHz, DMSO) δ 159.5, 156.4, 152.8, 150.8, 148.2, 129.1, 122.8, 121.5 (2C), 115.4 (2C), 114.4, 114.2, 103.8, 80.4, 73.6, 55.5, 30.8, 28.0 (3C).

_N_-Boc 7-(3-methoxyphenyl)-_O_-3-aminocoumarin (2.6c)

7-Hydroxy-3-acetamidocoumarin **2.4a** (0.500 g, 1.8 mmol), 3-methoxyphenylboronic acid **2.5c** (0.548 g, 3.6 mmol), $Cu(OAc)_2•H_2O$ (0.360 g, 1.8 mmol) and Et_3N (0.913 g, 9.0 mmol) afforded **2.6c** as a white solid (0.143 g, 23%). M.p.: 73-75 °C. ^{1}H NMR (300 MHz, DMSO-

d_6): δ 8.50 (s, 1H, H_2), 8.19 (s, 1H, H_3), 7.70 (d, J = 9.3 Hz, 1H, H_4), 7.33 (t, J = 8.2 Hz, 1H, H_9), 7.03 – 6.92 (m, 2H, H_5, H_6), 6.80 (ddd, J = 8.3, 2.4, 0.8 Hz, 1H, H_{10}), 6.69 (t, J = 2.3 Hz, 1H, H_7), 6.65 (ddd, J = 8.0, 2.3, 0.8 Hz, 1H, H_8), 3.75 (s, 3H, H_{11}), 1.47 (s, 9H, H_1); ^{13}C NMR (75 MHz, DMSO): δ 160.8, 157.9, 157.5, 156.6, 152.7, 150.7, 130.8, 129.1, 123.1, 115.3, 115.1, 111.4, 110.3, 105.5, 105.2, 80.4, 55.4, 30.8, 27.9 (3C).

_N_-Boc 7-(4-*tert*-butylphenyl)-_O_-8-methyl-3-aminocoumarin (2.6d)

7-Hydroxy-8-methyl-3-acetamidocoumarin **2.4b** (0.500 g, 1.7 mmol), 4-*tert*-butylphenylboronic acid **2.5a** (0.601 g, 3.4 mmol), $Cu(OAc)_2$ (0.306 g, 1.7 mmol) and Et_3N (0.853 g, 8.4 mmol) afforded **2.6d** as a white solid (0.080 g, 11%). M.p.: 227-230 °C. ^{1}H NMR (300 MHz, $CDCl_3$): δ 8.24 (s, 1H, H_2), 7.39 – 7.31 (m, 3H, H_3, H_8), 7.22 (d, J = 8.5 Hz, 1H, H_4), 6.92 – 6.85 (m, 2H, H_7), 6.81 (d, J = 8.6 Hz, 1H, H_5), 2.38 (s, 3H, H_6), 1.53 (s, 9H, H_{10}), 1.32 (s, 9H, H_1); ^{13}C NMR (75 MHz, $CDCl_3$): δ 159.0, 156.3, 154.6, 152.7, 149.1, 146.6, 126.8, 125.1, 122.9, 121.3, 118.1 (2C), 117.3, 115.6 (2C), 81.7, 34.5, 31.6 (3C), 29.8, 28.4 (3C), 8.7.

_N_-Boc 7-(4-methoxyphenyl)-_O_-8-methyl-3-aminocoumarin (2.6e)

7-Hydroxy-8-methyl-3-acetamidocoumarin **2.4b** (0.500 g, 1.7 mmol), 4-methoxyphenylboronic acid **2.5b** (0.523 g, 3.4 mmol), $Cu(OAc)_2$ (0.312 g, 1.7 mmol) and Et_3N (0.868 g, 8.6 mmol) afforded **2.6e** as a white solid (0.261 g, 38%). M.p.: 150-152 °C. ^1H NMR (300 MHz, $CDCl_3$): δ 8.25 (s, 1H, H_2), 7.37 (s, 1H, H_3), 7.21 (d, J = 8.6 Hz, 1H, H_4), 6.96 – 6.85 (m, 4H, H_7, H_8), 6.73 (d, J = 8.6 Hz, 1H, H_5), 3.83 (s, 3H, H_{10}), 2.42 (s, 3H, H_6), 1.55 (s, 9H, H_1); ^{13}C NMR (75 MHz, $CDCl_3$): δ 159.4, 157.5, 156.6, 153.1, 150.5, 149.5, 125.5, 123.1, 121.7, 120.7, 116.8, 115.6, 115.5, 114.7, 82.0, 56.2, 28.7 (3C), 9.0.

_N_-Boc 7-(3-methoxyphenyl)-_O_-8-methyl-3-aminocoumarin (2.6f)

7-Hydroxy-8-methyl-3-acetamidocoumarin **2.4b** (0.500 g, 1.7 mmol), 3-methoxyphenylboronic acid **2.5c** (0.523 g, 3.4 mmol), $Cu(OAc)_2$ (0.312 g, 1.7 mmol) and Et_3N (0.868 g, 8.6 mmol) afforded **2.6f** as a white solid (0.307 g, 45%). M.p.: 146-148 °C. ^1H NMR (300 MHz, $CDCl_3$): δ 8.24 (s, 1H, H_2), 7.36 (s, 1H, H_3), 7.26 – 7.18 (m, 2H, H, H_9, H_{10}), 6.85 (d, J = 8.5 Hz, 1H, H_4), 6.65 (ddd, J = 8.3, 2.3, 1.0 Hz, 1H, H_8), 6.53 – 6.48 (m, 2H, H_5, H_7), 3.77 (s, 3H, H_{11}), 2.36 (s, 3H, H_6), 1.53 (s, 9H, H_1); ^{13}C NMR (75 MHz, $CDCl_3$): δ 161.2, 158.9, 158.4, 155.5, 152.7, 149.1, 130.4, 125.2, 123.1, 121.1, 117.8, 116.4, 116.0, 110.3, 109.0, 104.4, 81.7, 55.5, 28.4 (3C), 8.7.

4.2.5. General procedure for synthesis of free 7-phenyloxy-3-aminocoumarins (2.7a-f)

A relevant *N*-Boc 7-phenyl-*O*-3-aminocoumarin (**2.6a-f**) was stirred in 4 M HCl in dioxane solution (3 mL) for 12 hours after which saturated $NaHCO_3$ solution (20 mL) was added with caution to neutralize the reaction solution. The product was extracted with DCM (3 × 25 mL). The organic layers were combined, dried ($MgSO_4$) and solvent removed *in vacuo* to afford aminocoumarins **2.7a-f**. Where necessary the product was purified by flash column chromatography (1% MeOH/DCM).

7-(4-*tert*-Butylphenyl)-*O*-3-aminocoumarin (2.7a)

N-Boc 7-(4-*tert*-butylphenyl)-*O*-3-aminocoumarin **2.6a** (0.200 g, 0.49 mmol) afforded **2.7a** as a brown solid (0.0802 g, 53%). M.p.: 103-106 °C. ^{1}H NMR (400 MHz, $CDCl_3$) δ 7.42 – 7.35 (m, 2H, H_7), 7.22 (d, J = 8.5 Hz, 1H, H_3), 7.00 – 6.95 (m, 2H, H_6), 6.90 (dd, J = 8.5, 2.4 Hz, 1H, H_4), 6.86 (d, J = 2.3 Hz, 1H, H_5), 6.70 (s, 1H, H_2), 3.86 (s, 2H, H_1), 1.34 (s, 9H, H_8); ^{13}C NMR (101 MHz, $CDCl_3$) δ 159.6, 157.4, 153.9, 150.2, 147.4, 130.6, 127.0, 126.1, 119.3, 116.3, 115.5, 111.7, 105.7, 34.6, 31.7 (3C).

7-(4-Methoxyphenyl)-*O*-3-aminocoumarin (2.7b)

N-Boc 7-(4-methoxyphenyl)-*O*-3-aminoocoumarin **2.6b** (0.200 g, 0.59 mmol) afforded **2.7b** as a brown solid (0.110 g, 66%). M.p.: 87-91 °C. ^{1}H NMR (600 MHz, DMSO): δ 7.39 (d, J = 8.4 Hz, 1H, H_3), 7.05 – 7.01 (m, 2H, H_7), 6.99 – 6.95 (m, 2H, H_6), 6.82 – 6.80 (m, 2H, H_4, H_5), 6.72 (s, 1H, H_2), 5.50 (br s, 2H, H_1), 3.75 (s, 3H, H_9); ^{13}C NMR (150 MHz, DMSO): δ 158.7, 156.1, 155.9, 149.1, 148.8, 131.8, 126.0, 120.9 (2C), 116.8, 115.2 (2C), 114.3, 108.3, 104.3, 55.5.

7-(3-Methoxyphenyl)-*O*-3-aminocoumarin (2.7c)

N-Boc 7-(3-methoxyphenyl)-*O*-3-aminocoumarin **2.6c** (0.120 g, 0.35 mmol) afforded **2.7c** as a dark-brown solid (0.098 g, 66%). M.p.: 74-75 °C. ^{1}H NMR (600 MHz, DMSO) δ 7.43 (d, J = 8.5 Hz, 1H, H, H_3), 7.29 (t, J = 8.2 Hz, 1H, H_8), 6.94 (d, J = 2.3 Hz, 1H, H_5), 6.90 (dd, J = 8.5, 2.4 Hz, 1H, H_4), 6.75 – 6.72 (m, 2H, H_2, H_9), 6.62 (t, J = 2.3 Hz, 1H, H_6), 6.58 (dd, J = 8.1, 2.1 Hz, 1H, H_7), 5.56 (s, 2H, H_1), 3.74 (s, 3H, H_{10}).

7-(4-*tert*-Butylphenyl)-*O*-8-methyl-3-aminocoumarin (2.7d)

N-Boc 7-(4-*tert*-butylphenyl)-*O*-8-methyl-3-aminocoumarin **2.6d** (0.220 g, 0.519 mmol) afforded **2.7d** as a light brown solid (0.128 g, 76%). M.p.: 120-123 °C. ^{1}H NMR (600 MHz, $CDCl_3$) δ 7.33 – 7.31 (m, 2H, H_8), 7.07 (d, J = 8.5 Hz, 1H, H_3), 6.86 – 6.85 (m, 2H, H_7), 6.80 (d, J = 8.5 Hz, 1H, H_4), 6.70 (s, 1H, H_2), 4.13 (br s, 2H, H_1), 2.36 (s, 3H, H_5), 1.31 (s, 9H. H_{10}); δ ^{13}C NMR (150 MHz, $CDCl_3$) δ 159.6, 155.1, 153.8, 148.4, 145.8, 130.4, 126.5 (2C), 122.7, 117.6, 117.2, 116.9 (2C), 116.0, 111.9, 40.9, 34.2, 31.5 (3C), 8.0.

7-(4-Methoxyphenyl)-*O*-8-methyl-3-aminocoumarin (2.7e)

N-Boc 7-(4-methoxyphenyl)-*O*-8-methyl-3-aminocoumarin **2.6e** (0.240 g, 0.60 mmol) afforded **2.7e** as a light-brown solid (0.172 g, 95%). M.p. 96-98 °C. ^{1}H NMR (300 MHz, $CDCl_3$): δ 7.04 (d, J = 8.5 Hz, 1H, H_3), 6.92 – 6.82 (m, 4H, H_7, H_8), 6.70 (d, J = 8.6 Hz, 1H, H_4), 6.68 (s, 1H, H_2), 3.79 (s, 3H, H_{10}), 2.37 (s, 3H, H_5); ^{13}C NMR (75 MHz, $CDCl_3$): δ 159.9, 155.9, 155.0, 151.0, 148.6, 130.5, 122.9, 119.7, 117.1, 116.7, 115.1, 115.0, 112.2, 55.9, 8.9.

7-(3-Methoxyphenyl)-*O*-8-methyl-3-aminocoumarin (2.7f)

N-Boc 7-(3-methoxyphenyl)-*O*-8-methyl-3-aminocoumarin **2.6f** (0.270 g, 0.68 mmol) afforded **2.7f** as a light-brown solid (0.199 g, 99%). M.p.: 78-80 °C. ^{1}H NMR (300 MHz, $CDCl_3$): δ 7.20 (t, J = 8.5 Hz, 1H, H_8), 7.09 (d, J = 8.5 Hz, 1H, H_3), 6.84 (d, J = 8.5 Hz, 1H, H_4), 6.70 (s, 1H, H_2), 6.65 – 6.60 (m, 1H, H_9), 6.50 – 6.45 (m, 2H, H_7, H_6), 4.18 (br s, 2H, H_1), 3.77 (s, 3H, H_{10}), 2.33 (s, 3H, H_5); ^{13}C NMR (75 MHz, $CDCl_3$): δ 161.5, 160.0, 159.4, 153.6, 148.8, 131.1, 130.7, 123.3, 118.6, 117.8, 117.1, 112.1, 110.1, 108.8, 104.2, 55.8, 9.2.

4.2.6. Synthesis of methyl 3-iodo-4-methoxybenzoate (2.9)

To a solution of 3-iodo-4-methoxybenzoic acid (2.00 g, 7.19 mmol) in methanol (40 ml), 8 drops of conc. H_2SO_4 (98%) were added and the solution was refluxed for 16 hours. The solution was cooled to room temperature and the product extracted with EtOAc (2 × 100 mL) and the solvent removed under reduced pressure to afford the product, methyl 3-iodo-4-methoxybenzoate **2.9**, as a white solid (1.70 g, 85%). M.p.: 71-72 °C. ^{1}H NMR (600 MHz, DMSO-d_6) δ 8.27 (d, J = 2.1 Hz, 1H, H_3), 7.96 (dd, J = 8.6, 2.2 Hz, 1H, H_2), 7.10 (d, J = 8.7 Hz, 1H, H_4), 3.91 (s, 3H, H_1), 3.82 (s, 3H, H_5); ^{13}C NMR (150 MHz, DMSO-d_6) δ 164.7, 161.5, 139.8, 131.4, 123.6, 111.2, 85.9, 56.8, 52.1.

4.2.7. Synthesis of methyl of methyl 4-methoxy-3-(3-methoxy)-phenylbenzoate (2.10)[4]

A solution of 2 M NaOH (0.08 g, 3.00 mmol) was added to a mixture of **2.9** (0.292 g, 1.00 mmol), 3-methoxyphenylboronic acid **2.5c** (0.456 g, 3.00 mmol) and 3% mol $PdCl_2$(dppf) in toluene (10 mL). The solution was refluxed under N_2 atmosphere, monitoring the reaction progress by TLC. After 24 hours, the reaction solution was diluted with distilled water, and the product extracted with ether (2 × 100 mL), washed with saturated brine and dried over magnesium sulphate ($MgSO_4$). The solvent was removed under reduced pressure, and the product purified by silica gel column chromatography (10% EtOAc/Hex) to afford **2.10** as a viscous, colourless oil. ^{1}H NMR (300 MHz, DMSO-d_6): δ 7.97 (dd, J = 8.7, 2.3 Hz, 1H, H_2), 7.83 (d, J = 2.2 Hz, 1H, H_3), 7.37 – 7.31 (m, 1H, H_7), 7.23 (d, J = 8.7 Hz, 1H, H_4), 7.04 – 7.00 (m, 2H, H_6, H_8), 6.96 – 6.91 (m, 1H, H_9), 3.85 (s, 3H, H_1), 3.82 (s, 3H, H_{10}), 3.78 (s, 3H, H_5);^{13}C NMR (75 MHz, DMSO-d_6): δ 165.9, 160.0, 159.0, 138.4, 131.3, 130.7, 129.8, 129.3, 121.9, 121.5, 114.0, 112.8, 111.7, 56.0, 55.1, 52.0.

4.2.8. Synthesis of 4-methoxy-3-(3-methoxy)-phenylbenzoic acid (2.11)

A solution of **2.10** (0.245 g, 0.898 mmol) in 3:1:1 tetrahydrofuran-methanol-water (10 mL) was heated at 70 °C for 8 hours. The reaction was cooled to room temperature and acidified to 1 – 2 pH with concentrated HCl (32%) to form a milky suspension. The product was extracted three times with ethyl acetate, dried over magnesium sulphate and concentrated under reduced pressure to afford **2.11** as an off-white solid (0.205 g, 89%). M.p.: 147-151 °C. ^{1}H NMR (300 MHz, DMSO-d_6): δ 12.73 (s, 1H,H_1), 7.95 (dd, J = 8.6, 2.2 Hz, 1H, H_2), 7.82 (d, J = 2.2 Hz, 1H, H_3), 7.38 – 7.30 (m, 1H, H_7), 7.21 (d, J = 8.7 Hz, 1H, H_4), 7.05 – 7.00 (m, 2H, H_6,H_8), 6.96

– 6.91 (m, 1H, H_9), 3.84 (s, 3H, H_{10}), 3.78 (s, 3H, H_5); ^{13}C NMR (75 MHz, DMSO-d_6): δ 167.0, 159.7, 158.9, 138.6, 131.5, 130.7, 129.5, 129.2, 123.0, 121.5, 114.9, 112.7, 111.5, 55.9, 55.1.

4.2.9. General procedure for synthesis of target phenylated Nb analogues (2.13a-f and 2.14a-f)[5]

A relevant free 7-phenyloxy-3-aminocoumarins (**2.7a-f**) (1.0 eq.) in 30% pyridine/DCM solution (2 mL) was stirred at room temperature for 10 minutes followed by addition of an appropriate diaryl acid (**2.11** or **2.12**) (2.0 eq.) and EDCI•HCl (3.0 eq.). The reaction mixture was stirred at room temperature for 1 to 3 days after which the solvent was removed *in vacuo* to afford a crude product. The ferrocene-containing novobiocin analogues were purified by silica gel column chromatography (10% EtOAc/Hex for **2.13a-f**) and the organic novobiocin analogues were purified by preparative TLC, using DCM as a mobile phase, to afford **2.14a-f**.

7-(4-*tert*-Butylphenyl)-*O*-3-ferrocenylcarboxamidocoumarin (2.13a)

7-(4-*tert*-Butylphenyl)-*O*-3-aminocoumarin **2.7a** (0.080 g, 0.26 mmol), ferrocene carboxylic acid **2.12** (0.119 g, 0.52 mmol) and EDCI•HCl (0.149 g, 0.78 mmol) afforded **2.13a** as an orange solid (0.0381 g, 28%). M.p.: 180-182 °C. IR ν_{max}/cm^{-1}: 3409 (N-H, amide), 3090 (C-H, pyrone C=C), 2959 (C-H, methyl), 1708 (C=O, lacone), 1658 (C=O, amide), 1501 (C=C, aromatic), 1168 (C-O, aromatic); ^{1}H NMR (300 MHz, $CDCl_3$): δ 8.71 (s, 1H, H_5), 8.27 (s, 1H, H_4), 7.45 (d, J = 8.6 Hz, 1H, H_6), 7.41 (d, J = 8.9 Hz, 2H, H_{10}), 7.04 – 6.95 (m, 3H, H_7, H_9), 6.88 (d, J = 2.4 Hz, 1H, H_8), 4.85 (t, J = 1.9 Hz, 2H, H_3), 4.50 (t, J = 1.9 Hz, 2H, H_2), 4.26 (s, 5H, H_1), 1.35 (s, 9H, H_{11}); ^{13}C NMR (75 MHz, $CDCl_3$): δ 170.0, 159.9, 159.2, 153.0, 151.0, 147.9, 128.8, 127.1 (2C), 123.0, 122.5, 119.8 (2C), 115.5, 114.9, 105.0, 75.2, 71.6 (2C), 70.2 (5C), 68.5 (2C), 34.6, 31.6 (3C); HRMS (ESI$^+$) *m/z* calcd for $C_{30}H_{27}FeNO_4$: 521.1290, found 522.1381 $[M+H]^+$. Anal. calcd for $C_{30}H_{27}FeNO_4$: C, 69.11; H, 5.22; N, 2.69. Found: C, 68.23; H, 6.03; N, 2.57%.

7-(4-Methoxyphenoxy)-*O*-3-ferrocenylcarboxamidocoumarin (2.13b)

7-(4-Methoxyphenyl)-*O*-3-aminocoumarin **2.7b** (0.0950 g, 0.34 mmol), ferrocene carboxylic acid **2.12** (0.154 g, 0.67 mmol) and EDCI•HCl (0.192 g, 1.0 mmol) afforded **2.13b** as a dark red solid (0.0867 g, 52%). M.p.: 114-115 °C. IR ν_{max}/cm^{-1}: 3394 (N-H, amide), 3054 (C-H, pyrone C=C), 2928 (C-H, methyl), 1690 (C=O, lactone), 1667 (C=O, amide), 1502 (C=C, aromatic), 1168 (C-O, aromatic ether); ^{1}H NMR (300 MHz, $CDCl_3$): δ 8.70 (s, 1H, H_5), 8.26 (s, 1H, H_4), 7.43 (d, J = 8.6 Hz, 1H, H_6), 7.06 – 7.01 (m, 2H, H_{10}), 6.96 – 6.90 (m, 3H, H_7, H_9), 6.83 (d, J = 2.4 Hz, 1H, H_8), 4.82 (t, J = 2.0 Hz, 2H, H_3), 4.47 (t, J = 1.9 Hz, 2H, H_2), 4.26 (s, 5H, H_1), 3.83 (s, 3H, H_{11}); ^{13}C NMR (75 MHz, $CDCl_3$): δ 170.0, 160.5, 159.2, 156.9, 151.0, 148.6, 128.8, 123.0, 122.4, 121.8 (2C), 115.2 (2C), 114.9, 114.6, 104.4, 77.2, 75.1, 71.6 (2C), 70.2 (5C), 68.5 (2C), 55.8; HRMS (ESI) *m/z* calcd for $C_{27}H_{21}FeNO_5$: 495.0769, Found 496.0851 [M+H]$^+$. Anal. calcd $C_{27}H_{21}FeNO_5$: C, 65.47; H, 4.27; N, 2.83. Found: C, 65.54; H, 4.95; N, 2.74%.

7-(3-Methoxyphenoxy)-*O*-3-ferrocenylcarboxamidocoumarin (2.13c)

7-(3-Methoxyphenyl)-*O*-3-aminocoumarin **2.7c** (0.0780 g, 0.28 mmol), ferrocene carboxylic acid **2.12** (0.127 g, 0.55 mmol) and EDCI•HCl (0.158 g, 1.0 mmol) afforded **2.13c** as a dark red solid (0.056 g, 41%). M.p.: 180-183 °C. IR ν_{max}/cm^{-1}: 3400 (N-H, amide), 3056 (C-H, methylene), 2927 (C-H, methyl), 1693 (C=O, lactone), 1668 (C=O, amide), 1513 (C=C, aromatic), 1158 (C-O, aromatic ether); ^{1}H NMR (600 MHz, $CDCl_3$): δ 8.71 (s, 1H, H_4), 8.28 (s, 1H, H_5), 7.46 (d, J = 8.6 Hz, 1H, H_7), 7.29 (t, J = 8.2 Hz, 1H, H_{11}), 6.98 (dd, J = 8.5, 2.3 Hz, 1H, H_7), 6.93 (d, J = 2.2 Hz, 1H, H_8), 6.75 (dd, J = 8.3, 2.2 Hz, 1H, H_{12}), 6.66 (dd, J = 8.0, 1.8 Hz, 1H, H_{10}), 6.63 (t, J = 2.3 Hz, 1H, H_9), 4.84 (t, J = 1.8 Hz, 2H, H_3), 4.49 (t, J = 1.8 Hz, 2H, H_2), 4.26 (s, 5H, H_1), 3.80 (s, 3H, H_3); ^{13}C NMR (150 MHz, $CDCl_3$) δ 170.1, 161.2, 159.2, 159.1, 156.7, 150.9, 130.6, 128.9, 122.9, 122.7, 115.8, 115.2, 112.1, 110.4, 106.1, 105.6, 75.0, 71.6 (2C), 70.2 (5C), 68.5 (2C), 55.6; HRMS (ESI$^+$) *m/z* calcd for $C_{27}H_{21}FeNO_5$: 495.0769, Found 496.0835 [M+H]$^+$. Anal. calcd $C_{27}H_{21}FeNO_5$: C, 65.47; H, 4.27; N, 2.83. Found: C, 65.88; H, 4.97; N, 2.75%.

7-(4-*tert*-butylphenyl)-*O*-8-methyl-3-ferrocenylcarboxamidocoumarin (2.13d)

7-(4-*tert*-Phenyl)-*O*-8-methyl-3-aminocoumarin **2.7d** (0.0600 g, 0.19 mmol), ferrocene carboxylic acid (0.0856 g, 0.37 mmol) and EDCI•HCl (0.107 g, 0.56 mmol) afforded **2.13d** as an orange solid (0.0446g g, 45%). M.p.: 188-191 °C. IR ν_{max}/cm^{-1} 3389 (N-H, amide), 3090

(C-H, pyrone C=C), 2960 (C-H, methyl), 1712 (C=O, lactone), 1698 (C=O, amide), 1506 (C=C, aromatic), 1170 (C-O, aromatic); ^{1}H NMR (600 MHz, $CDCl_3$): δ 8.70 (s, 1H, H_5), 8.32 (br s, 1H, H_4), 7.38 – 7.35 (m, 2H, H_{10}), 7.28 (d, J = 8.8 Hz, 1H, H_6), 6.92 – 6.84 (m, 2H, H_9), 6.84 (d, J = 8.6 Hz, 1H, H_7), 4.85 (t, J = 1.9 Hz, 2H, H_3), 4.48 (t, J = 1.9 Hz, 2H, H_2), 4.27 (s, 5H, H_1), 2.42 (s, 3H, H_8), 1.33 (s, 9H, H_{11}); ^{13}C NMR (150 MHz, $CDCl_3$): δ 170.0, 159.4, 156.7, 154.5, 149.4, 146.7, 126.9 (2C), 125.6, 123.4, 122.5, 118.2 (2C), 117.3, 115.6, 115.6, 75.2, 71.5 (2C), 70.2 (5C), 68.6 (2C), 34.5, 31.6 (3C); HRMS (ESI$^+$) *m/z* calcd for $C_{31}H_{25}NO_7$: 535.1446, Found 536.1520 [M+H]$^+$. Anal. calcd $C_{31}H_{29}NO_4$: C, 69.54; H, 5.46; N, 2.62. Found: C, 70.23; H, 3.92; N, 2.72%.

_N_-(7-(4-Methoxyphenyl)-_O_-8-methyl-3-ferrocenylcarboxamidocoumarin (2.13e)

7-(4-Methoxyphenyl)-*O*-8-methyl-3-aminocoumarin **2.7e** (0.0750 g, 0.25 mmol), ferrocene carboxylic acid (0.116 g, 0.50 mmol) and EDCI•HCl (0.145 g, 0.76 mmol) afforded **2.13e** as an orange solid (0.0245 g, 19%). M.p.: 167-169 °C. IR ν_{max}/cm^{-1} 3407 (N-H, amide), 3097 (C-H, pyrone C=C), 2920 (C-H, methyl), 1704 (C=O, lactone), 1667 (C=O, amide), 1499 (C=C, aromatic), 1202 (C-O, aromatic ether); ^{1}H NMR (600 MHz, $CDCl_3$): δ 8.70 (s, 1H, H_4), 8.33 (br s, 1H, H_5), 7.28 (d, J = 8.6 Hz, 1H, H_6), 6.99 – 6.95 (m, 2H, H_{10}), 6.94 – 6.89 (m, 2H, H_9), 6.75 (d, J = 8.6 Hz, 1H, H_7), 4.86 (t, J = 1.9 Hz, 2H, H_3), 4.51 – 4.48 (m, 2H, H_2), 4.29 (s, 5H, H_1), 3.83 (s, 3H, H_{11}), 2.45 (s, 3H, H_8); ^{13}C NMR (150 MHz, $CDCl_3$): δ 170.0, 159.5, 157.6, 156.2, 150.0, 149.3, 125.5, 123.4, 122.3, 120.5 (2C), 116.4, 115.1 (3C), 114.3, 75.2, 71.5 (2C), 70.2 (5C), 68.5 (2C), 55.8, 8.7; HRMS (ESI$^+$) *m/z* calcd for $C_{28}H_{23}FeNO_5$: 509.0926, Found 510.1004 [M+H]$^+$. Anal. calcd $C_{28}H_{23}FeNO_5$: C, 66.03; H, 4.55; N, 2.75. Found: C, 66.77; H, 4.59; N, 2.66%.

7-(3-Methoxyphenoxy)-_O_-8-methyl-3-ferrocenylcarboxamidocoumarin (2.13f)

7-(3-Methoxyphenyl)-*O*-8-methyl-3-aminocoumarin **2.7f** (0.080 g, 0.27 mmol), ferrocene carboxylic acid (0.124 g, 0.54 mmol) and EDCI•HCl (0.155 g, 0.81 mmol) afforded **2.13f** as an orange solid (0.0615 g, 45%). M.p.: 162-164 °C. IR ν_{max}/cm^{-1} 3396 (N-H, amide), 3080 (C-H, pyrone C=C), 2924 (C-H, methyl), 1716(C=O, lactone), 1663 (C=O, amide), 1510 (C=C, aromatic), 1170 (C-O, aromatic ether); ^{1}H NMR (600 MHz, $CDCl_3$): δ 8.71 (s, 1H, H_4), 8.32 (s, 1H, H_5), 7.31 (d, J = 8.5 Hz, 1H, H_6), 7.23 (t, J = 8.7 Hz, 1H, H_{11}), 6.89 (d, J = 8.5 Hz, 1H, H_7), 6.67 (dd, J = 8.2, 2.5 Hz, 1H, H_{10}), 6.54 – 6.51 (m, 2H, H_9, H_{12}), 4.85 (t, J = 1.9 Hz, 2H, H_3), 4.48 (t, J = 1.9 Hz, 2H, H_3), 4.27 (s, 5H, H_5), 3.79 (s, 3H, H_{13}), 2.39 (s, 3H, H_8); ^{13}C NMR (150 MHz, $CDCl_3$) δ 170.1, 161.2, 159.3, 158.3, 155.9, 149.3, 130.5, 125.7, 123.2, 122.7,

117.8, 116.4, 116.0, 110.4, 109.1, 104.5, 75.1, 71.6 (2C), 70.2 (5C), 68.6 (2C), 55.5, 8.8; HRMS (ESI) *m/z* calcd for $C_{28}H_{23}FeNO_5$: 509.0926, Found 510.1004 $[M+H]^+$. Anal. calcd $C_{28}H_{23}FeNO_5$: C, 66.03; H, 4.55; N, 2.75. Found: C, 66.46; H, 4.61; N, 2.66%.

7-(4-*tert*-Butylphenyl)-*O*-3-(3',6-dimethoxy-[1,1'-biphenyl])-3-carboxamidocoumarin (2.14a)

7-(4-*tert*-Butylphenyl)-*O*-3-aminocoumarin **2.7a** (0.0630 g, 0.20 mmol), 4-methoxy-3-(3-methoxy)-phenylbenzoic acid (0.12 g, 0.41 mmol) and EDCI•HCl (0.117 g, 0.61 mmol) afforded **2.14a** as a yellow solid (0.041 g, 37%). M.p.: 182-185 °C. IR ν_{max}/cm^{-1}: 3369 (N-H, amide), 3070 (C-H, pyrone C=C), 2920 (C-H, methyl), 1700 (C=O, lactone), 1665 (C=O, amide), 1601 (C=C, aromatic), 1177 (C-O, aromatic); ^{1}H NMR (600 MHz, $CDCl_3$): δ 8.83 (s, 1H, H_{10}), 8.71 (s, 1H, H_{11}), 7.91 (dd, *J* = 8.6, 2.4 Hz, 1H, H_8), 7.88 (d, *J* = 2.3 Hz, 1H, H_9), 7.47 (d, *J* = 8.6 Hz, 1H, H_7), 7.42 – 7.41 (m, 2H, H_{16}), 7.36 (t, *J* = 7.9 Hz, 1H, H_4), 7.11 (dt, *J* = 7.5, 1.2 Hz, 1H, H_5), 7.08 (t, *J* = 1.1 Hz, 1H, H_2), 7.06 (d, *J* = 8.6 Hz, 1H, H_{12}), 7.03 – 7.00 (m, 2H, H_{15}), 6.98 (dd, *J* = 8.6, 2.4 Hz, 1H, H_{13}), 6.93 (dd, *J* = 8.2, 2.3 Hz, 1H, H_3), 6.87 (d, *J* = 2.3 Hz, 1H, H_{14}), 3.90 (s, 3H, H_1), 3.86 (s, 3H, H_6), 1.35 (s, 9H, H_{17}); ^{13}C NMR (150 MHz, $CDCl_3$): δ 165.6, 160.1, 160.0, 159.4, 159.3, 153.0, 151.2, 148.0, 138.7, 131.2, 130.0, 129.3, 129.0, 128.3, 127.1 (2C), 126.0, 123.7, 122.6, 122.1, 119.9 (2C), 115.4, 114.7, 113.2, 111.1, 105.0, 56.0, 55.5, 34.6, 31.6, 29.8 (3C); HRMS (ESI^+) *m/z* calcd for $C_{34}H_{31}NO_6$: 549.2151, Found 550.2216 $[M+H]^+$. Anal. calcd for $C_{34}H_{31}NO_6$: C, 74.30; H, 5.69; N, 2.55. Found: C, 74.63; H, 5.95; N, 2.66%.

7-(4-Methoxyphenyl)-*O*-3-(3',6-dimethoxy-[1,1'-biphenyl])-3-carboxamidocoumarin (2.14b)

7-(4-Methoxyphenyl)-*O*-3-aminocoumarin **2.7b** (0.100 g, 0.35 mmol), 4-methoxy-3-(3-methoxy)-phenylbenzoic acid (0.162 g, 0.71 mmol) and EDCI•HCl (0.203 g, 1.1 mmol) afforded **2.14b** as an off-white solid (0.0260 g, 13%). M.p.: 182-184 °C. IR ν_{max}/cm^{-1}: 3366 (N-H, amide), 3085 (C-H, pyrone C=C), 2922 (C-H, methyl), 1698 (C=O, lactone), 1663 (C=O, amide), 1601 (C=C, aromatic), 1180 (C-O, aromatic ether); ^{1}H NMR (300 MHz, $CDCl_3$): δ 8.82 (s, 1H, H_{11}), 8.70 (s, 1H, H_{10}), 7.91 (dd, *J* = 8.6, 2.4 Hz, 1H, H_8), 7.88 (d, *J* = 2.4 Hz, 1H, H_9), 7.46 (d, *J* = 8.7 Hz, 1H, H_7), 7.36 (t, *J* = 7.9 Hz, 1H, H_4), 7.11 (d, *J* = 7.8 Hz, 1H, H_5), 7.10 – 7.07 (m, 2H, H_2, H_3), 7.05 – 7.01 (m, 2H, H_{16}), 6.96 – 6.91 (m, 4H, H_{12}, H_{13}, H_{15}), 6.84 (d, *J* = 2.3 Hz, 1H, H_{14}), 3.90 (s, 3H, H_1), 3.86 (s, 3H, H_6), 3.83 (s, 3H, H_{17}); ^{13}C NMR (150 MHz, $CDCl_3$): δ 165.6, 160.7, 159.9, 159.4, 159.3, 156.9, 151.20, 148.5, 138.7, 131.1, 130.0, 129.3,

129.0 128.2, 126.0, 123.7, 122.5, 122.1, 121.8 (2C), 115.4, 115.3 (2C), 114.9, 114.5, 113.2, 111.1, 104.3, 56.0, 55.8, 55.4; HRMS (ESI^+) *m/z* calcd for $C_{31}H_{25}NO_7$: 523.1631, Found 524.1700 $[M+H]^+$. Anal. calcd $C_{31}H_{25}NO_7$: C, 71.12; H, 4.81; N, 2.68. Found: C, 70.44; H, 4.84; N, 2.27%.

7-(3-Methoxyphenyl)-*O*-3-(3',6-dimethoxy-[1,1'-biphenyl])-3-carboxamidocoumarin (2.14c)

7-(3-Methoxyphenyl)-*O*-3-aminocoumarin **2.7c** (0.120 g, 0.42 mmol), 4-methoxy-3-(3-methoxy)-phenylbenzoic acid (0.195 g, 0.85 mmol) and EDCI•HCl (0.244 g, 1.3 mmol) afforded **2.14c** as a yellow solid (0.0588 g, 27%). M.p.: 152-153 °C. IR ν_{max}/cm^{-1}: 3365 (N-H, amide), 3085 (C-H, pyrone C=C), 2919 (C-H, methyl), 1697 (C=O, lactone), 1663 (C=O, amide), 1601 (C=C, aromatic), 1178 (C-O, aromatic ether); ^{1}H NMR (600 MHz, $CDCl_3$): δ 8.83 (s, 1H, H_{11}), 8.72 (s, 1H, H_{10}), 7.91 (dd, J = 8.6, 2.5 Hz, 1H, H_8), 7.88 (d, J = 2.5 Hz, 1H, H_9), 7.48 (d, J = 8.6 Hz, 1H, H_7), 7.36 (t, J = 7.9 Hz, 1H, H_4), 7.29 (t, J = 8.2 Hz, 1H, H_{17}), 7.12 (d, J = 7.6 Hz, 1H, H_5), 7.10 – 7.08 (m, 1H, H_{15}), 7.06 (d, J = 8.6 Hz, 1H, H_{12}), 6.99 (dd, J = 8.5, 2.3 Hz, 1H, H_{13}), 6.95 – 6.90 (m, 2H, H_{14}, H_{16}), 6.76 (dd, J = 8.3, 2.3 Hz, 1H, H_5), 6.66 (dd, J = 8.0, 2.1 Hz, H_3), 6.64 (t, J = 2.2 Hz, 1H, H_2), 3.90 (s, 3H, H_1), 3.86 (s, 3H, H_6), 3.80 (s, 3H, H_{19}); ^{13}C NMR (150 MHz, $CDCl_3$) δ 165.6, 161.2, 159.9, 159.4, 159.3, 159.2, 156.7, 151.2, 138.6, 131.1, 130.6, 130.0, 129.3, 129.0, 128.3, 126.0, 123.5, 122.8, 122.1, 115.8, 115.4, 115.1, 113.2, 112.1, 111.1, 110.5, 106.1, 105.6, 56.0, 55.6, 55.4; HRMS (ESI$^+$) *m/z* calcd for $C_{31}H_{25}NO_7$: 523.1631, Found 524.1714 $[M+H]^+$. Anal. calcd $C_{31}H_{25}NO_7$: C, 71.12; H, 4.81; N, 2.68. Found: C, 71.62; H, 5.25; N, 2.53%.

7-(4-*tert*-Butylphenyl)-*O*-8-methyl-3-(3',6-dimethoxy-[1,1'-biphenyl])-3-carboxamidocoumarin (2.14d)

7-(4-*tert*-Butylphenyl)-*O*-8-methyl-3-aminocoumarin **2.7d** (0.0420 g, 0.13 mmol), (0.0653 g, 0.26 mmol) and EDCI•HCl (0.0750 g, 0.39 mmol) afforded **2.14d** as a yellow solid (0.0404 g, 55%). M.p.: 179-181 °C. IR ν_{max}/cm^{-1} 3413 (N-H, amide), 3078 (C-H, pyrone C=C), 2962 (C-H, methyl), 1698 (C=O, lactone), 1672 (C=O, amide), 1599 (C=C, aromatic), 1175 (C-O, aromatic); ^{1}H NMR (600 MHz, $CDCl_3$): δ 8.83 (s, 1H, H_{11}), 8.75 (s, 1H, H_{10}), 7.93 (dd, J = 8.5, 2.4 Hz, 1H, H_8), 7.91 (d, J = 2.4 Hz, 1H, H_9), 7.39 – 7.35 (m, 3H, H_4, H_{16}), 7.31 (d, J = 8.6 Hz,1H, H_7), 7.13 (dt, J = 7.6, 1.2 Hz, 1H, H_5), 7.10 (t, J = 2.1 Hz, 1H, H_2), 7.08 (d, J = 8.7 Hz, 1H, H_{12}), 6.96 – 6.90 (m, 3H, H_{15}, H_3), 6.84 (d, J = 8.6 Hz, 1H, H_{13}), 3.90 (s, 3H, H_1), 3.86 (s, 3H, H_6), 2.42 (s, 3H, H_{14}), 1.33 (s, 9H, H_{17}); ^{13}C NMR (150 MHz, $CDCl_3$) δ 165.7, 159.9, 159.4, 159.4, 156.9, 154.4, 149.5, 146.7, 138.7, 131.1, 130.1, 129.3, 128.3, 126.9 (2C), 126.1, 125.7, 124.0, 122.6, 122.1, 118.2 (2C), 117.2, 115.5, 115.4, 115.3, 113.2, 111.1, 56.0, 55.4, 34.5, 31.6 (3C), 8.7; HRMS (ESI$^+$) *m/z* calcd for $C_{35}H_{33}NO_6$: 563.2308, Found 564.2377

$[M+H]^+$. Anal. calcd $C_{35}H_{33}NO_6$: C, 74.58; H, 5.90; N, 2.49. Found: C, 74.07; H, 4.95; N, 2.61%.

7-(4-Methoxyphenyl)-*O*-8-methyl-3-(3',6-dimethoxy-[1,1'-biphenyl])-3-carboxamidocoumarin (2.14e)

7-(4-Methoxyphenyl)-*O*-8-methyl-3-aminocoumarin **2.7e** (0.0500 g, 0.17 mmol), 4-methoxy-3-(3-methoxy)-phenylbenzoic acid (0.0826 g, 0.32 mmol) and EDCI•HCl (0.0920 g, 0.48 mmol) afforded **2.14e** as a pale yellow solid (0.0640 g, 71%). M.p.: 156-159 °C. IR ν_{max}/cm^{-1} 3412 (N-H, amide), 3058 (C-H, pyrone C=C), 2921 (C-H, methyl), 1698 (C=O, lactone), 1672 (C=O, amide), 1671 (C=C, aromatic), 1207 (C-O, aromatic ether); ^1H NMR (600 MHz, $CDCl_3$): δ 8.81 (s, 1H, H_{11}), 8.74 (br s, 1H, H_{10}), 7.92 (dd, J = 8.5, 2.5 Hz, 1H, H_8), 7.90 (d, J = 2.4 Hz, 1H, H_9), 7.37 (t, J = 7.9 Hz, 1H, H_4), 7.27 (d, J = 8.8 Hz, 1H, H_7), 7.13 (dt, J = 7.6, 1.2 Hz, 1H, H_5), 7.10 (t, J = 0.3, 1H, H_2), 7.07 (d, J = 8.5 Hz, 1H, H_{12}), 6.98 – 6.87 (m, 5H, H_{15}, H_{16}, H_3), 6.74 (d, J = 8.6 Hz, 1H, H_{13}), 3.90 (s, 3H, H_1), 3.86 (s, 3H, H_6), 3.81 (s, 3H, H_{17}), 2.43 (s, 3H, H_{14}); ^{13}C NMR (150 MHz, $CDCl_3$) δ 165.7, 159.9, 159.5, 159.4, 157.8, 156.2, 149.9, 149.5, 138.7, 131.1, 130.1, 129.3, 128.3, 126.1, 125.7, 124.1, 122.4, 122.1, 120.6 (2C), 116.4, 115.3, 115.1, 115.0 (2C), 114.2, 113.2, 111.1, 56.0, 55.8, 55.4, 8.7; HRMS (ESI^+) *m/z* calcd for $C_{31}H_{25}NO_7$: 537.1788, Found 538.1881 $[M+H]^+$. Anal. calcd $C_{32}H_{27}NO_7$: C, 71.50; H, 5.06; N, 2.61. Found: C, 70.14; H, 4.61; N, 2.60%.

7-(3-Methoxyphenyl)-*O*-8-methyl-3-(3',6-dimethoxy-[1,1'-biphenyl])-3-carboxamidocoumarin (2.13f)

7-(3-Methoxyphenyl)-8-methyl-*O*-3-aminocoumarin **2.7f** (0.0800 g, 0.27 mmol), 4-methoxy-3-(3-methoxy)-phenylbenzoic acid (0.139 g, 0.54 mmol) and EDCI•HCl (0.155 g, 0.81 mmol) afforded **2.13f** as a yellow solid (0.0750 g, 52%). M.p.: 112-114 °C. IR ν_{max}/cm^{-1} 3405 (N-H, amide), 3082 (C-H, pyrone C=C), 2933 (C-H, methyl), 1705 (C=O, lactone), 1669 (C=O, amide), 1601 (C=C, aromatic), 1185 (C-O, aromatic ether); ^{1}H NMR (600 MHz, $CDCl_3$): δ 8.83 (s, 1H, H_{11}), 8.75 (br s, 1H, H_{10}), 7.93 (dd, J = 8.5, 2.4 Hz, 1H, H_8), 7.90 (d, J = 2.4 Hz, 1H, H_9), 7.37 (t, J = 7.9 Hz, 1H, H_4), 7.33 (d, J = 8.5 Hz, 1H, H_7), 7.24 (t, J = 8.6 Hz, 1H, H_{17}), 7.13 (dt, J = 7.6, 1.2 Hz, 1H, H_5), 7.10 (t, J = 2.1 Hz, 1H, H_{15}), 7.08 (d, J = 8.6 Hz, 1H, H_{12}), 6.94 (ddd, J = 8.3, 2.6, 0.9 Hz, 1H, H_{16}), 6.89 (d, J = 8.5 Hz, 1H, H_{13}), 6.68 (ddd, J = 8.3, 2.4, 1.0 Hz, 1H, H_{18}), 6.55 – 6.52 (m, 2H, H_2, H_3), 3.90 (s, 3H, H_1), 3.86 (s, 3H, H_6), 3.79 (s, 3H, H_{19}), 2.39 (s, 3H, H_{14}); ^{13}C NMR (150 MHz, $CDCl_3$): δ 165.7, 161.2, 160.0, 159.4, 159.4, 158.2, 156.1, 149.5, 138.7, 131.2, 130.5, 130.1, 129.3, 128.3, 126.0, 125.8, 123.9, 122.8, 122.1, 117.8, 116.3, 115.9, 115.4, 113.3, 111.1, 110.5, 109.2, 104.5, 56.0, 55.5, 55.4, 8.8; HRMS (ESI^+) *m/z* calcd for $C_{32}H_{27}NO_7$: 537.1788, Found 538.1852 $[M+H]^+$. Anal. calcd $C_{32}H_{27}NO_7$: C, 71.50; H, 5.06; N, 2.61. Found: C, 70.17; H, 5.19; N, 2.61%.

4.2.10. General procedure for synthesis of *N*Boc-protected piperidinols (2.15e-f)

A suspension of an appropriate 3- or 4-hydroxy piperidinol (**2.15c-d**) (1.0 eq.) and Boc_2O (1.2 eq.) in THF (10 mL) was stirred at room temperature for 20 minutes after which DMAP (ca. 10 mg) was added. The resulting light yellow solution was further stirred for 30 minutes and concentrated *in vacuo*. The product was purified by silica gel flash column chromatography (5% MeOH/DCM) to give the relevant product.

***N*-Boc 4-piperidinol (2.15e)**

4-Piperidinol **2.15c** (0.500 g, 4.94 mmol), Boc_2O (1.29 g) and DMAP (ca. 10 mg) afforded **2.15e** as a white solid (1.02 g, 96%). M.p.: 39-40 °C. ^{1}H NMR (400 MHz, $CDCl_3$): δ 3.85 – 3.79 (m, 4H, H_2), 3.01 (ddd, J = 13.3, 9.8, 3.3 Hz, 1H, H_1), 1.86 – 1.82 (m, 4H, H_3), 1.44 (s, 9H, H_4); ^{13}C NMR (101 MHz, $CDCl_3$): δ 155.0, 79.7, 67.9, 41.4 (2C), 34.4 (2C), 28.6 (3C).

***N*-Boc 3-piperidonol (2.15f)**

3-Piperidinol **2.15d** (0.500 g, 4.94 mmol), Boc_2O (1.29 g) and DMAP (ca. 10 mg) afforded **2.15f** as a yellow oil (1.04 g, 98%). ^{1}H NMR (400 MHz, $CDCl_3$): δ 3.77 – 3.73 (m, 2H, H_6), 3.54 – 3.28 (m, 2H, H_5), 2.99 – 2.92 (m, 3H, H_1, H_3), 1.92 – 1.65 (m, 2H, H_4), 1.41 (s, 9H, H_7); ^{13}C NMR (101 MHz, $CDCl_3$): δ 155.2, 79.68, 66.1, 39.5, 32.6, 28.4 (3C), 27.7, 22.6.

4.2.11. General procedure for synthesis of *N*-Boc-protected 7-benzyloxy-3-aminocoumarins (2.16a-b)

A suspension of an appropriate *N*Boc 7-hydroxycoumarin **2.4a-b** (1.0 eq.), benzylbromide (1.0 eq.) and K_2CO_3 (4.0 eq.) in acetone (20 mL) was refluxed for 3 hours. The reaction mixture was diluted with distilled water (50 mL) and the product extracted with EtOAc (3 × 30 mL). The collected organic layers were combined, dried ($MgSO_4$) and concentrated under reduced pressure to afford a crude product, which was purified by silica gel chromatography (5% EtOAc/Hex) to yield the desired product as a white solid.

***N*-Boc 7-benzyloxy-3-aminocoumarin (2.16a)**

7-Hydroxy-3-acetamidocoumarin **2.4a** (0.500 g, 1.8 mmol), benzylbromide (0.879 g, 1.8 mmol) and K_2CO_3 (1.00 g, 7.2 mmol) afforded **2.16a** as a white solid (0.479 g, 91%). M.p.: 111-113 °C. ^{1}H NMR (300 MHz, $CDCl_3$): δ 8.23 (s, 1H, H_2), 7.44 – 7.29 (m, 7H, H_3, H_4, H_8, H_9, H_{10}), 6.93 (dd, J = 8.6, 2.5 Hz, 1H, H_5), 6.88 (d, J = 2.4 Hz, 1H, H_6), 5.10 (s, 2H, H_7), 1.53 (s, 9H, H_1); ^{13}C NMR (75 MHz, $CDCl_3$): δ 160.0, 159.0, 152.8, 151.0, 136.2, 128.9 (2C), 128.5, 128.3, 127.7 (2C), 122.4, 121.3, 113.9, 113.7, 101.9, 81.6, 70.7, 28.4 (3C).

***N*-Boc 7-benzyloxy-8-methyl-3-aminocoumarin (2.16b)**

7-Hydroxy-3-acetamidocoumarin **2.4b** (1.18 g, 4.05 mmol), benzylbromide (0.693 g, 1.8 mmol) and K_2CO_3 (2.24 g, 16.2 mmol) afforded **2.16b** as a white solid (1.05 g, 81%). M.p.: 147-152 °C. ^{1}H NMR (600 MHz, $CDCl_3$): δ 8.22 (s, 1H, H_2), 7.44 (d, J = 7.3 Hz, 2H, H_8), 7.40

(t, J = 7.5 Hz, 1H, H_9), 7.36 – 7.31 (m, 2H, H_{10}, H_3), 7.24 (d, J = 8.6 Hz, 1H, H_4), 6.89 (d, J = 8.6 Hz, 1H, H_5), 5.15 (s, 2H, H_7), 2.36 (s, 3H, H_6), 1.53 (s, 9H, H_1); ^{13}C NMR (150 MHz, $CDCl_3$): δ 159.3, 157.8, 152.8, 148.9, 136.8, 128.8 (2C), 128.2, 127.3 (2C), 125.2, 122.0, 121.8, 114.6, 113.9, 109.4, 81.6, 70.7, 28.4 (3C), 8.5.

4.2.12. General procedure for synthesis of free 7-benzyloxy-3-aminocoumarins (2.17a-b)

Compounds **2.16a-b** were Boc-deprotected according to the procedure highlighted in **Section 4.6** to yield free 7-benzyloxy-3-aminocoumarins (**2.17a-b**).

7-Benzyloxy-3-aminocoumarin (2.17a)

N-Boc 7-benzyloxy-3-aminocoumarin **2.16a** (0.264 g, 0.72 mmol) afforded **2.17a** as a light-yellow solid (0.178 g, 93%). M.p.: 116-118 °C. ^{1}H NMR (300 MHz, $CDCl_3$): δ 7.47 – 7.30 (m, 5H, H_7, H_8, H_9), 7.22 – 7.16 (m, 1H, H_3), 6.92 – 6.85 (m, 2H, H_4, H_5), 6.69 (s, 1H, H_2), 5.09 (s, 2H, H_6), 4.06 (s, 2H, H_1); ^{13}C NMR (75 MHz, $CDCl_3$): δ 159.9, 158.3, 150.4, 136.5, 130.0, 128.9 (2C), 128.4, 127.7 (2C), 126.0, 114.8, 113.5, 112.3, 102.1, 70.6.

7-Benzyloxy-8-methyl-3-aminocoumarin (2.17b)

N-Boc 7-benzyloxy-8-methyl-3-aminocoumarin **2.16b** (0.800 g, 2.51 mmol) afforded **2.17b** as a light-yellow solid (0.706 g, 71%). M.p.: 83 – 84 °C. ^{1}H NMR (400 MHz, $CDCl_3$): δ 7.44 - 7.37 (m, 5H, H_7, H_8, H_9), 7.07 (d, J = 8.7 Hz, 1H, H_3), 6.84 (d, J = 8.7 Hz, 1H, H_4), 6.69 (s, 1H, H_2), 5.12 (s, 2H, H_6), 3.15 (s, 2H, H_1), 2.37 (s, 3H, H_5); ^{13}C NMR (100 MHz, $CDCl_3$): δ 160.1, 156.2, 148.6, 137.1, 129.6, 128.8 (2C), 128.2, 127.3 (2C), 122.7, 115.0, 114.7, 112.9, 109.4, 70.9, 8.6.

4.2.13. General procedure for synthesis of 7-OBn analogues (2.18a-d)[6]

To a suspension of a relevant free 7-benzyl-*O*-3-aminocoumarin **2.17a-b** (1.0 eq.) and an appropriate diaryl carboxylic acid (**2.10** or **2.11**) (1.0 eq.) in 1:2 pyridine/$CHCl_3$ solution (2 mL) on ice was added 50% T3P®/EtOAc solution (2.0 eq.). The reaction mixture was refluxed at 75 °C for 1 – 2 days after which the solvents were removed under reduced pressure to afford a crude product, which was purified by silica gel chromatography (100% DCM) to afford the desired product.

7-Benzyl-*O*-3-ferrocenylcarboxamidocoumarin (2.18a)

7-Benzyl-*O*-3-aminocoumarin **2.17a** (0.350 g, 1.31 mmol), ferrocene carboxylic acid (0.301, 1.31 mmol), 50% T3P®/EtOAc solution (0.452 g, 2.00 mmol) afforded **2.18a** as a red solid (0.502 g, 80%). Mp.: 155-160 °C. IR ν_{max}/cm^{-1} 3387 (N-H, amide), 2957 (C-H, pyrone C=C), 1700 (C=O, lactone), 1635 (C=O, amide), ^{1}H NMR (300 MHz, $CDCl_3$): δ 8.69 (s, 1H, H_4), 8.26 (s, 1H, H_5), 7.47 – 7.34 (m, 6H, H_6, H_{10}, H_{11}, H_{12}), 6.98 (dd, J = 8.6, 2.4 Hz, 1H, H_7), 6.93 (d, J = 2.3 Hz, 1H, H_8), 5.13 (s, 2H, H_9), 4.83 (t, 2H, J = 1.9 Hz, H_3), 4.47 (t, J = 1.9 Hz, 2H, H_2), 4.26 (s, 5H, H_1); ^{13}C NMR (75 MHz, $CDCl_3$): δ 170.0, 160.3, 159.5, 151.4, 136.1, 128.9 (2C), 128.8, 128.5, 127.7 (2C), 123.4, 122.1, 114.1, 113.8, 102.1, 75.4, 71.6 (2C), 70.7, 70.2 (5C), 68.6 (2C); HRMS (ESI$^+$) *m/z* calcd for $C_{30}H_{24}FeNO_4$: 479.0820, Found 480.0905 $[M+H]^+$.

7-Benzyl-*O*-8-methyl-3-ferrocenylcarboxamidocoumarin (2.18b)

7-Benzyl-*O*-8-methyl-3-aminocoumarin **2.17b** (0.400 g, 1.42 mmol), ferrocene carboxylic acid (0.327 g, 1.42 mmol), 50% T3P®/EtOAc solution (0.904 g, 2.84 mmol) afforded **2.18b** as a red solid (0.475 g, 68%). Mp.: 92-94 °C. IR ν_{max}/cm^{-1} 3355 (N-H, amide), 3094 (C-H, pyrone C=C), 1701 (C=O, lactone), 1650 (C=O, amide), ^1H NMR (600 MHz, $CDCl_3$): δ 8.68 (s, 1H, H_4), 8.28 (s, 1H, H_5), 7.45 (d, J = 7.2 Hz, 2H, H_{11}), 7.41 (t, J = 7.5 Hz, 2H, H_{10}), 7.35 (t, J = 7.2 Hz, 1H, H_{12}), 7.31 (d, J = 8.6 Hz, 1H, H_6), 6.93 (d, J = 8.6 Hz, 1H, H_7), 5.17 (s, 2H, H_9), 4.84 (t, J = 1.9 Hz, 2H, H_3), 4.47 (t, J = 1.9 Hz, 2H, H_2), 4.26 (s, 5H, H_1), 2.40 (s, 3H, H_8); ^{13}C NMR (150 MHz, $CDCl_3$): δ 170.0, 160.0, 158.1, 149.2, 136.7, 128.8 (2C), 128.3, 127.3 (2C), 125.7, 123.9, 121.7, 114.7, 113.9, 109.5, 75.4, 71.5 (2C), 70.7, 70.2 (5C), 68.6 (2C), 8.5; HRMS (ESI^+) *m/z* calcd for $C_{28}H_{23}NO_4$: 493.0977, Found 494.1056 $[M+H]^+$.

7-Benzyl-*O*-3-(3',6-dimethoxy-[1,1'-biphenyl])-3-carboxamidocoumarin (2.18c)

7-Benzyl-*O*-8-methyl-3-aminocoumarin **2.17a** (0.259 g, 0.97 mmol), 4-methoxy-3-(3-methoxy)-phenylbenzoic acid (0.250 g, 0.97 mmol), 50% T3P®/EtOAc solution (0.617 g, 2.0 mmol) afforded **2.18c** as a red solid (0.244 g, 50%). Mp.: 148-150 °C. IR ν_{max}/cm^{-1}: 3411 (N-H, amide), 3070 (C-H, pyrone C=C), 2920 (C-H, methyl), 1698 (C=O, lactone), 1666 (C=O, amide), ^1H NMR (400 MHz, $CDCl_3$) δ 8.82 (s, 1H, H_{10}), 8.68 (s, 1H, H_{11}), 7.91 (dd, J = 8.5, 2.4 Hz, 1H, H_8), 7.88 (d, J = 2.3 Hz, 1H, H_9), 7.47 – 7.40 (m, 5H, H_{16}, H_{17}, H_{18}), 7.40 – 7.34 (m, 2H, H_4, H_7), 7.12 (d, J = 7.7 Hz, 1H, H_5), 7.10 – 7.08 (m, 1H, H_3), 7.07 (d, J = 8.6 Hz, 1H, H_{12}), 6.98 (dd, J = 8.6, 2.4 Hz, 1H, H_{13}), 6.95 – 6.92 (m, 2H, H_2, H_{14}), 5.13 (s, 2H, H_{15}), 3.90 (s, 3H, H_1), 3.86 (s, 3H, H_6); ^{13}C NMR (101 MHz, $CDCl_3$) δ 172.2, 165.7, 160.5, 160.0, 159.5, 151.5, 138.8, 136.1, 131.3, 130.1, 129.4, 129.0 (2C), 128.9, 128.6, 128.4, 127.7 (2C), 126.2, 124.1, 122.2 (2C), 115.5, 114.1, 113.7, 113.3, 111.2, 102.1, 70.7 56.1, 55.5; HRMS (ESI^+) *m/z* calcd for $C_{31}H_{25}NO_6$: 507.1682, Found 508.1739 $[M+H]^+$.

7-Benzyl-*O*-8-methyl-3-(3',6-dimethoxy-[1,1'-biphenyl])-3-carboxamidocoumarin (2.18d)

7-Benzyl-*O*-8-methyl-3-aminocoumarin **5e** (0.273 g, 0.67 mmol), 4-methoxy-3-(3-methoxy)-phenylbenzoic acid (0.250 g, 0.97 mmol), 50% T3P®/EtOAc solution (0.617 g, 2 mmol) afforded **6j** as a red solid (0.214 g, 42%). Mp.: 155-157 °C. IR ν_{max}/cm^{-1}: 3416 (N-H, amide), 3033 (C-H, pyrone C=C), 2957 (C-H, methyl), 1733 (C=O, lactone), 1702 (C=O, amide); ^1H NMR (400 MHz, $CDCl_3$) δ 8.80 (s, 1H, H_{10}), 8.70 (s, 1H, H_{11}), 7.92 (dd, J = 8.5, 2.3 Hz, 1H,

H_8), 7.90 (d, J = 2.2 Hz, 1H, H_9), 7.46 – 7.43 (m, 3H, H_3, H_4, H_7), 7.41 – 7. 40 (m, 2H, H_{16}), 7.36 – 7.33 (m, 3H, H_{17}, H_{18}), 7.13 (d, J = 7.7 Hz, 1H, H_5), 7.10 (t, J = 2.0 Hz, 1H, H_2), 7.07 (d, J = 8.5 Hz, 1H, H_{12}), 6.94 (d, J = 8.5, 1H, H_{13}), 5.18 (s, 2H, H_{15}), 3.90 (s, 3H, H_1), 3.86 (s, 3H, H_6), 2.40 (s, 3H, H_{14}); ^{13}C NMR (101 MHz, $CDCl_3$) δ 165.7, 160.0, 159.7, 159.5, 158.3, 149.4, 138.8, 136.8, 131.4, 130.2, 129.4, 128.9 (2C), 128.3 (2C), 127.3 (2C), 126.3, 125.8, 124.5, 122.2, 121.9, 115.4, 114.8, 113.8, 113.4, 111.2, 109.6, 70.8, 56.1, 55.5, 8.5; HRMS (ESI^+) *m/z* calcd for $C_{32}H_{27}NO_6$: 521.1838, Found 508.1739 $[M+H]^+$.

4.2.14. General procedure for synthesis of 7-OH Nb analogues (2.19a-d)

A mixture of a relevant OBn Nb analogue **2.18a-d** (1.0 eq.) and 10 mol % Pd/C in THF (15 mL) was stirred under H_2 atmosphere for 12 hours at room temperature. The product was filtered through a small pad of silica gel, eluting with 100% EtOAc. The solvent was removed under reduce pressure to afford the desired product **2.19a-d**.

7-Hydroxy-3-ferrocenylcarboxamidocoumarin (2.19a)

7-Benzyl-*O*-3-ferrocenylcarboxamidocoumarin **2.18a** (0.140 g, 0.29 mmol) and 10 mol % Pd/C afforded **2.19a** as a light red solid (0.116 g, 96%). M.p.: >300 °C. IR ν_{max}/cm^{-1} 3243 (N-H, amide & OH), 2981 (C-H, pyrone C=C), 1732 (C=O, lactone), 1688 (C=O, amide); ^{1}H NMR (600 MHz, DMSO-d_6): δ 10.49 (br s, 1H, OH), 8.83 (s, 1H, H_4), 8.30 (s, 1H, H_5), 7.57 (d, J = 8.5 Hz, 1H, H_6), 6.82 (dd, J = 8.5, 2.0 Hz, 1H, H_7), 6.78 (d, J = 1.8 Hz, 1H, H_8), 4.95 (s, 2H, H_3), 4.48 (s, 2H, H_2), 4.27 (s, 5H, H_1); ^{13}C NMR (150 MHz, DMSO-d_6): δ 168.8, 160.0, 158.5, 152.1, 129.5, 129.2, 120.3, 113.7, 111.4, 102.1, 75.3, 70.9 (2C), 69.7 (5C), 68.5 (2C); HRMS (ESI^+) *m/z* calcd for $C_{20}H_{15}FeNO_4$: 389.0351, Found 390.0392 $[M+H]^+$.

7-Hydroxy-8-methyl-3-ferrocenylcarboxamidocoumarin (2.19b)

7-Benzyl-*O*-8-methyl-3-ferrocenylcarboxamidocoumarin **2.18b** (0.550 g, 1.1 mmol) and 10 mol % Pd/C (10 mol%) afforded **2.19b** as a light red solid (0.150, 33%). M.p.: 94-96 °C.IR ν_{max}/cm^{-1} 3352 (N-H, amide & OH), 2927 (C-H, pyrone C=C), 1703 (C=O, lactone), 1656 (C=O, amide); ^{1}H NMR (600 MHz, DMSO-d_6): δ 10.37 (br s, 1H, OH), 8.83 (s, 1H, H_4), 8.28 (s, 1H, H_5), 7.40 (d, J = 8.4 Hz, 1H, H_6), 6.88 (d, J = 8.4 Hz, 1H, H_7), 4.96 (s, 2H, H_3), 4.48 (s, 2H, H_2), 4.27 (s, 5H, H_1), 2.19 (s, 3H, H_8); ^{13}C NMR (150 MHz, DMSO-d_6): δ 168.8, 158.7, 157.8, 150.2, 129.9, 125.9, 119.9, 112.6, 111.4, 110.6, 75.3, 70.9 (2C), 69.7 (5C), 68.5 (2C), 8.0; HRMS (ESI^+) *m/z* calcd for $C_{21}H_{17}FeNO_4$: 403.0507, Found 413.2609 $[C_{20}H_{15}FeNO_4+Na]^+$.

7-Hydroxy-3-(3',6-dimethoxy-[1,1'-biphenyl])-3-carboxamidocoumarin (2.19c)

7-Benzyl-*O*-3-(3',6-dimethoxy-[1,1'-biphenyl])-3-carboxamidocoumarin **2.18c** (0.200 g, 1.1 mmol) and Pd/C (10 mol%) afforded **2.19c** as an off-white solid (0.115, 70%). M.p.: 201-205 °C. IR ν_{max}/cm^{-1}: 3258 (N-H, amide & OH), 2940 (C-H, pyrone C=C), 2836 (C-H, methyl), 1715 (C=O, lactone), 1600 (C=O, amide); ^{1}H NMR (400 MHz, DMSO-d_6): δ 10.46 (s, 1H, OH), 9.60 (s, 1H, H_{10}), 8.42 (s, 1H, H_{11}), 7.98 (dd, J = 8.6, 2.3 Hz, 1H, H_8), 7.92 (d, J = 2.3 Hz, 1H, H_9), 7.58 (d, J = 8.6 Hz, 1H, H_7), 7.36 (t, J = 7.9 Hz, 1H, H_4), 7.25 (d, J = 8.8 Hz, 1H, H_{12}), 7.12 – 7.09 (m, 2H, H_2, H_3), 6.95 (dd, J = 7.9, 2.2 Hz, 1H, H_5), 6.83 (dd, J = 8.5, 2.3 Hz, 1H, H_{13}), 6.78 (d, J = 2.2 Hz, 1H, H_{14}), 3.86 (s, 3H, H_1), 3.79 (s, 3H, H_6); ^{13}C NMR (100 MHz, DMSO-d_6): δ 165.1, 160.0, 159.1, 158.9, 158.3, 152.3, 138.7, 130.0, 129.9, 129.4, 129.3, 129.1, 129.0, 125.8, 121.7, 120.5, 115.2, 113.6, 112.6, 111.6, 111.3, 102.0, 55.1, 39.5; HRMS (ESI$^+$) *m/z* calcd for $C_{24}H_{19}NO_6$: 417.1212, Found 418.1270 $[M+H]^+$.

7-Hydroxy-8-methyl-3-(3',6-dimethoxy-[1,1'-biphenyl])-3-carboxamidocoumarin (2.19d)

7-Benzyl-*O*-8-methyl-3-(3',6-dimethoxy-[1,1'-biphenyl])-3-carboxamidocoumarin **2.18d** (0.200 g, 0.38 mmol) and Pd/C (10 mol%) afforded **2.19d** as an off-white solid (0.0665 g, 40%). M.p.: 140-144 °C. IR ν_{max}/cm^{-1}: 3228 (N-H, amide & hydroxyl), 2919 (C-H, pyrone C=C), 2856(C-H, methyl), 1679 (C=O, lactone), 1603 (C=O, amide); ^{1}H NMR (400 MHz, $CDCl_3$): δ 8.78 (s, 1H, H_{10}), 8.68 (s, 1H, H_{11}), 7.94 – 7.87 (m, 2H, H_8, H_9), 7.36 (t, J = 7.9 Hz, 1H, H_4), 7.24 – 2.23 (m, 1H, H_7), 7.16 – 7.10 (m, 1H, H_{12}), 7.13 – 7.09 (m, 2H, H_2, H_3), 7.07 (d, J = 8.7 Hz, 1H, H_{13}), 6.94 – 6.91 (m, 1H, H_5), 3.90 (s, 3H, H_1), 3.86 (s, 3H, H_6), 2.35 (s, 3H, H_{14}); HRMS (ESI$^+$) *m/z* calcd for $C_{25}H_{21}NO_6$: 431.1369, Found 432.1434 $[M+H]^+$.

4.2.15. Mitsunobi etheration for synthesis of piperidinyl Fc-Nb analogues (2.20a-f)[7]

An appropriate volume of DIAD (2.0 eq.) was added to as suspension of a relevant phenolic substrate **2.19a-b** (1.0 eq.), piperidinol (**2.15a-b** or **2.15e-f**) (1.0 eq.) and PPh_3 (2.0 eq.) in THF (20 mL) on ice. The reaction mixture was stirred at 0 °C for 5 hours followed by removal of solvent under reduced pressure. The resulting orange residue was purified by silica gel chromatography (5% MeOH/DCM) to afford the desired product **2.20a-f**.

7-(*N*-methyl-4-piperidinyl)-*O*-3-ferrocenylcarboxamidocoumarin (2.20a)

7-Hydroxy-3-ferrocenylcarboxamidocoumarin **2.19a** (0.100 g, 0.26 mmol), *N*-methyl-4-piperidinol **2.15a** (0.030 g, 0.26 mmol), PPh_3 (0.135 g, 0.51 mmol) and DIAD (0.104 g, 0.51 mmol) afforded **2.20a** as red solid (0.051 g, 41%). M.p.: 161-163 °C. IR ν_{max}/cm^{-1} 3355 (N-H,

amide), 3107 (C-H, pyrone C=C), 2935 (C-H, methyl), 1704 (C=O, lactone), 1659 (C=O, amide), 1501 (C=C, aromatic), 1173 (C-O, aromatic ether); ^{1}H NMR (600 MHz, $CDCl_3$): δ 8.68 (s, 1H, H_4), 8.25 (s, 1H, H_5), 7.40 (d, J = 8.6 Hz, 1H, H_6), 6.89 (dd, J = 8.6, 2.4 Hz, 1H, H_7), 6.85 (d, J = 2.4 Hz, 1H, H_8), 4.82 (t, J = 1.9 Hz, 2H, H_3), 4.46 (t, J = 1.9 Hz, 2H, H_2), 4.39 (br s, 1H, H_{10}), 4.26 (s, 5H, H_1), 2.73 (s, 2H, $_{13}$), 2.34 (br s, 5H, H_{14}, H_{15}), 2.09 – 2.04 (m, 2H, H_{12}), 1.92 – 1.85 (m, 2H, H_{11}); ^{13}C NMR (150 MHz, $CDCl_3$): δ 170.0, 159.5, 159.1, 151.5, 128.8, 123.5, 122.0, 114.7, 113.5, 102.7, 75.4, 71.5 (2C), 70.2 (6C), 68.6 (2C), 52.6 (2C), 46.2, 30.7 (2C), 29.9; HRMS (ESI$^+$) *m/z* calcd for $C_{26}H_{26}FeN_2O_4$: 486.1242, Found 487.1318 $[M+H]^+$.

7-(*N*-methyl-3-piperidinyl)-*O*-3-ferrocenylcarboxamidocoumarin (2.20b)

7-Hydroxy-3-ferrocenylcarboxamidocoumarin **2.19a** (0.100 g, 0.26 mmol), *N*-methyl-4-piperidinol **2.15b** (0.030 g, 0.26 mmol), PPh_3 (0.135 g, 0.51 mmol) and DIAD (0.104 g, 0.51 mmol) afforded **2.20b** as red solid (0.046 g, 37%). M.p.: 161-163 °C. IR ν_{max}/cm^{-1} 3380 (N-H, amide), 3068 (C-H, pyrone C=C), 2923 (C-H, methyl), 1706 (C=O, lactone), 1663 (C=O, amide), 1518 (C=C, aromatic), 1237 (C-O, aromatic ether); ^{1}H NMR (600 MHz, $CDCl_3$): δ 8.68 (s, 1H, H_4), 8.25 (s, 1H, H_5), 7.40 (d, J = 8.6 Hz, 1H, H_6), 6.92 (dd, J = 8.6, 1.9 Hz, 1H, H_7), 6.89 (d, J = 1.6, 1H, H_8), 4.82 (br s, 2H, H_3), 4.46 – 4.44 (m, 3H, H_2, H_9), 4.26 (s, 5H, H_1), 2.96 – 2.52 (m, 2H, H_{13}), 2.34 – 2.18 (m, 5H, H_{12}, H_{14}), 2.02 – 1.86 (m, 2H, H_{11}), 1.69 – 1.51 (m, 2H, H_{10}); ^{13}C NMR (150 MHz, $CDCl_3$): δ 170.3, 159.8, 159.6, 151.7, 129.1, 123.8, 122.3, 114.8, 113.9, 103.1, 75.7, 73.7, 71.8 (2C), 70.5 (5C), 68.9 (2C), 59.9, 55.8, 46.8, 29.3, 23.2; HRMS (ESI$^+$) *m/z* calcd for $C_{26}H_{26}FeN_2O_4$: 486.1242, Found 487.1328 $[M+H]^+$.

7-(*N*-methyl-4-piperidinyl)-*O*-8-methyl-3-ferrocenylcarboxamidocoumarin (2.20c)

7-Hydroxy-3-ferrocenylcarboxamidocoumarin **2.19b** (0.060 g, 0.15 mmol), *N*-methyl-4-piperidinol (0.017 g, 0.15 mmol), PPh_3 (0.078 g, 0.30 mmol) and DIAD (0.060 g, 0.30 mmol) afforded **2.20c** as an red solid (0,016 g, 22%). M.p.: 161-163 °C. IR ν_{max}/cm^{-1} 3363 (N-H, amide), 3079 (C-H, pyrone C=C), 2921 (C-H, methyl), 1704 (C=O, lactone), 1658 (C=O, amide), 1521 (C=C, aromatic), 1107 (C-O, aromatic ether); ^{1}H NMR (600 MHz, $CDCl_3$): δ 8.67 (s, 1H, H_4), 8.27 (s, 1H, H_5), 7.29 (d, J = 8.6 Hz, 1H,H_6), 6.87 (d, J = 8.6 Hz, 1H, H_7), 4.85 – 4.82 (m, 2H, H_3), 4.49 – 4.43 (m, 3H, H_2, H_{10}), 4.26 (s, 5H, H_1), 2.66 (s, 2H, H_{11}), 2.38 (s, 2H, H_{12}), 2.35 (s, 3H, H_{15}), 2.33 (br s, 3H, H_8), 2.07 – 1.99 (m, 2H, H_{13}), 1.95 – 1.87 (m, 2H, H_{14}); ^{13}C NMR (150 MHz, $CDCl_3$): δ 169.9, 159.7, 156.9, 149.5, 125.5, 123.9, 121.7,

115.4, 113.6, 110.7, 75.4, 71.5 (2C), 70.2 (5C), 68.5 (2C), 52.5 (2C), 46.4, 30.9 (2C), 29.8, 8.5; HRMS (ESI^+) *m/z* calcd for $C_{27}H_{28}FeN_2O_4$: 500.1398, Found 501.1471 $[M+H]^+$.

7-(*N*-methyl-3-piperidinyl)-*O*-8-methyl-3-ferrocenylcarboxamidocoumarin (2.20d)

7-Hydroxy-3-ferrocenylcarboxamidocoumarin **2.19b** (0.060 g, 0.15 mmol), *N*-methyl-3-piperidinol (0.017 g, 0.15 mmol), PPh_3 (0.078 g, 0.30 mmol) and DIAD (0.060 g, 0.30 mmol) afforded **2.20d** as a red solid (0,016 g, 38%). M.p.: 100-102 °C. IR ν_{max}/cm^{-1} 3361 (N-H, amide), 3088 (C-H, pyrone C=C), 2925 (C-H, methyl), 1702 (C=O, lactone), 1660 (C=O, amide), 1517 (C=C, aromatic), 1107 (C-O, aromatic ether); ^1H NMR (300 MHz, $CDCl_3$): δ 8.67 (s, 1H, H_4), 8.27 (s, 1H, H_5), 7.31 (d, *J* = 8.6 Hz, 1H, H_6), 6.97 (d, *J* = 8.7 Hz, 1H, H_7), 4.83 (t, *J* = 1.95 Hz, 2H, H_3), 4.58 (s, 1H, H_9), 4.83 (t, *J* = 1.95 Hz, 2H, H_2), 4.60 (s, 5H, H_1), 3.31 – 3.06 (m, 2H, H_{13}), 2.89 – 2.79 (m, 2H, H_{12}), 2.43 (s, 3H, H_{14}), 2.31 (s, 3H, H_8), 1.92 – 1.79 (4H, H_{10}, H_{11}); ^{13}C NMR (150 MHz, $CDCl_3$): δ 170.0, 159.7, 156.7, 149.4, 125.7, 123.8, 121.8, 115.5, 114.0, 111.1, 75.4, 71.5 (2C), 70.2 (5C), 68.6 (2C), 55.3, 53.6, 46.0, 31.1, 29.9, 22.1, 8.6; HRMS (ESI^+) *m/z* calcd for $C_{27}H_{28}FeN_2O_4$: 500.1398, Found 501.1474 $[M+H]^+$.

7-(*N*-Boc-4-piperidinyl)-*O*-3-ferrocenylcarboxamidocoumarin (2.20e)

7-Hydroxy-3-ferrocenylcarboxamidocoumarin **2.19a** (0.100 g, 0.26 mmol), *N*-Boc 4-piperidinol **2.15e** (0.061 g, 0.28 mmol), PPh_3 (0.135 g, 0.51 mmol) and DIAD (0.104 g, 0.51 mmol) afforded **2.20c** as a red solid (0.055 g, 37%). M.p.: 159-161 °C. IR ν_{max}/cm^{-1} 3399 (N-H, amide), 3089 (C-H, pyrone C=C), 2934 (C-H, methyl), 1692 (C=O, lactone), 1662 (C=O, amide), 1520 (C=C, aromatic), 1234 (C-O, aromatic ether); ^1H NMR (600 MHz, $CDCl_3$): δ 8.69 (s, 1H, H_4), 8.26 (s, 1H, H_5), 7.42 (d, *J* = 8.6 Hz, 1H, H_6), 6.89 (dd, *J* = 8.6, 2.4 Hz, 1H, H_7), 6.86 (d, *J* = 2.3 Hz, 1H, H_8), 4.82 (t, *J* = 1.8 Hz, 2H, H_3), 4.55 – 4.51 (m, 1H, H_9), 4.48 – 4.45 (t, *J* = 1.8 Hz, 2H, H_2), 4.26 (s, 5H, H_1), 3.75 – 3.66 (m, 2H, H_{13}), 3.41 – 3.33 (m, 2H, H_{12}), 2.00 – 1.93 (m, 2H, H_{10}), 1.82 – 1.75 (m, 2H, H_{11}), 1.47 (s, 9H, H_{15}); ^{13}C NMR (150 MHz, $CDCl_3$): δ 170.0, 167.6, 159.4, 158.9, 155.0, 151.4, 128.9, 123.4, 122.1, 114.7, 113.7, 102.8, 80.0, 73.1, 71.8 (2C), 70.3 (5C), 68.9 (2C), 68.6, 28.6 (3C), 21.9; HRMS (ESI^+) *m/z* calcd for $C_{30}H_{32}FeN_2O_6$: 572.1610, Found 494.1045 $[C_{25}H_{23}FeN_2O_4+Na]^+$.

7-(*N*-Boc-3-piperidinyl)-*O*-3-ferrocenylcarboxamidocoumarin (2.20f)

7-Hydroxy-3-ferrocenylcarboxamidocoumarin **2.19a** (0.100 g, 0.26 mmol), *N*-Boc-3-piperidinol **2.15d** (0.030 g, 0.26 mmol), PPh_3 (0.135 g, 0.51 mmol) and DIAD (0.104 g, 0.51 mmol) afforded **2.20d** as a red solid (0.060 g, 37%). M.p.: 112-114 °C. IR ν_{max}/cm^{-1} 3384 (N-

H, amide), 3056 (C-H, pyrone C=C), 2926 (C-H, methyl), 1698 (C=O, lactone), 1663 (C=O, amide), 1518 (C=C, aromatic), 1232 (C-O, aromatic ether); ^{1}H NMR (400 MHz, $CDCl_3$): δ 8.68 (s, 1H, H_4), 8.27 (s, 1H, H_5), 7.41 (d, J = 8.6 Hz, 1H, H_6), 7.05 (d, J = 2.2 Hz, 1H, H_8), 6.99 (dd, J = 8.6, 2.2 Hz, 1H, H_7), 5.14 – 4.88 (m, 1H, H_9), 4.82 (t, J = 1.29 Hz, H_3), 4.46 (t, J = 1.26 Hz, H_2), 4.26 (s, 5H, H_1), 4.10 – 3.94 (m, 2H, H_{13}), 2.30 – 2.08 (m, 4H, H_{11}, H_{12}), 2.08 – 1.90 (m, 2H, H_{10}), 1.47 – 1.37 (m, 9H, H_{15}); ^{13}C NMR (101 MHz, $CDCl_3$): δ 169.8, 159.3, 158.6, 155.7, 151.0, 128.4, 123.3, 122.0, 114.7, 113.9, 103.9, 102.6, 75.2, 71.3, 70.6, 70.1 (2C), 68.5 (5C), 68.4 (3C), 32.7, 28.4 (3C), 23.3; HRMS (ESI^+) *m/z* calcd for $C_{30}H_{32}FeN_2O_6$: 572.1610, Found 373.1765 $[C_{20}H_{15}FeNO_3+H]^+$.

4.2.16. General procedure synthesis of 3'- and 4'-NH piperidinyl Fc-Nb analogues (2.20g-h)

An appropriate *N*Boc-protected piperidinyl Fc-Nb analogue **2.20e-f** (1.0 eq.) was stirred in 10% TFA/DCM solution (2 mL) for 12 hours at room temperature. The solvents were removed under reduced pressure to obtain a crude product, which was purified by silica gel column chromatography (10% MeOH/DCM) to afford the desired product **2.20g-h**.

7-(4-Piperidinyl)-*O*-3-ferrocenylcarboxamidocoumarin (2.20g)

7-(*N*-Boc-4-piperininyl)-*O*-3-ferrocenylcarboxamidocoumarin **2.20e** (0.045 g, 0.079 mmol) afforded **2.20g** as a light red solid (0.035 g, 95%). Mp.: 76-80 °C. IR ν_{max}/cm^{-1} 3397 (N-H, amide and piperidinyl amine), 2931 (C-H, pyrone C=C), 2708 (C-H, methyl), 1658 (C=O, lactone), 1610 (C=O, amide), 1530 (C=C, aromatic), 1131 (C-O, aromatic ether); ^{1}H NMR (300 MHz, $CDCl_3$): δ 8.69 (s, 1H, H_4), 8.26 (s, 1H, H_5), 7.45 (d, J = 8.6 Hz, 1H, H_6), 6.90 (dd, J = 8.6, 2.2 Hz, 1H, H_7), 6.85 (d, J = 1.7 Hz, 1H, H_8), 4.82 (t, J = 1.8 Hz, 2H, H_3), 4.72 (br s, 1H, H_9), 4.47 (t, J = 1.8 Hz, 2H, H_2), 4.26 (s, 5H, H_1), 3.31 (br s, 4H, H_{12}, H_{13}), 2.19 (br s, 4H, H_{10}, H_{11}); ^{13}C NMR (75 MHz, $CDCl_3$): δ 170.1, 159.5, 158.8, 151.2, 128.6, 123.5, 122.1, 114.9, 114.1, 104.0, 102.8, 75.3, 71.6 (2C), 70.3 (5C), 68.6 (3C), 32.9 (2C), 23.5(2C); HRMS (ESI^+) *m/z* calcd for $C_{25}H_{24}FeN_2O_4$: 472.1085, Found 473.1156 $[M+H]^+$.

7-(3-Piperidinyl)-*O*-3-ferrocenylcarboxamidocoumarin (2.20h)

7-(*N*-Boc-4-piperininyl)-*O*-3-ferrocenylcarboxamidocoumarin **2.20e** (0.045 g, 0.079 mmol) afforded **2.20h** as a light red solid (0.036 g, 97%). Mp.: >300 °C. IR ν_{max}/cm^{-1} 3385 (N-H, amide and piperidinyl amine), 2920 (C-H, pyrone C=C), 1702 (C=O, lactone), 1607 (C=O, amide), 1607 (C=C, aromatic), 1533 (C-O, ether); ^{1}H NMR (300 MHz, $CDCl_3$): δ 8.68 (s, 1H, H_4), 8.26 (s, 1H, H_5), 7.40 (d, J = 8.7 Hz, 1H, H_6), 7.04 (d, J = 2.3 Hz, 1H, H_8), 6.98 (dd, J = 8.6, 2.4 Hz, 1H, H_7), 5.89 – 5.80 (m, 1H, H_{13}), 4.82 (t, J = 1.92 Hz, 2H, H_3), 4.46 (t, J = 1.92, 2H, H_2), 4.34 – 4.31 (m, 1H, H_9), 4.26 (s, 5H, H_1), 4.06 – 3.92 (m, 2H, H_{14}), 2.52 – 1.92 (m, 6H, H_{10}, H_{11}, H_{12}); ^{13}C NMR (75 MHz, $CDCl_3$): δ 170.0, 159.5, 158.8, 151.1, 128.6, 123.5, 122.1, 114.8, 114.0, 104.0, 102.7, 75.3, 71.5 (2C), 70.2 (5C), 68.6, 68.5 (2C), 32.9, 28.0, 23.5; HRMS (ESI^+) *m/z* calcd for $C_{25}H_{24}FeN_2O_4$: 472.1085, Found 473.3404 $[M+H]^+$.

4.2.17. Synthesis of organic piperidinyl Nb analogues (2.20i-k)

An appropriate organic phenolic coumarin **2.19c-d** was subjected to Mitsunobi conditions as described in **Section 4.16** using a relevant 3'- or 4'-*N*-Boc piperidinol **2.15c-d**. The resultant residue was stirred in 10%TFA/DCM (2 mL) solution for 12 hours as described in **Section 4.17** after which the solvents were removed under reduced pressure to yield a pale-yellow paste. The crude products were purified by silica gel preparative TLC purification to yield the desired products **2.20i-k**.

7-(4-Piperidinyl)-*O*-3-(3',6-dimethoxy-[1,1'-biphenyl])-3-carboxamidocoumarin (2.20i)

7-Hydroxy-3-(3',6-dimethoxy-[1,1'-biphenyl])-3-carboxamidocoumarin **2.19a** (0.100 g, 0.24 mmol), *N*-Boc-4-piperidinol **2.15b** (0.514 g, 0.24 mmol), PPh_3 (0.126 g, 0.48 mmol) and DIAD (0.097, 0.48 mmol) afforded **2.20i** as an off-white solid (0.0110 g, 9%). M.p.: 145-149 °C. IR ν_{max}/cm^{-1} 3415 (N-H, amide) 3382 (N-H, piperidinyl amine), 2919 (C-H, pyrone C=C), 2850 (C-H, methyl), 1702(C=O, lactone), 1662 (C=O, amide), 1531 (C=C, aromatic), 1178 (C-O, aromatic ether); ^{1}H NMR (600 MHz, $CDCl_3$): δ 8.81 (s, 1H, H_{10}), 8.70 (s, 1H, H_{11}), 7.91 (dd, J = 8.6, 2.4 Hz, 1H, H_8), 7.88 (d, J = 2.4 Hz, 1H, H_9), 7.44 (d, J = 8.6 Hz, 1H, H_7), 7.36 (t, J = 7.9 Hz, 1H, H_4), 7.12 (d, J = 7.6 Hz, 1H, H_2), 7.10 – 7.08 (m, 1H, H_3), 7.07 (d, J = 8.6 Hz, 1H, H_{12}), 7.05 (d, J = 2.3 Hz, 1H, H_9), 7.00 (dd, J = 8.6, 2.3 Hz, 1H, H_{13}), 6.93 (dd, J = 8.3, 1.9 Hz, 1H, H_5), 5.85 (d, J = 3.7 Hz, 1H, H_{18}), 4.08 – 3.95 (m, 2H, H_{17}), 3.90 (s, 3H, H_1), 3.86 (s, 3H, H_6), 3.84 – 3.64 (m, 1H, H_{15}), 2.28 – 1.83 (m, 4H, H_{19}, H_{20}), 1.55 – 1.30 (m, 2H, H_{16}); ^{13}C NMR (150 MHz, $CDCl_3$): δ 165.7, 160.0, 159.6, 159.5, 159.0, 151.3, 138.8, 131.3, 130.1, 129.4, 128.8, 128.3, 126.3, 124.1, 122.2, 115.4, 114.9, 114.0, 113.3, 111.2, 104.1, 102.8, 68.7 (2C), 56.1, 55.5, 32.9 (2C), 23.5; HRMS (ESI^+) *m/z* calcd for $C_{29}H_{28}N_2O_6$: 500.1947, Found 501.3754 $[M+H]^+$.

7-(3-Piperidinyl)-*O*-3-(3',6-dimethoxy-[1,1'-biphenyl])-3-carboxamidocoumarin (2.20j)

7-Hydroxy-3-(3',6-dimethoxy-[1,1'-biphenyl])-3-carboxamidocoumarin **2.19a** (0.100 g, 0.24 mmol), *N*-Boc-4-piperidinol **2.15b** (0.514 g, 0.24 mmol), PPh_3 (0.126 g, 0.48 mmol) and DIAD (0.097, 0.48 mmol) afforded **2.20j** as an off-white solid (0.013 g, 16%). M.p.: 115-117 °C. IR ν_{max}/cm^{-1} 3415 (N-H, amide) 3384 (N-H, piperidinyl amine), 2920 (C-H, pyrone C=C), 2851 (C-H, methyl), 1702(C=O, lactone), 1667 (C=O, amide), 1607 (C=C, aromatic), 1178 (C-O, aromatic ether); ^{1}H NMR (400 MHz, $CDCl_3$) δ 8.81 (s, 1H, H_{10}), 8.70 (s, 1H, H_{11}), 7.91 (dd, J = 8.5, 2.4 Hz, 1H, H_8), 7.88 (d, J = 2.3 Hz, 1H, H_9), 7.44 (d, J = 8.6 Hz, 1H, H_7), 7.36 (t, J = 7.9 Hz, 1H, H_4), 7.14 – 7.11 (m, 1H, H_2), 7.10 – 7.07 (m, 2H, H_3, H_{12}), 7.05 (d, J = 2.2 Hz, 1H, H_{14}), 7.00 (dd, J = 8.6, 2.3 Hz, 1H, H_{13}), 6.93 (dd, J = 8.2, 2.4 Hz, 1H, H_5), 5.85 (d, J = 3.8 Hz, 1H, H_{19}), 4.10 – 3.95 (m, 2H, H_{18}), 3.90 (s, 3H, H_6), 3.86 (s, 3H, H_1), 3.80 – 3.70 (m, 1H, H_{15}), 3.70 – 3.54 (m, 2H, H_{20}), 2.17 (s, 4H, H_{16}, H_{17}); ^{13}C NMR (100 MHz, $CDCl_3$) δ 165.9, 160.3, 159.8, 159.2, 151.6, 151.2, 131.5, 130.4, 129.6, 129.0, 128.6, 126.5, 124.3, 122.6, 122.4, 115.7, 115.2, 114.3, 113.6, 111.5, 104.3, 103.0, 77.5, 68.7, 56.1, 55.5, 32.9, 29.9, 23.5; HRMS (ESI^+) *m/z* calcd for $C_{29}H_{28}N_2O_6$: 500.1947, Found 500.3809 $[M]^+$.

7-(4-Piperidinyl)-*O*-8-methyl-3-(3',6-dimethoxy-[1,1'-biphenyl])-3-carboxamidocoumarin (2.20k)

7-Hydroxy-8-methyl-3-(3',6-dimethoxy-[1,1'-biphenyl])-3-carboxamidocoumarin **2.19b** (0.100 g, 0.23 mmol), *N*-Boc-4-piperidinol **2.15b** (0.514 g, 0.23 mmol), PPh_3 (0.126 g, 0.46 mmol) and DIAD (0.097, 0.46 mmol) afforded **2.20k** as an off-white solid (0.015g, 13%). M.p.: 140-141 °C. IR ν_{max}/cm^{-1} 3387 (N-H, amide) 3173 (N-H, piperidinyl amine), 2924 (C-H, pyrone C=C), 2850 (C-H, methyl), 1705 (C=O, lactone), 1628 (C=O, amide), 1600 (C=C, aromatic), 1240 (C-O, aromatic ether); ^{1}H NMR (400 MHz, $CDCl_3$): δ 8.80 (s, 1H, H_{10}), 8.69 (s, 1H, H_{11}), 7.92 (dd, J = 8.5, 2.4 Hz, 1H, H_8), 7.90 – 7.87 (d, J = 2.3 Hz, 1H, H_9), 7.36 – 7.32 (m, 2H, H_4, H_7), 7.17 (d, J = 8.7 Hz, 1H, H_{12}), 7.13 – 7.11 (m, 1H, H_3), 7.10 – 7.08 (m, 1H, H_2), 7.07 (d, J = 8.6 Hz, 1H, H_{13}), 6.93 (dd, J = 8.2, 2.5 Hz, 1H, H_5), 5.87 (d, J = 3.9 Hz, 1H, H_{18}), 4.14 – 3.95 (m, 3H, H_{15}, H_{19}), 3.90 (s, 3H, H_6), 2.36 (s, 3H, H_1), 2.30 (s, 3H, H_{14}) 2.35 – 2.11 (m, 4H, H_{16}, H_{17}), 2.06 – 1.84 (m, 2H, H_{20}); ^{13}C NMR (100 MHz, $CDCl_3$): δ 165.8, 160.0, 159.7, 159.5, 155.8, 149.7, 138.8, 131.3, 130.2, 129.4, 128.3, 126.0, 124.8, 122.2, 121.6, 115.5, 113.5, 113.4, 113.2, 112.5, 112.0, 111.2; HRMS (ESI^+) *m/z* calcd for $C_{29}H_{28}N_2O_6$: 514.2104, Found 454.1254 $[C_{25}H_{21}NO_6+Na]^+$.

4.3. HCC38 BREAST CANCER CELL LINE INHIBITION ASSAY

The toxicity of novobiocin and novobiocin analogues was assessed in the human breast cancer HCC38 cell line (ATCC CRL-2314) using a WST-1 cell proliferation kit (Roche) carried out according to manufacturer's instructions. All compounds were resuspended to a final concentration of 100 mM in DMSO. Cells of equal density (4×10^4 cells/mL at 50 μL/well) were seeded in a 96 well plate and treated the following day with a range of compound concentrations (0, 0.32, 1.6, 8, 40, 200, 1000 μM). After 72 hours, media containing compounds were removed from the wells and 5 μL of a 5 mg/mL WST-1 reagent in 100 μL of medium was added to each of the wells and incubated for 4 hours prior to reading absorbance at 450 nm. The cell viability was determined by cleavage of the tetrazolium salt, WST-1, to formazan by metabolically active cells to produce a coloured product. This viability assay was carried out in triplicate and the dose response and half-maximal inhibitory concentrations (IC_{50}) determined by non-linear regression using GraphPad Prism 4.

4.4. HeLa CELL CYTOTOXICITY ASSAY

HeLa cells (Cellonex) were cultured in DMEM medium (Lonza) supplemented with 10% fetal calf serum and antibiotics (penicillin/streptomycin/amphotericin B) at 37 °C in a 5% CO_2 incubator. Cells were plated in 96-well plates at a cell density of 2×10^4 cells/well and grown overnight. Serial dilutions of test compounds were incubated with the cells for an additional 24 hours, and cell viability in the wells assessed by adding 20 μL resazurin toxicology reagent (Sigma-Aldrich) for an additional 2 – 4 hours. Fluorescence readings (excitation 560 nm, emission 590 nm) obtained for the individual wells were converted to % cell viability relative the average readings obtained from untreated control wells.

4.5. 3D7 ANTIPLASMODIAL ASSAY

The 3D7 strain of *P. falciparum* was routinely cultured in medium consisting of RPMI1640 containing 25 mM Hepes (Lonza), supplemented with 0.5% (w/v) Albumax II (Thermo Fisher Scientific), 22 mM glucose, 0.65 mM hypoxanthine, 0.05 mg/mL gentamicin and 2-4% (v/v) human erythrocytes. Cultures were maintained at 37 °C under an atmosphere of 5% CO_2, 5% O_2, 90% N_2. To assess antiplasmodial activity, three-fold serial dilutions of test compounds in culture medium were added to parasite cultures (adjusted to 2% parasitaemia, 1% haematocrit) in 96-well plates and incubated for 48 hours. Duplicate wells per compound concentration were used. Parasite lactate dehydrogenase (pLDH) enzyme activity in the individual wells was

determined by removing 20 μL of the parasite cultures and mixing it with 125 μL colorimetric substrate solution containing 0.18 M L-lactic acid, 0.13 mM acetylpyridine adenine dinucleotide, 0.39 mM nitrotetrazolium blue chloride, 0.048 mM phenazineethosulphate and 0.16% (v/v) Triton X-100 in 44 mM Tris buffer (pH 9). Color development was monitored by measuring absorbance at 620 nm in a Spectramax M3 plate reader (Molecular Devices). Absorbance values were converted to percentage parasite viability relative to untreated control cultures and plotted against log[compound] to derive IC_{50} values by non-linear regression, using GraphPad Prism (v. 5.02) software.

4.6. HSP90 INHIBITION ASSAY

The *Saccharomyces cerevisiae* strains used were: DP552 (wild type/parental strain), DP553 (expressing *Pf*Hsp90), DP555 (expressing hHsp90α) and DP584 (expressing hHsp90β). A 1/500 dilution of a 2-day culture was used to seed a 5 mL test tube culture in YEP rich media (1% w/v yeast extract, 2% w/v bacterial peptone, 2% w/v glucose, 0.2% w/v adenine). The cells were treated at seeding in triplicate with either DMSO (vehicle control), or 50 μM of either compound **2.13a** or **2.20c** before culturing at 28 °C with shaking at 200 rpm. Samples were collected at 6, 16, 24, 30 and 40-hour intervals and absorbance measured at 600 nm using a Powerwave microplate reader.

REFERENCES

1. W. L. Mendelson and S. Hayden, *Synthetic Communications*, **1996**, *26*, 603-610.
2. A. A. Kudale, J. Kendall, C. C. Warford, N. D. Wilkins and G. J. Bodwell, *Tetrahedron Lett.*, **2007**, *48*, 5077-5080.
3. A. Medda, G. Pal, R. Singha, T. Hossain, A. Saha and A. R. Das, *Synth. Commun.*, **2013**, *43*, 169-181.
4. N. Miyaura and A. Suzuki, *Synth. Commun.*, *11*, 513-519.
5. J. A. Burlison, C. Avila, G. Vielhauer, D. J. Lubbers, J. Holzbeierlein and B. S. Blagg, *J. Org. Chem.*, **2008**, *73*, 2130-2137.
6. J. R. Dunetz, Y. Xiang, A. Baldwin and J. Ringling, *Org. Lett.*, **2011**, *13*, 5048-5051.
7. A. C. Donnelly, H. Zhao, B. R. Kusuma and B. S. Blagg, *Med. Chem. Commun.*, **2010**, *1*, 165-170.